Supplementary Information

Macrocyclization of Native Peptides through (Thio)urea Crosslinking of Two Amines

Jinyao Liu [1], Peiru Chen [1], Meilin Tang [1], Qiuyu Chen [1], Yixin Liao [1], Yu Liu [1], Shafi Ullah [1], Jinwu Zhao*[1], Yubo Long*[2], Gong Chen*[3], Wenfang Xiong*[1]

[1] *School of Pharmacy, Guangdong Medical University, Dongguan, China*
** E-mail: jwzhao@gdmu.edu.cn, xiongwf@gdmu.edu.cn*
[2] *Research Institute of Interdisciplinary Science, School of Materials Science and Engineering, Dongguan University of Technology, Dongguan, China*
** E-mail: longyubo@dgut.edu.cn*
[3] *State Key Laboratory and Institute of Elemento-Organic Chemistry, College of Chemistry, Nankai University, Tianjin, China*
** E-mail: gongchen@nankai.edu.cn*

List of contents

A. Reagents & Instruments

All commercial chemical reagents were used as received without further purification unless otherwise noted. Chemicals were purchased from Shanghai Macklin Biochemical Co., Ltd., Bide Pharmatech Ltd., Shanghai Yinli Chemical Technology Co., Ltd., Energy Chemical, Sarn Chemical Technology (Shanghai) Co., Ltd., Shanghai Aladdin Biochemical Technology Co., Ltd..

Linear peptides were synthesized by peptide Biotechnology Co., Ltd (Hangzhou, China), Gutuo Biotechnology Co., Ltd (Hangzhou, China), Tengyi Biotechnology Co., Ltd (Nanjing, China) and Pharmaceutical Technology Co., Ltd (Shanghai, China), Jill Biochemical (Shanghai) Co., Ltd (Shanghai China).

All commercial biological reagents were used as received without further purification unless otherwise noted. Biological reagents were purchased from Grand Island Biological Company, Procell Life Science&Technology Co., Ltd., Shanghai Biyuntian Biotechnology Co., Ltd., Lianke Biotechnology Co., Ltd..

All cell lines were used without further authentication unless otherwise noted. Cells were obtained from Guangzhou Xinyuan Technology Co., Ltd., including A549-Luc (human non-small-cell lung carcinoma), Caco-2 (human colorectal adenocarcinoma), and A498 (human renal carcinoma).

^{1}H NMR spectra were recorded on a Bruker AMX-400 (400 MHz). Chemical shifts were expressed in parts per million (ppm) with respect to the residue solvent peak. The following abbreviations were used to explain multiplicities: s = singlet, d = doublet, t = triplet, q = quartet, m = multiplet, br = broad. Coupling constants (J) were reported in Hertz (Hz). ^{13}C NMR spectra were recorded on Bruker AMX-400 instrument (100 MHz), and were fully decoupled by broadband proton decoupling.

High Resolution Mass Spectra (HRMS) were recorded on a Thermo Fisher Scientific Q Exactive HR LCMS equipped with an ESI source, operated in positive or negative ion mode, over a range of m/z 150-2200. The purified peptide samples were dissolved in methanol/0.1% aqueous formic acid (7:3, v/v) and directly infused into the ESI source at 0.2 mL/min using a syringe pump. Data were processed using Xcalibur

software (Thermo Fisher Scientific). Each compound was independently analyzed with three sample replicates to ensure the reliability of the results.

Analytical HPLC were performed on an Agilent 1260 Infinity II system and an E-Classical 3200 Liquid Chromatography system. Each compound was dissolved in 50% MeCN at a concentration of 0.15 mg/mL, filtered through a 0.22 um syringe filter, and analyzed on a HPLCONE 10C18A (10 μm, 4.6 x 250 mm) or Supersil ODS2 column (5 μm, 4.6mm x 250 mm) using a mobile phase of 0.1% TFA in water/acetonitrile (v/v) with a gradient of 10-60% MeCN (0-30 min) and 60-95% MeCN (30-35 min) at 1 mL/min. Fractions were collected by UV monitoring (210 -280 nm). This method was applied to all compounds.

Preparative HPLC was performed on a preparative HPLC system (Ruihe Technology, China) equipped with a YMC-1025-S-10 column (10 mm × 250 mm; Wuhan Ruihe Chromatography Technology Co., Ltd.). The mobile phase consisted of 0.1% TFA in water / MeCN (v/v) with a gradient of 10-50% MeCN (0-30 min), held at 50% MeCN (30-40 min), 50%-95% MeCN (40-45 min) at 3 mL/min. Fractions were collected by UV detection monitoring at 210 nm and 220 nm, and dried under reduced pressure.

A freeze dryer was purchased from Beijing Songyuan Huaxing Technology Development Co., Ltd.. **Fluorescence imaging** was conducted using a Leica SP8 laser scanning confocal microscope equipped with a 63×/1.40 oil immersion objective. The following excitation/emission settings were used: 405 nm / 410-480 nm for Hoechst and 488 nm / 494-631 nm for FITC. **Flow cytometry** was performed on a FongCyte™ flow cytometer.

B. Optimization of reaction conditions

Create the standard calibration curve using the standard sample 1a

The lyophilized product **1a**, was dissolved in 50% aqueous MeCN to prepare a series of standard solutions with varying concentrations (0.25, 0.5, 1.0, 2.0, and 4.0 mg/mL). Subsequently, under the HPLC conditions described in the manuscript, 10 μL of each solution was injected into the analytical HPLC. The peak areas were measured using EClassical 3200 Liquid Chromatography system, and standard calibration curves were

plotted using GraphPad Prism with the peak areas versus sample concentrations. The calibration curve of **1a** is shown in Figure S1, with the corresponding equation $Y = 0.0009720 * X - 0.01813$ (Figure S1).

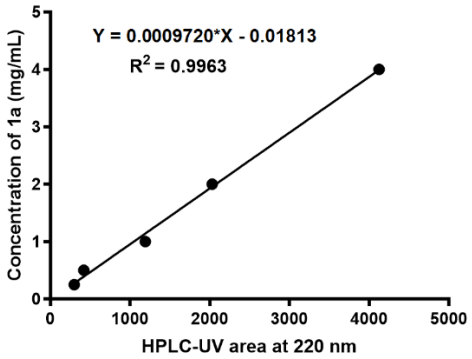

Figure S1. The standard calibration curve of **1a**

Calibration Yield Calculation Formula:

$$\boldsymbol{Yeild}(\%) = \frac{(\mathbf{0.0009720}*\boldsymbol{a}-\mathbf{0.01813})*\boldsymbol{v}}{\mathbf{5.68}} * \mathbf{100}\% \qquad \mathbf{(1)}$$

$\boldsymbol{a}$: refers to peak area of **1a** at 220 nm

$\boldsymbol{v}$: refers to the volume of the reaction mixture of compound **1a**

5.68: refers to the theoretical mass of compound **1a**

Screening of reaction conditions

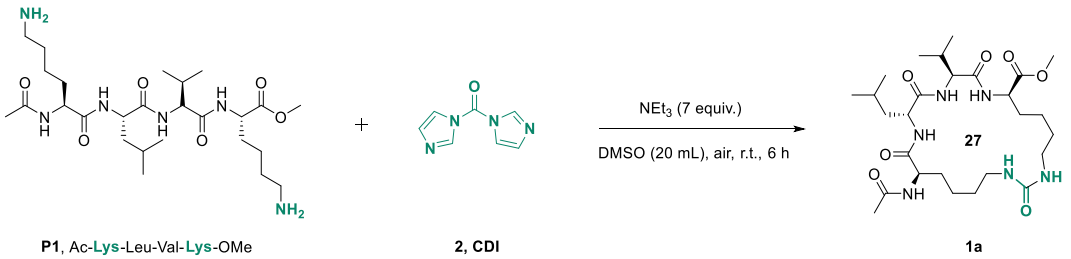

Table S1. Optimization of reaction conditions.

Entry	Variations from the above conditions	Yield [a] (%)
1	none	84 (76[b])
2	DIPEA instead of NEt_3	58
3	DBU instead of NEt_3	n.d.
4	DABCO instead of NEt_3	65
5	TBD instead of NEt_3	n.r.
6	*t*-BuOK instead of NEt_3	52

7	no NEt_3	22
8	DMF instead of DMSO	48
9	MeCN instead of DMSO	4
10	MeOH instead of DMSO	n.r.
11	PBS buffer (pH 8.5, 1 M) instead of DMSO	n.r.
12	DMSO: PBS buffer (pH 8.5, 1 M) (*v*: *v* = 1:1) instead of DMSO	n.d.
13	1.0 mM instead of 0.5 mM reaction molarity	47
14	2.0 mM instead of 0.5 mM reaction molarity	13

Reaction conditions: **P1** (0.01 mmol), **2** (1.5 equiv.), base (7 equiv.), air, r.t., 6 h. [a] Yield of **1a** was determined by analytical HPLC with the external standard method based on absorbance at 220 nm. [b] Isolated yields. n. r. = no reaction. n. d. = no detected.

Example Procedure (Entry 1):

To a solution of **P1** in DMSO (0.01 mmol, 0.001 M, 10 mL), a solution of *N*, *N'*-carbonyldiimidazole (CDI, 1.5 equiv., 0.015 M in DMSO, 10 mL) and NEt_3 (7 equiv., 0.0035 M) was added dropwise successively *via* a constant-pressure dropping funnel under stirring. The reaction mixture was stirred at room temperature for 6 hours. After the reaction was completed, the crude mixture was quenched with excess 1,3-propanediamine and lyophilized to remove DMSO. The resulting residue was dissolved in 4 mL of MeCN/H_2O. Then, an aliquot of 20 μL was filtered and subjected to HPLC analysis, record the peak area for **1a**, and calculate its concentration using Equation. Determine the conversion rate using Formula.

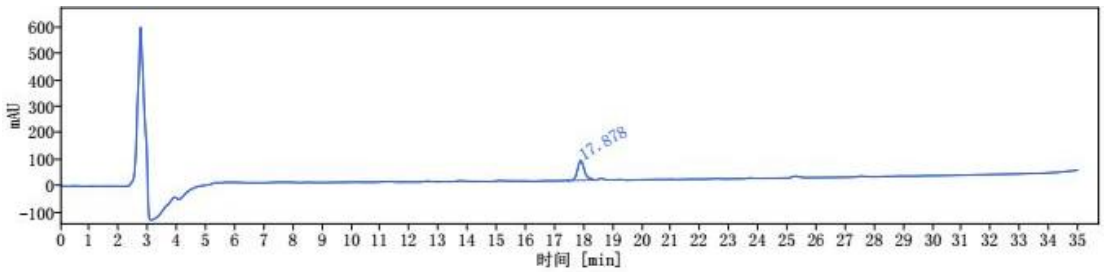

	RT	Area	%Area	Height
1a	17.878	1244.5	88	74.5

Figure S2. HPLC-UV chromatogram at 220 nm of the reaction solution of entry 1.

C. Characterization of (thio)urea-containing cyclic peptides

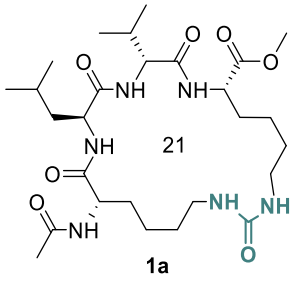

1a

Compound 1a was isolated in 76% yield (4.3 mg, 0.0076 mmol) as a white powder; the HPLC yield was 88% based on absorbance at 220 nm.

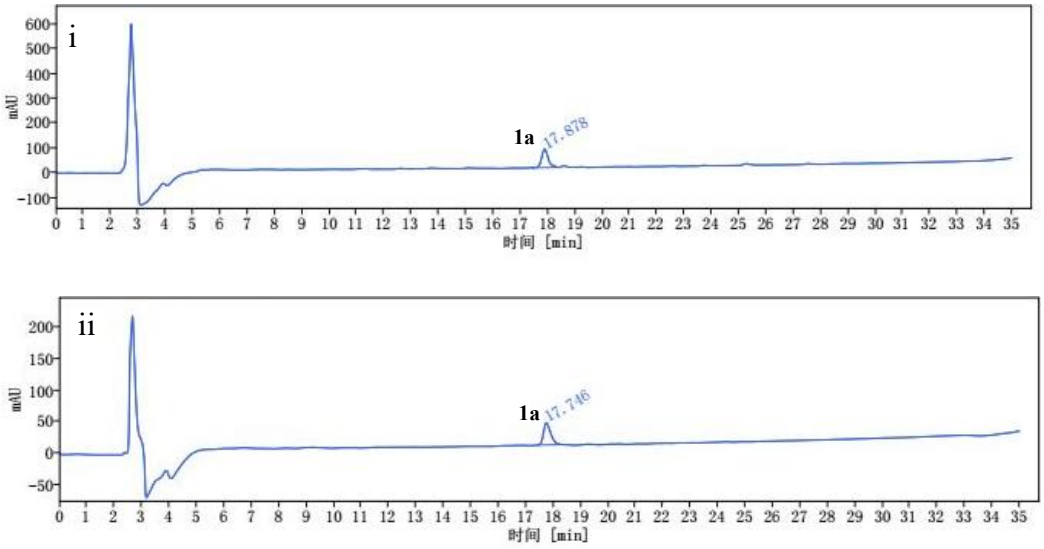

Figure S3. i) HPLC trace of reaction mixture of compound **1a**. ii) HPLC trace of purified compound **1a** [1 mL/min, 10% to 60% MeCN for 30 min, then 60% to 95% MeCN 30-35 min, HPLCONE 10C18A (10 μm, 4.6 x 250 mm), λ = 220 nm].

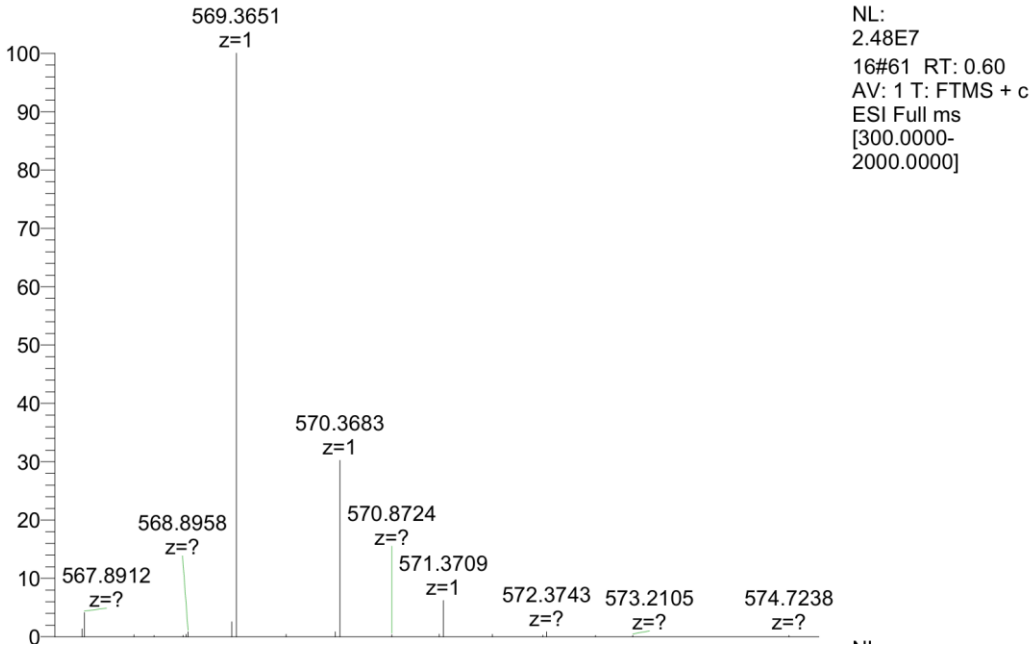

HRMS of compound 1a: Calcd for $[M+H]^+$ $C_{27}H_{49}N_6O_7^+$: 569.3657; found: 569.3651. **^{1}H NMR (400 MHz, DMSO-*d*$_6$)** δ 8.34 – 8.22 (m, 2 H), 8.07 (d, *J* = 5.6 Hz, 1 H), 7.91 (d, *J* = 7.8 Hz, 1 H), 5.95 (s, 1 H), 5.41 (s, 1 H), 4.37 – 4.26 (m, 2 H), 4.23 – 4.18 (m, 1 H), 3.99 – 3.95 (m, 1 H), 3.60 (s, 3 H), 3.22 – 2.84 (m, 5 H), 1.98 – 1.90 (m, 1 H), 1.82 (s, 3 H), 1.73 – 1.50 (m, 6 H), 1.44 – 1.39 (m, 2 H), 1.36 – 1.24 (m, 6 H), 0.97 – 0.81 (m, 12 H). **^{13}C NMR (100 MHz, DMSO-*d*$_6$)** δ 173.9, 173.0, 171.6, 171.5, 169.1, 158.6, 59.2, 52.2, 52.2, 51.6, 51.2, 40.8, 31.8, 30.0, 29.7, 28.4, 27.9, 24.3, 23.4, 22.9, 22.4, 22.1, 21.7, 19.7, 19.4.

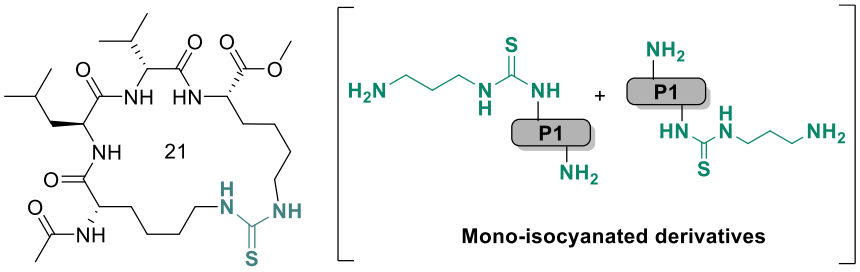

Compound 1b was isolated in 45% yield (2.6 mg, 0.0045 mmol) as a white powder; the HPLC yield was 50% based on absorbance at 250 nm.

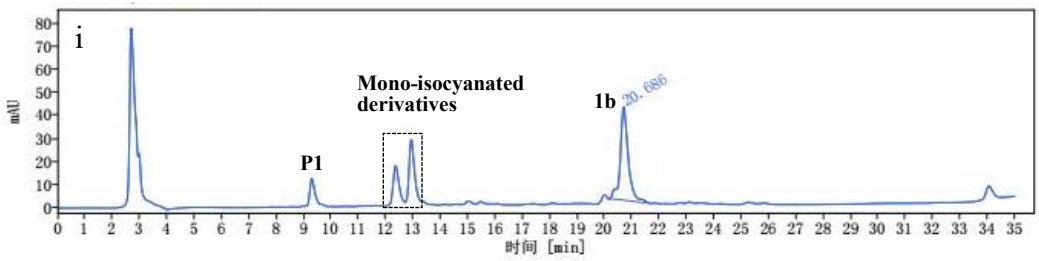

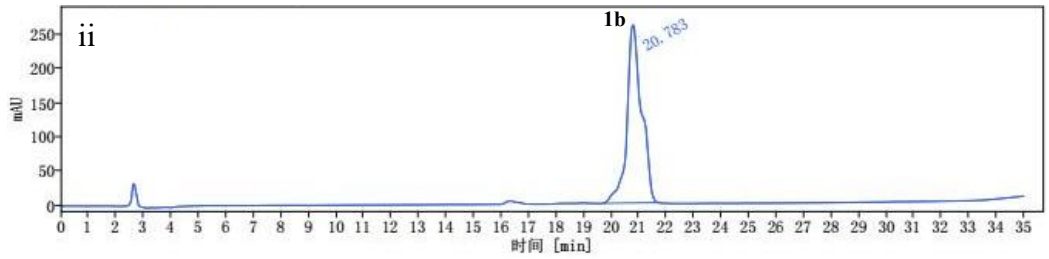

Figure S4. i) HPLC trace of reaction mixture of compound **1b**. ii) HPLC trace of purified compound **1b** [1 mL/min, 10% to 60% MeCN for 30 min, then 60% to 95% MeCN 30-35 min, HPLCONE 10C18A (10 μm, 4.6 x 250 mm), λ = 250 nm].

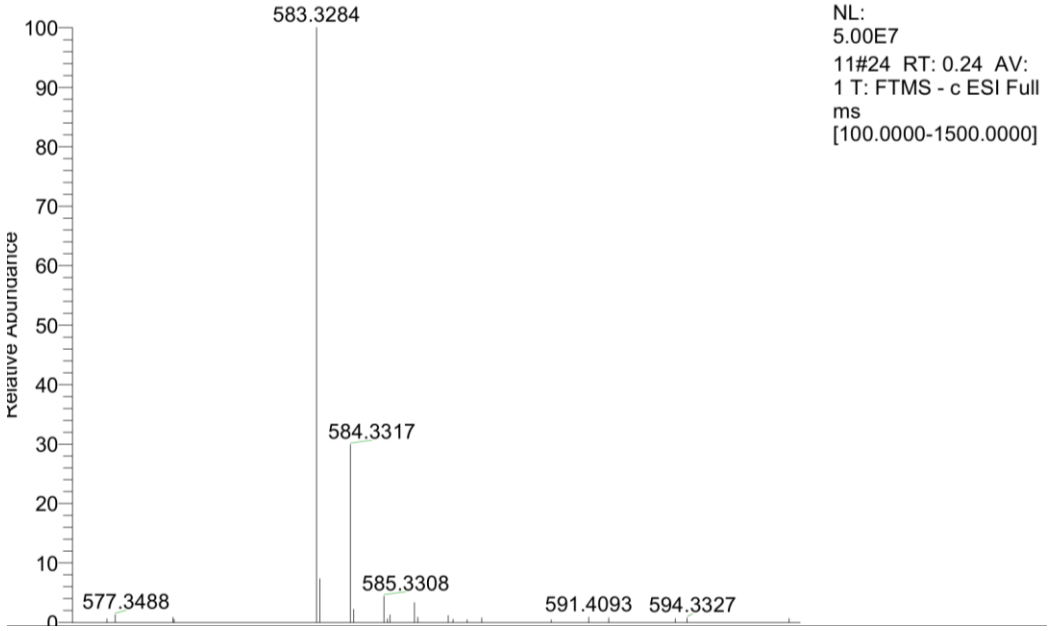

HRMS of compound 1b: Calcd for $[M-H]^-$ $C_{27}H_{47}N_6O_6S^-$: 583.3283; found:583.3284.

^{1}H NMR (400 MHz, DMSO-*d*$_6$) δ 8.30 (d, *J* = 8.4 Hz, 1 H), 8.18 (d, *J* = 6.0 Hz, 1 H), 7.99 – 7.90 (m, 1 H), 7.87 – 7.66 (m, 1 H), 7.37 (s, 1 H), 7.14 – 6.59 (m, 1 H), 4.38 – 4.16 (m, 3 H), 3.97 (t, *J* = 7.8 Hz, 1 H), 3.53 – 3.41 (m, 5 H), 3.25 – 3.13 (m, 2 H), 3.04 – 2.69 (m, 1 H), 2.00 – 1.89 (m, 1 H), 1.80 (s, 3 H), 1.77 – 1.53 (m, 6 H), 1.47 – 1.26 (m, 8 H), 0.98 – 0.81 (m, 12 H).

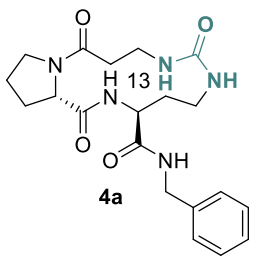

4a

Compound 4a was isolated in 61% yield (2.4 mg, 0.0061 mmol) as a white powder; the HPLC yield was 71% based on absorbance at 210 nm.

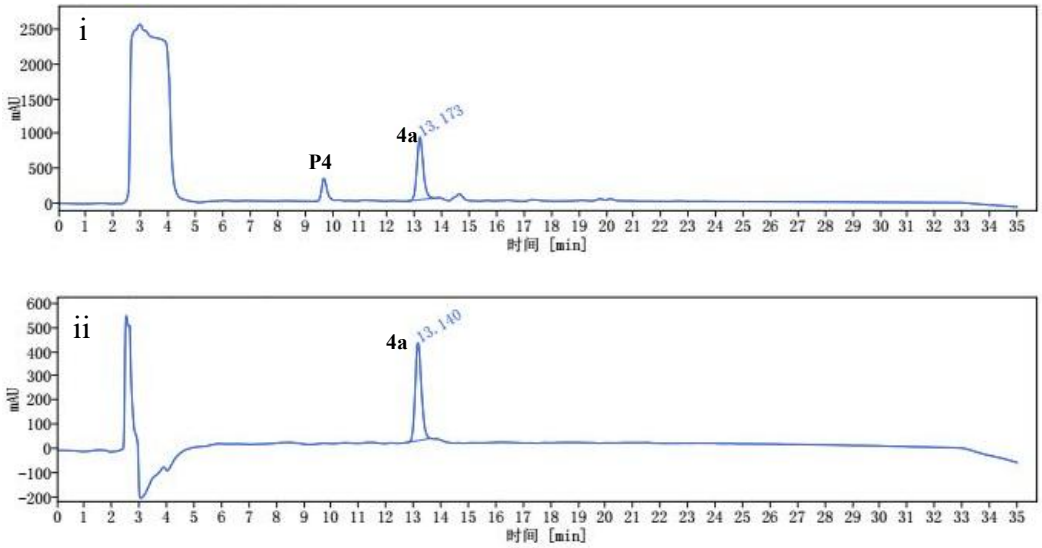

Figure S5. i) HPLC trace of reaction mixture of compound **4a**. ii) HPLC trace of purified compound **4a** [1 mL/min, 10% to 60% MeCN for 30 min, then 60% to 95% MeCN 30-35 min, HPLCONE 10C18A (10 μm, 4.6 x 250 mm), λ = 210 nm].

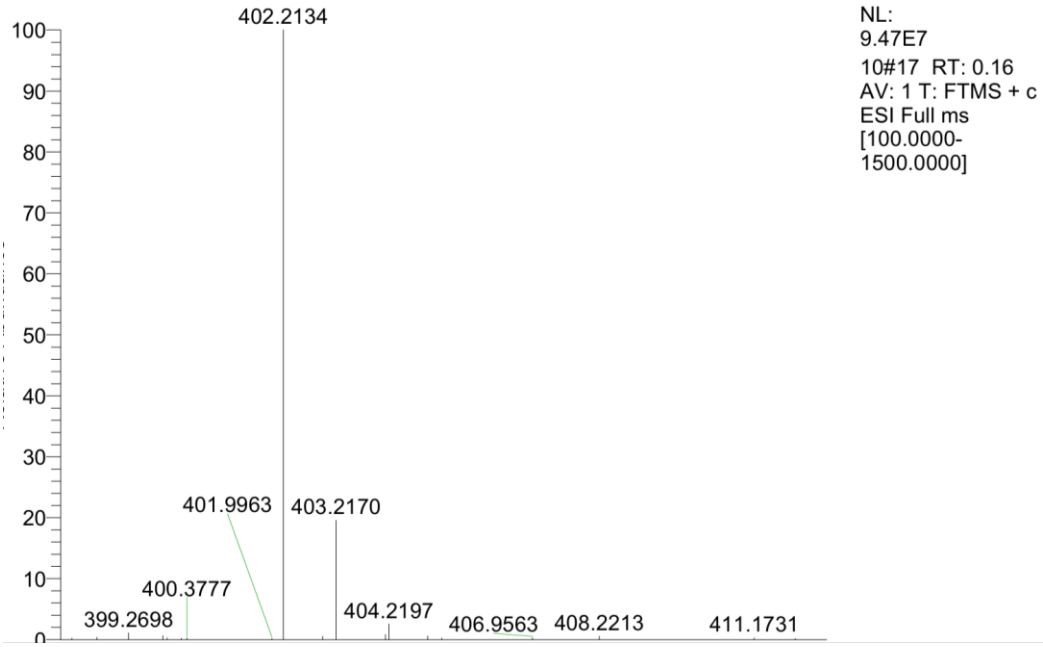

HRMS of compound 4a: Calcd for $[M+H]^+$ $C_{20}H_{28}N_5O_4^+$: 402.2136; found: 402.2134

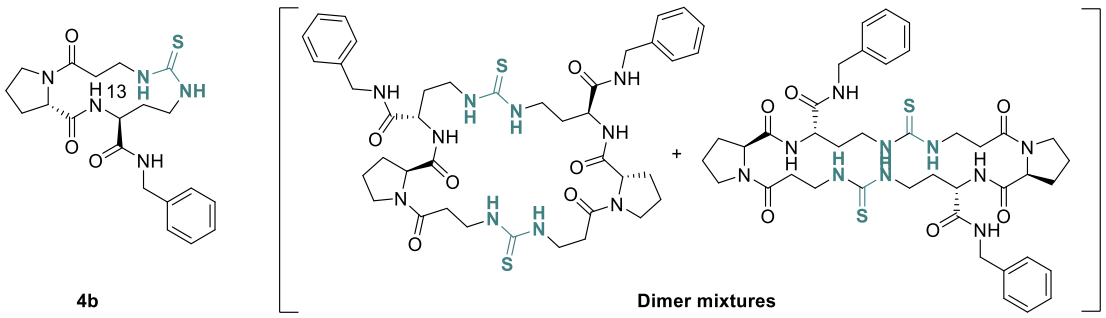

Compound 4b was isolated in 54% yield (2.3 mg, 0.0054 mmol) as a white powder; the HPLC yield was 65% based on absorbance at 250 nm.

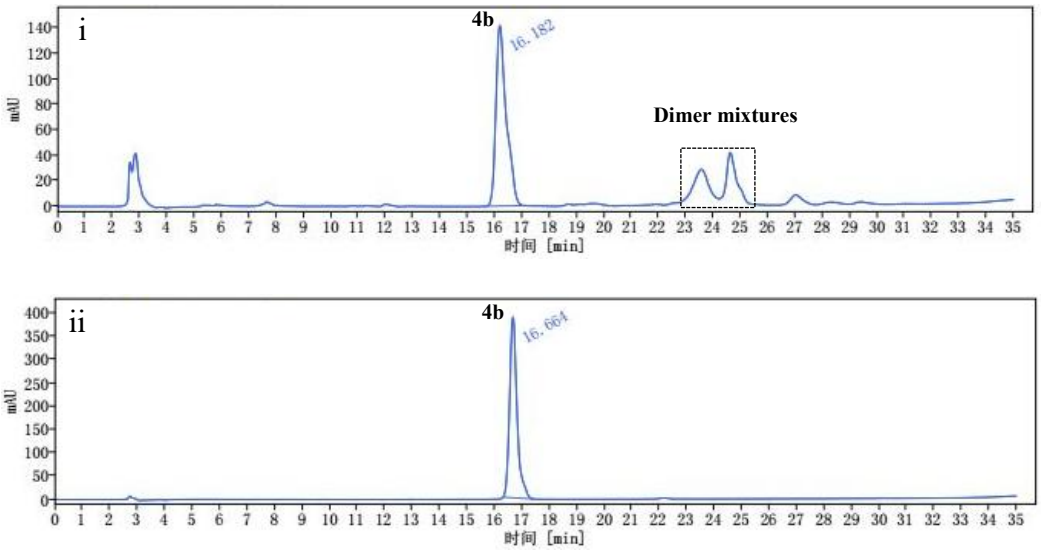

Figure S6. i) HPLC trace of reaction mixture of compound **4b**. ii) HPLC trace of purified compound **4b** [1 mL/min, 10% to 60% MeCN for 30 min, then 60% to 95% MeCN 30-35 min, HPLCONE 10C18A (10 μm, 4.6 x 250 mm), λ = 250 nm].

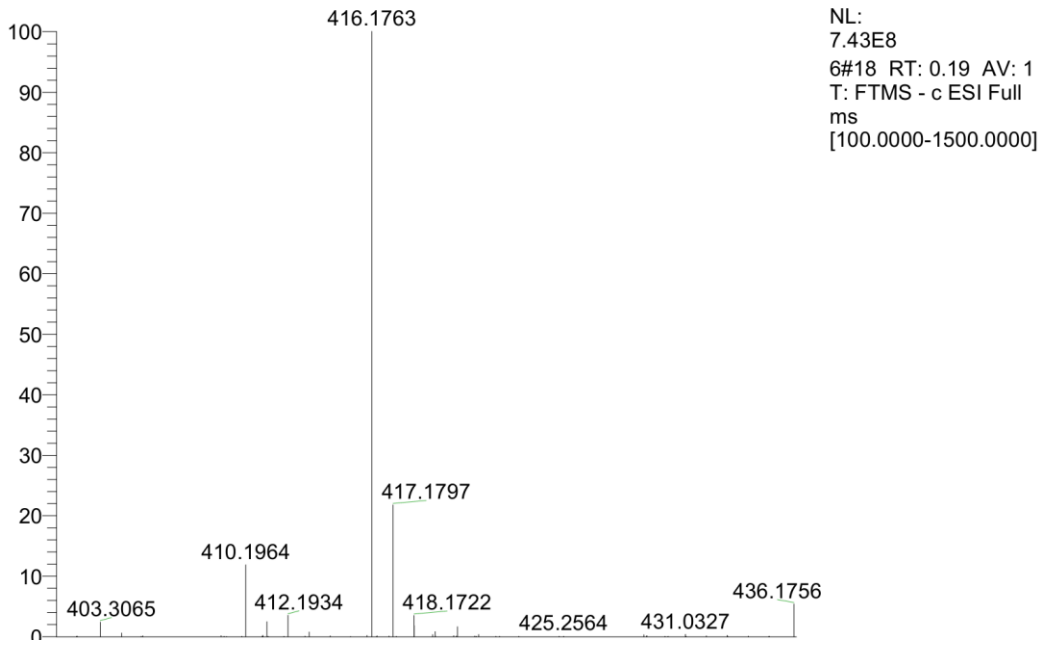

HRMS of compound 4b: Calcd for $[M-H]^-$ $C_{20}H_{26}N_5O_3S^-$: 416.1762; found: 416.1763.

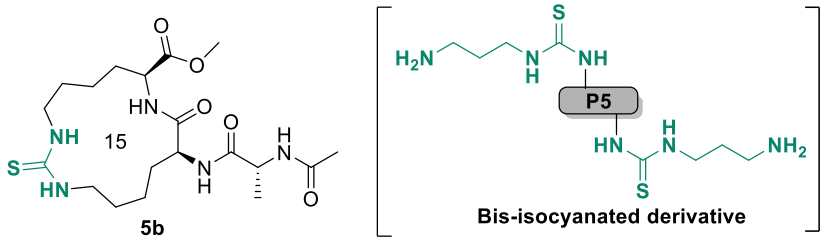

Compound 5b was isolated in 38% yield (1.7 mg, 0.0038 mmol) as a white powder; the HPLC yield was 44% based on absorbance at 240 nm.

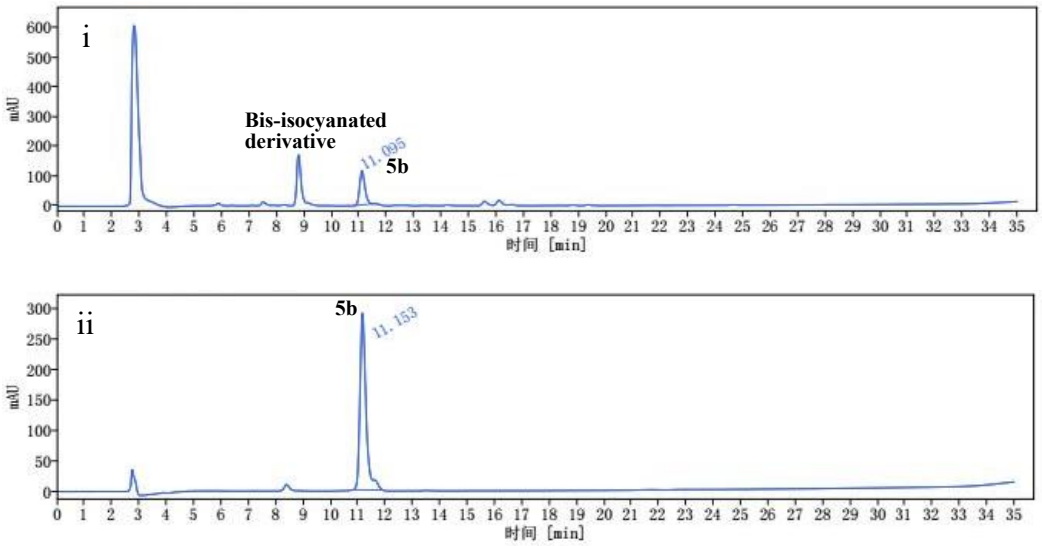

Figure S7. i) HPLC trace of reaction mixture of compound **5b**. ii) HPLC trace of purified compound **5b** [1 mL/min, 10% to 60% MeCN for 30 min, then 60% to 95% MeCN 30-35 min, HPLCONE 10C18A (10 μm, 4.6 x 250 mm), λ = 240 nm].

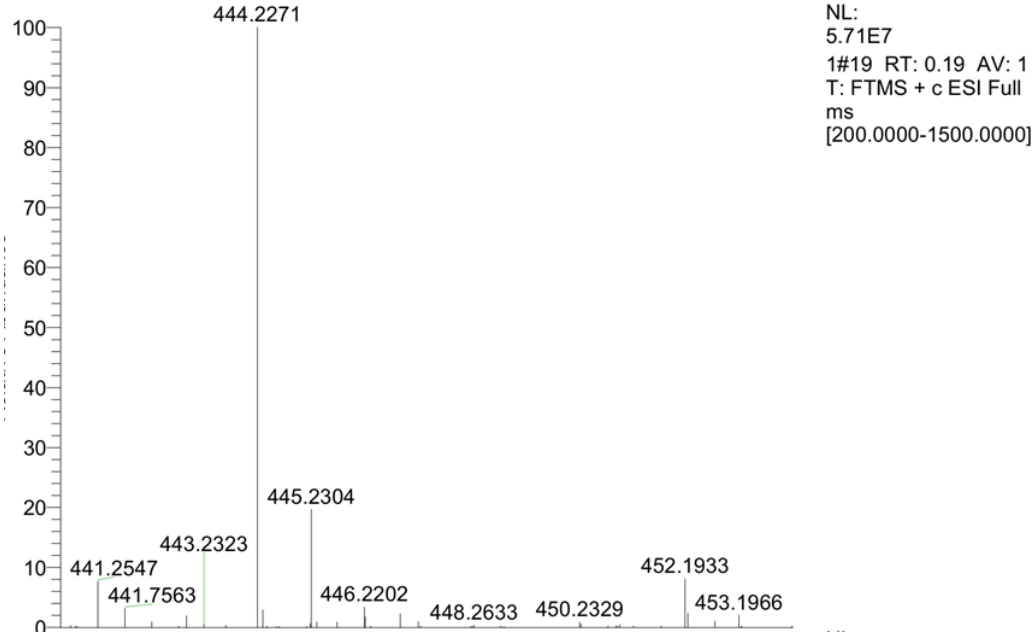

HRMS of compound 5b: Calcd for $[M+H]^+$ $C_{19}H_{34}N_5O_5S^+$: 444.2275; found: 444.2271.

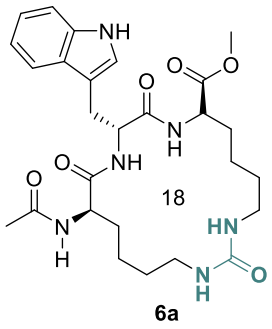

6a

Compound 6a was isolated in 39% yield (2.1 mg, 0.0039 mmol) as a white powder; the HPLC yield was 45% based on absorbance at 220 nm.

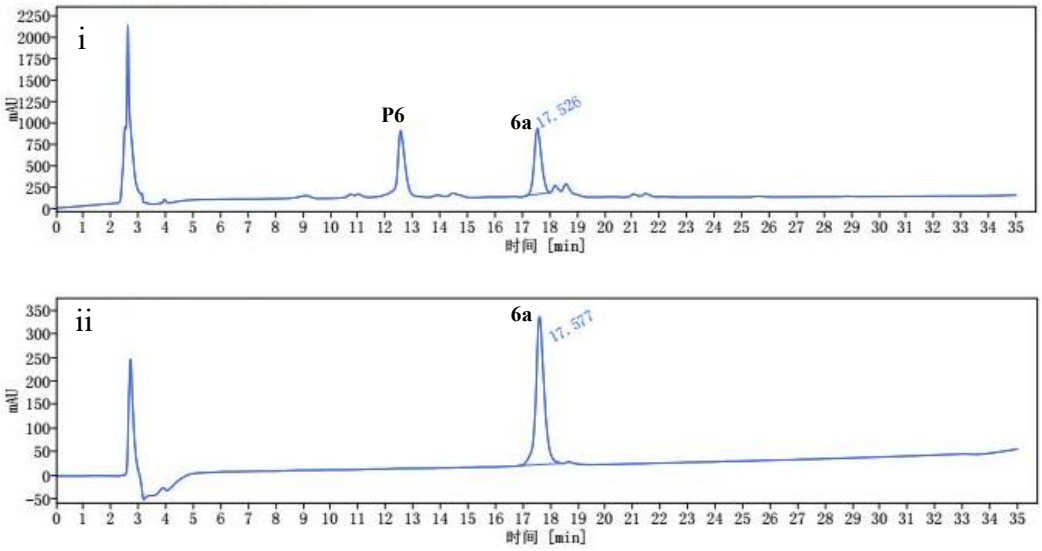

Figure S8. i) HPLC trace of reaction mixture of compound **6a**. ii) HPLC trace of purified compound **6a** [1 mL/min, 10% to 60% MeCN for 30 min, then 60% to 95% MeCN 30-35 min, HPLCONE 10C18A (10 µm, 4.6 x 250 mm), λ = 220 nm].

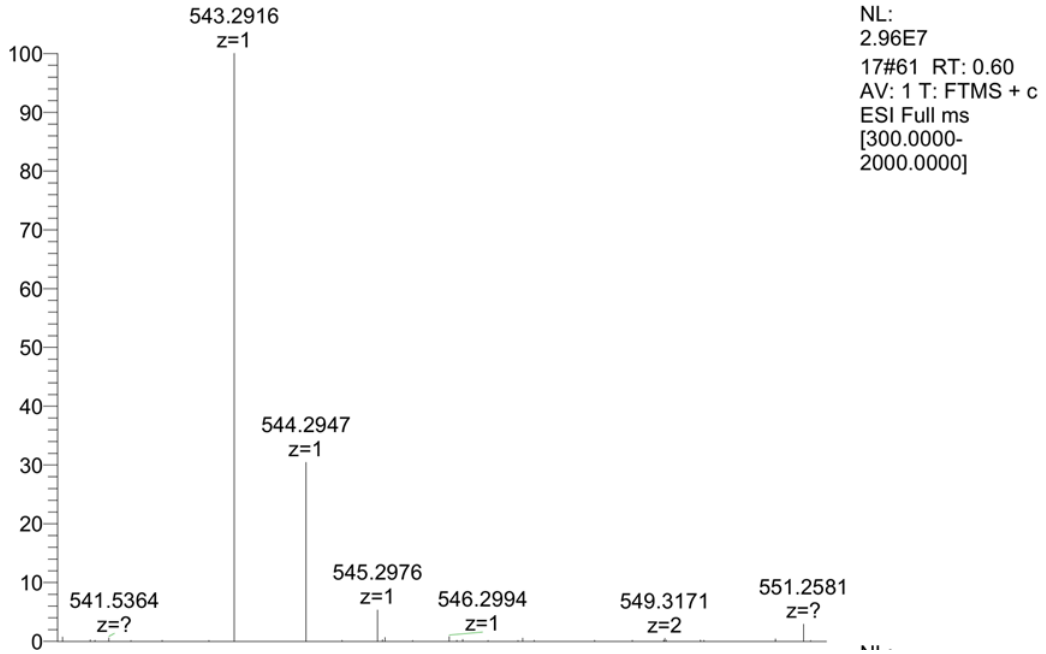

HRMS of compound 6a: Calcd for $[M+H]^+C_{27}H_{39}N_6O_6^+$: 543.2926; found: 543.2916. **^{1}H NMR (400 MHz, DMSO-*d*$_6$)** δ 10.81 (s, 1 H), 8.33 (d, *J* = 8.3 Hz, 1 H), 8.08 (d, *J* = 8.4 Hz, 1 H), 7.83 (d, *J* = 7.7 Hz, 1 H), 7.57 (d, *J* = 7.8 Hz, 1 H), 7.30 (d, *J* = 8.0 Hz, 1 H), 7.10 (d, *J* = 2.3 Hz, 1 H), 7.04 (t, *J* = 7.5 Hz, 1 H), 6.95 (t, *J* = 7.4 Hz, 1 H), 5.66 – 5.56 (m, 2 H), 4.70 – 4.63 (m, 1 H), 4.38 – 4.29 (m, 2 H), 3.59 (s, 3 H), 3.21 – 3.11 (m, 2 H), 3.09 – 3.05 (m, 1 H), 2.94 – 2.90 (m, 1 H), 2.87 – 2.81 (m, 2 H), 1.83 (s, 3 H), 1.72 – 1.53 (m, 4 H), 1.50 – 1.35 (m, 4 H), 1.24 – 1.19 (m, 4 H). **^{13}C NMR (100 MHz, DMSO-d$_6$)** δ 172.9, 171.7, 171.4, 169.2, 158.5, 136.4, 128.0, 124.1, 121.2, 118.8, 118.6, 111.6, 110.0, 53.4, 52.5, 52.3, 51.9, 40.9, 39.2, 32.6, 31.5, 29.8, 29.6, 28.7, 23.2, 22.9, 22.4.

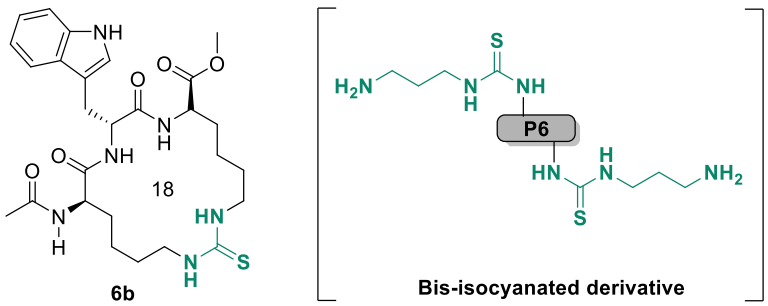

Compound 6b was isolated in 53% yield (3.0 mg, 0.0053 mmol) as a white powder; the HPLC yield was 61% based on absorbance at 210 nm.

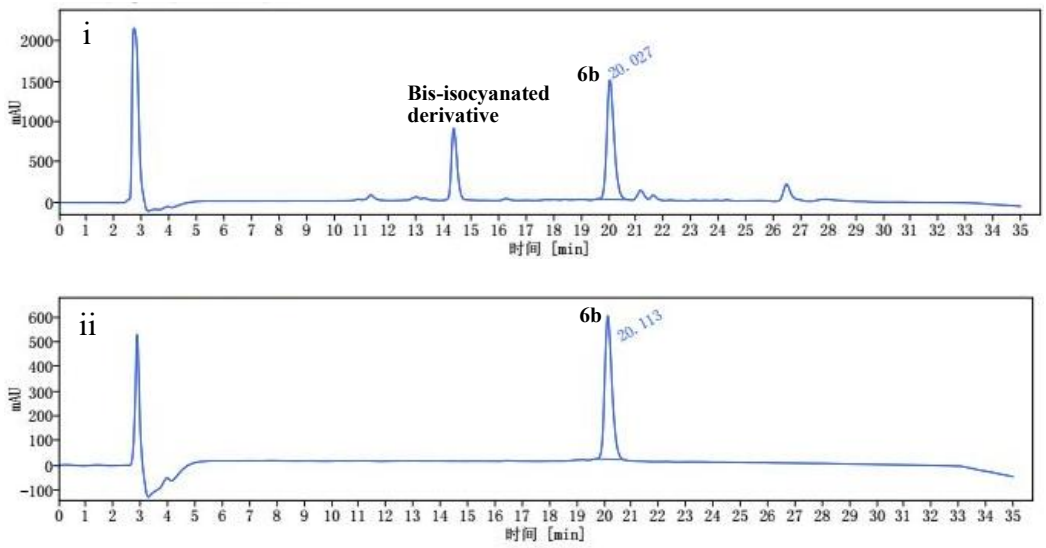

Figure S9. i) HPLC trace of reaction mixture of compound **6b**. ii) HPLC trace of purified compound **6b** [1 mL/min, 10% to 60% MeCN for 30 min, then 60% to 95% MeCN 30-35 min, HPLCONE 10C18A (10 μm, 4.6 x 250 mm), λ = 210 nm].

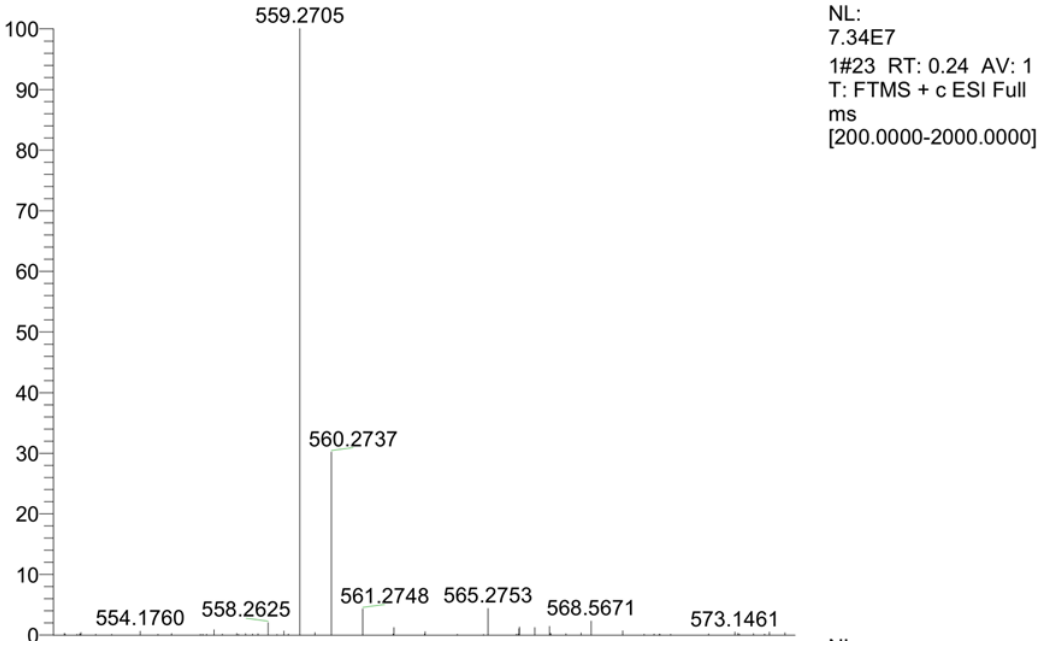

HRMS of compound 6b: Calcd for $[M+H]^+C_{27}H_{39}N_6O_5S^+$: 559.2697; found:559.2705.

^{1}H NMR (400 MHz, DMSO-*d*$_6$) δ10.80 (s, 1 H), 8.37 – 8.03 (m, 2 H), 7.83 (d, *J* = 7.7 Hz, 1 H), 7.57 (d, *J* = 7.8 Hz, 1 H), 7.30 (d, *J* = 8.0 Hz, 1 H), 7.27 – 7.17 (m, 1 H), 7.10 (d, *J* = 2.3 Hz, 1 H), 7.04 (t, *J* = 7.5 Hz, 1 H), 6.95 (t, *J* = 7.4 Hz, 1 H), 4.67 – 4.56 (m, 1 H), 4.40 – 4.22 (m, 2 H), 3.78 – 3.72 (m, 3 H), 3.30 – 3.19 (m, 2 H), 3.12 – 3.05 (m,

1 H), 2.96 – 2.89 (m, 1 H), 1.83 (s, 3 H), 1.70 – 1.58 (m, 3 H), 1.56 – 1.45 (m, 3 H), 1.41 – 1.21 (m, 6 H).

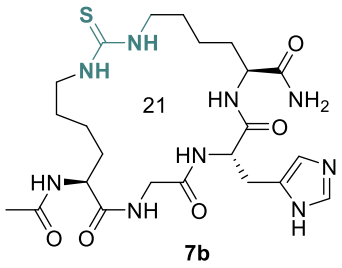

Compounds 7b was isolated in 65% yield (3.6 mg, 0.0065 mmol) as a white powder; the HPLC yield was 72% based on absorbance at 210 nm.

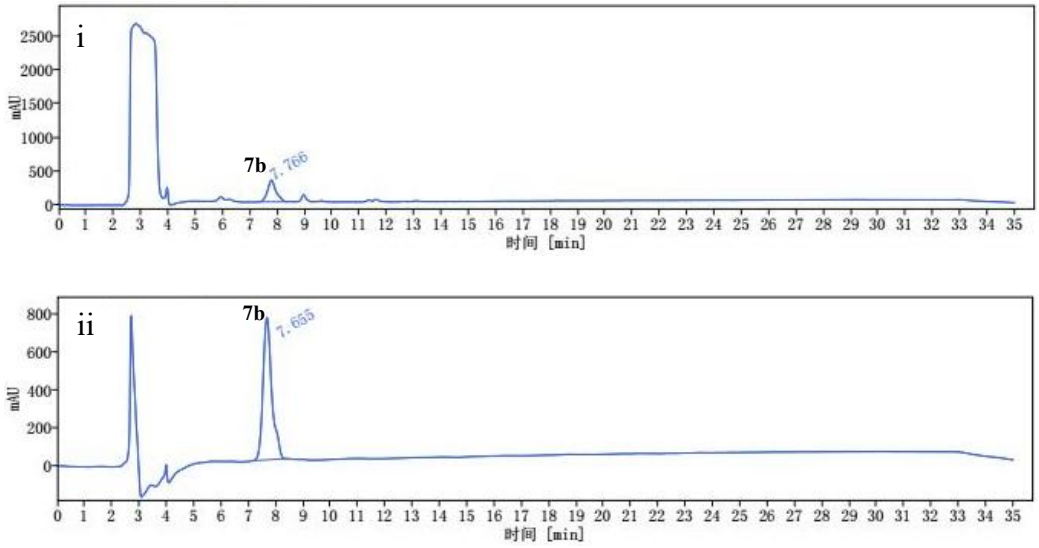

Figure S10. i) HPLC trace of reaction mixture of compound **7b**. ii) HPLC trace of purified compound **7b** [1 mL/min, 10% to 60% MeCN for 30 min, then 60% to 95% MeCN 30-35 min, HPLCONE 10C18A (10 μm, 4.6 x 250 mm), λ = 210 nm].

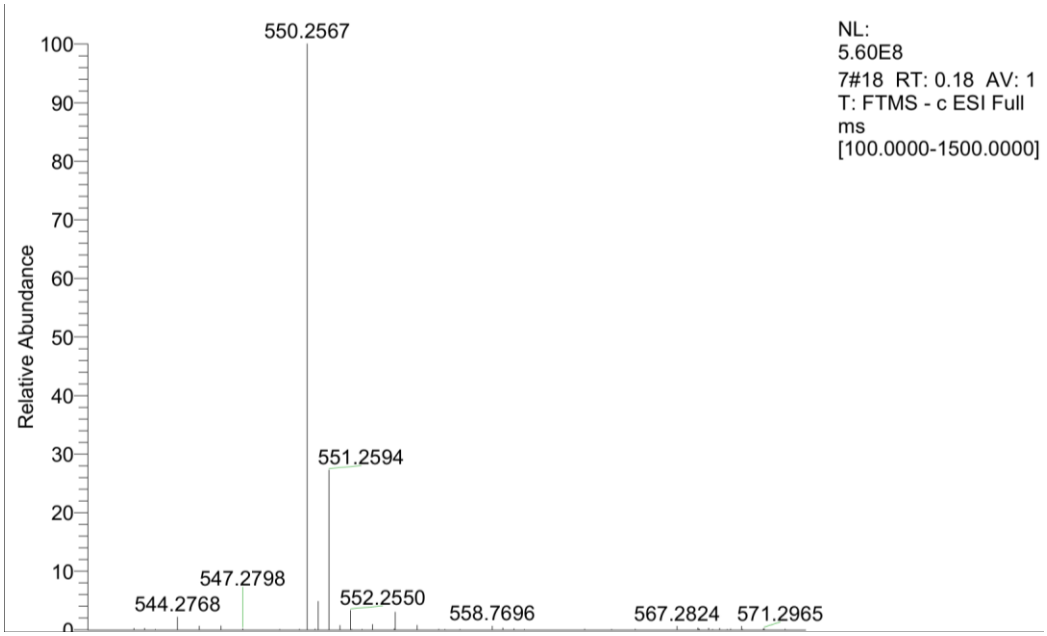

HRMS of compound 7b: Calcd for $[M-H]^-C_{23}H_{36}N_9O_5S^-$: 550.2566; found: 550.2567.

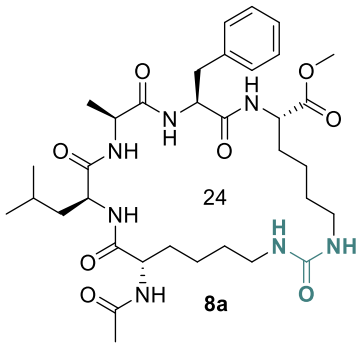

Compound 8a was isolated in 10% yield (0.69 mg, 0.0010 mmol) as a white powder; the HPLC yield was 14% based on absorbance at 220 nm.

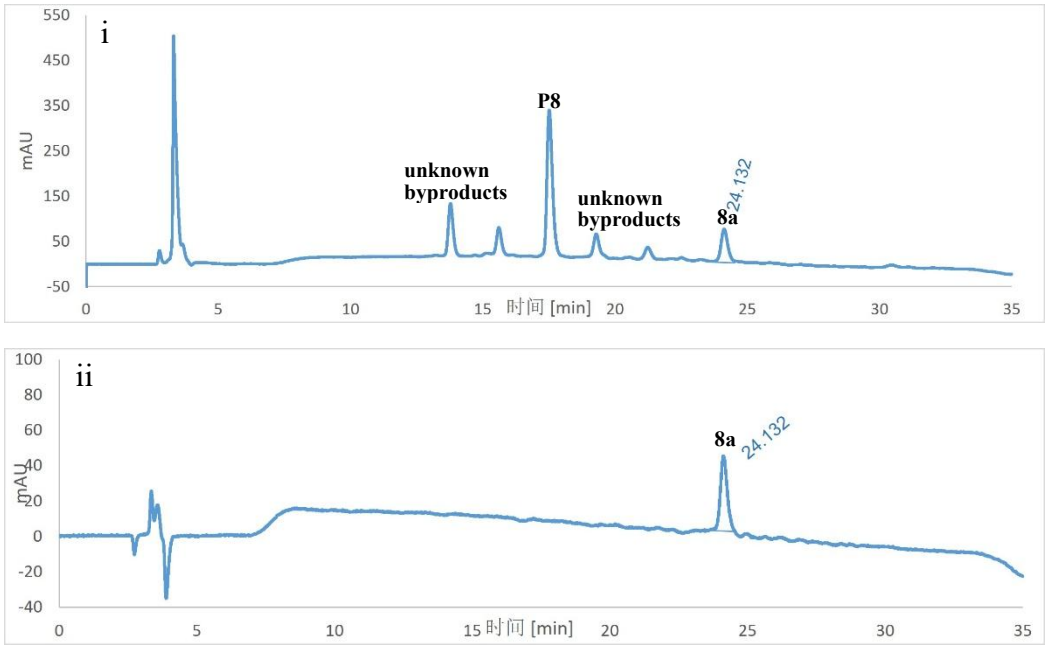

Figure S11. i) HPLC trace of reaction mixture of compound **8a**. ii) HPLC trace of purified compound **8a** [1 mL/min, 10% to 60% MeCN for 30 min, then 60% to 95% MeCN 30-35 min, Supersil ODS2 5μm, E3614696: 4.6mm x 250 mm, λ = 220 nm].

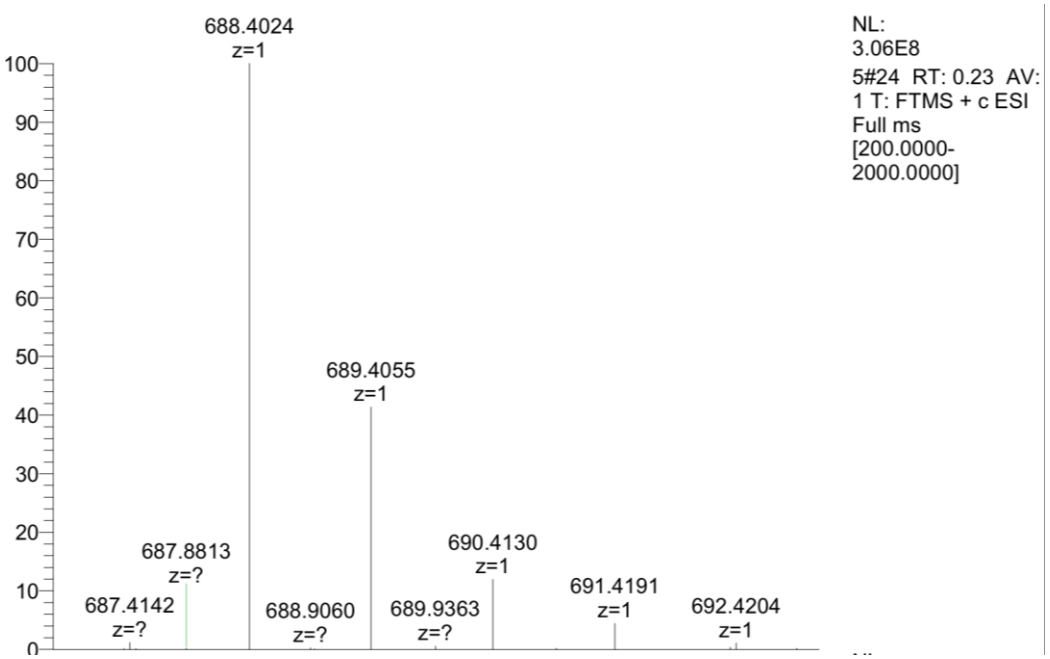

HRMS of compound 8a: Calcd for $[M+H]^+C_{34}H_{54}N_7O_8^+$: 688.4028; found: 688.4024.

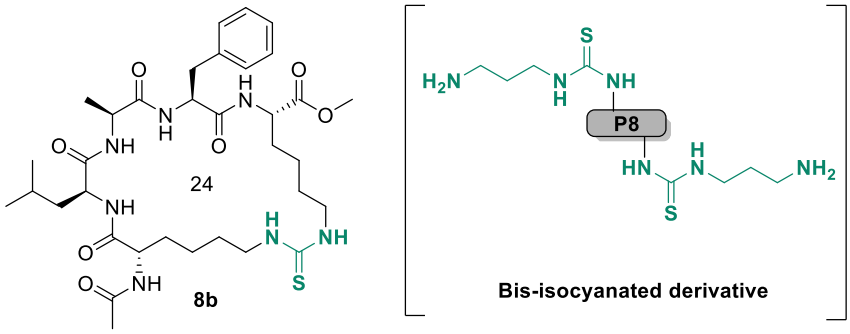

Compound 8b was isolated in 61% yield (4.3 mg, 0.0061 mmol) as a white powder; the HPLC yield was 67% based on absorbance at 250 nm.

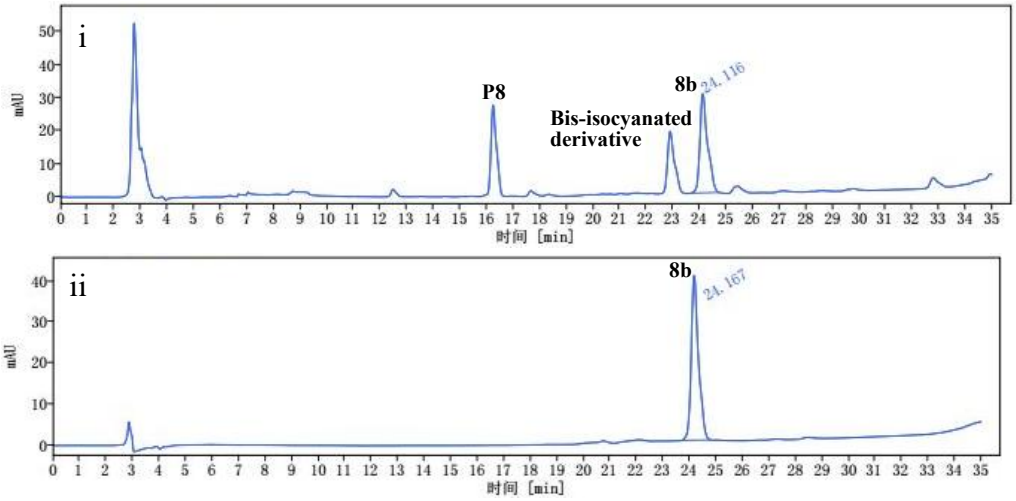

Figure S12. i) HPLC trace of reaction mixture of compound **8b**. ii) HPLC trace of purified compound **8b** [1 mL/min, 10% to 60% MeCN for 30 min, then 60% to 95% MeCN 30-35 min, HPLCONE 10C18A (10 μm, 4.6 x 250 mm), λ = 250 nm].

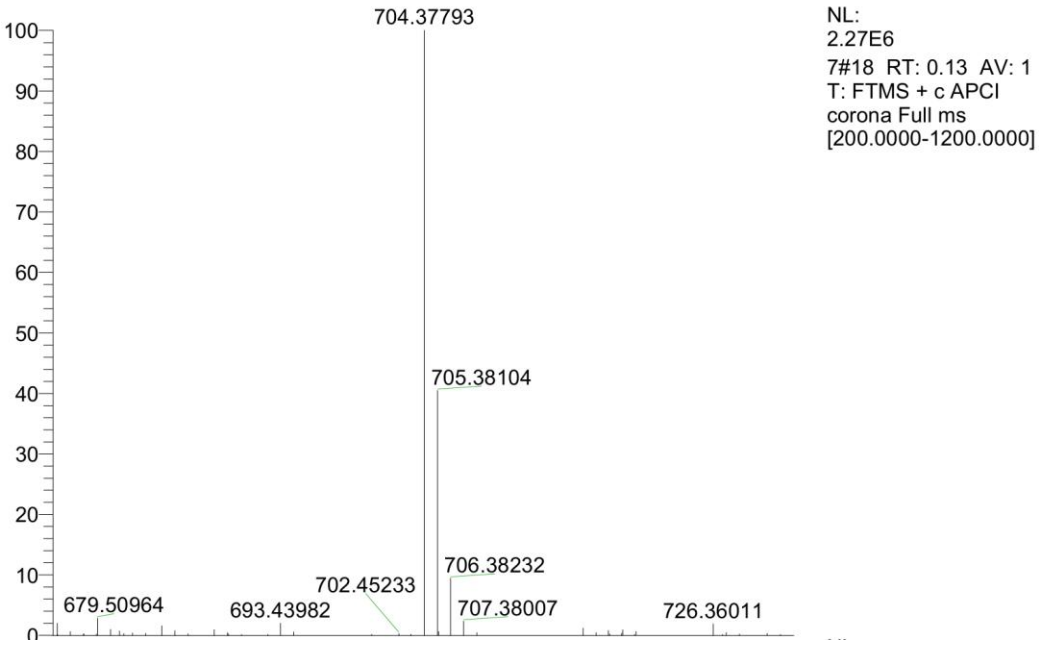

HRMS of compound 8b: Calcd for $[M+H]^+C_{34}H_{54}N_7O_7S^+$:704.37999; found:

704.37793.

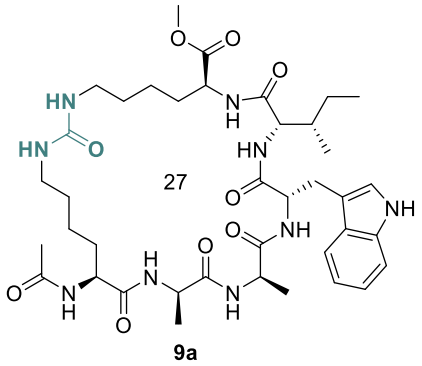

Compound 9a was isolated in 71% yield (5.7 mg, 0.0071 mmol) as a white powder; the HPLC yield was 78% based on absorbance at 220 nm.

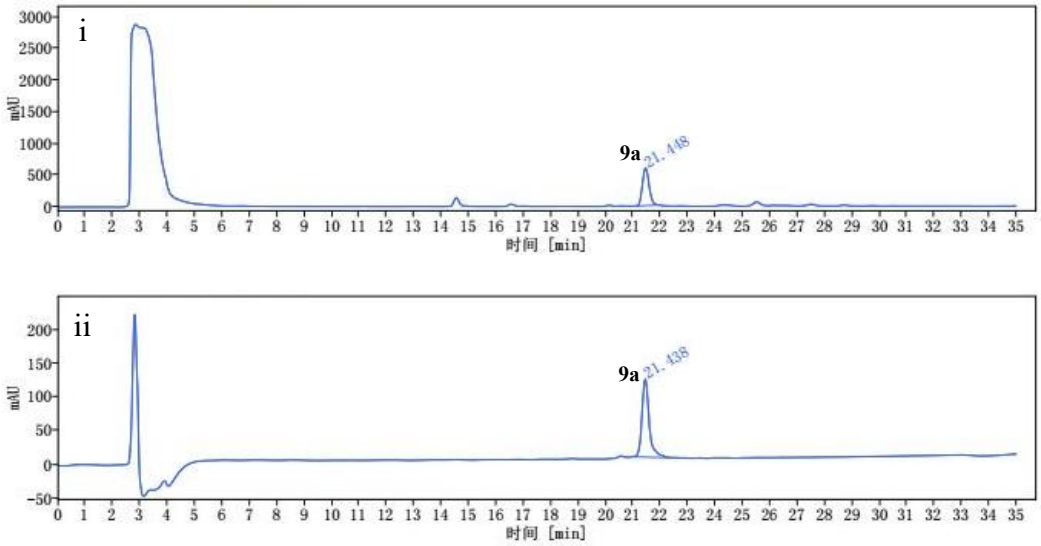

Figure S13. i) HPLC trace of reaction mixture of compound **9a**. ii) HPLC trace of purified compound **9a** [1 mL/min, 10% to 60% MeCN for 30 min, then 60% to 95% MeCN 30-35 min, HPLCONE 10C18A (10 μm, 4.6 x 250 mm), λ = 220 nm].

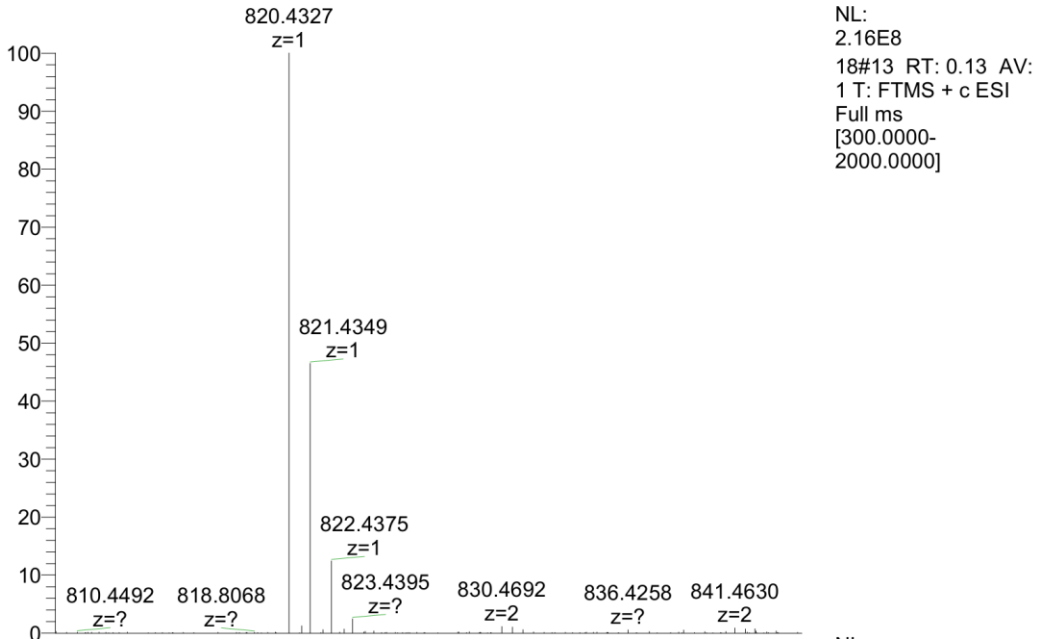

HRMS of compound 9a: Calcd for $[M+Na]^+$ $C_{39}H_{59}N_9O_9Na^+$: 820.4328; found: 820.4327.

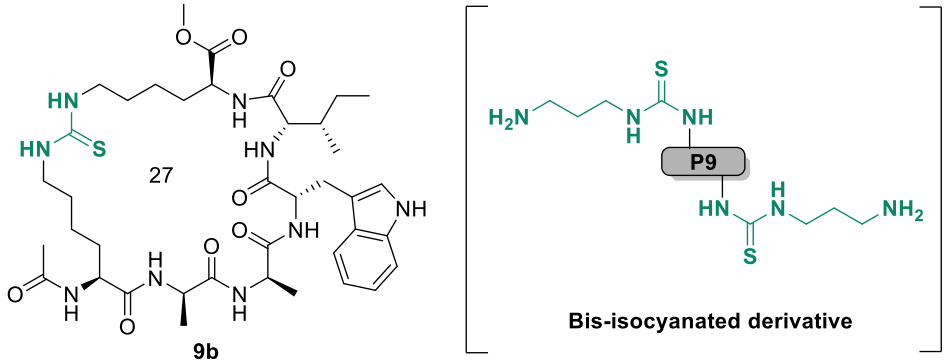

Compound 9b was isolated in 51% yield (4.2 mg, 0.0051 mmol) as a white powder; the HPLC yield was 77% based on absorbance at 250 nm.

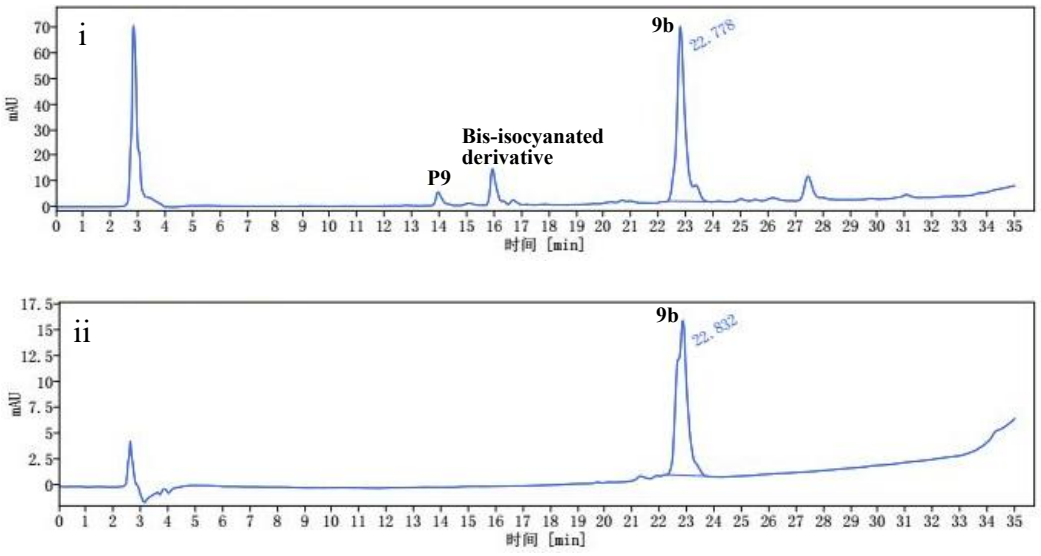

Figure S14. i) HPLC trace of reaction mixture of compound **9b**. ii) HPLC trace of purified compound **9b** [1 mL/min, 10% to 60% MeCN for 30 min, then 60% to 95% MeCN 30-35 min, HPLCONE 10C18A (10 μm, 4.6 x 250 mm), λ = 250 nm].

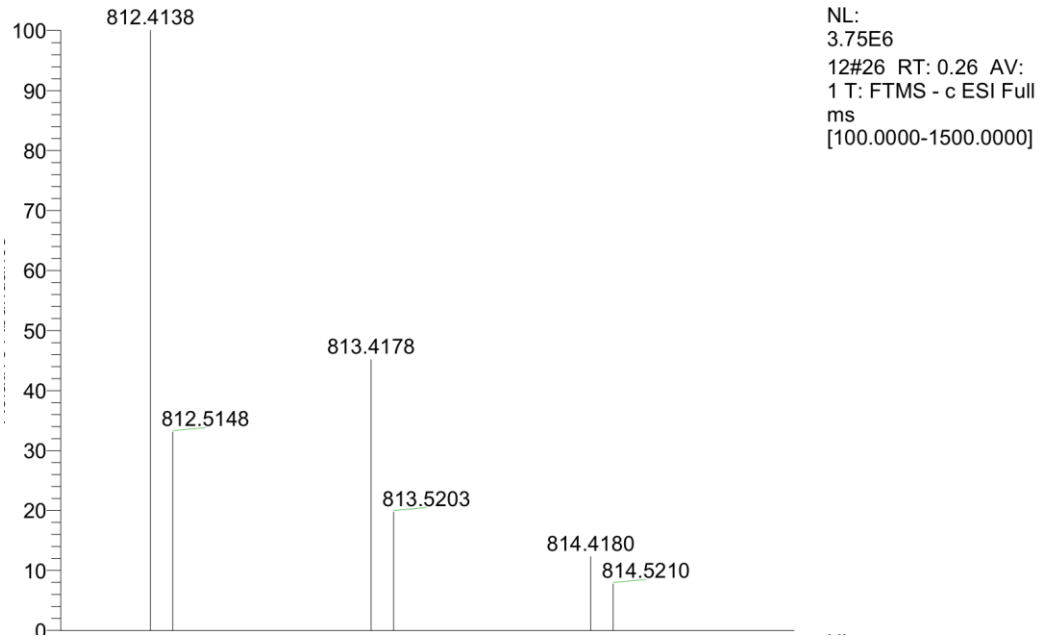

HRMS of compound 9b: Calcd for $[M-H]^-$ $C_{39}H_{58}N_9O_8S^-$: 812.4135; found: 812.4138.

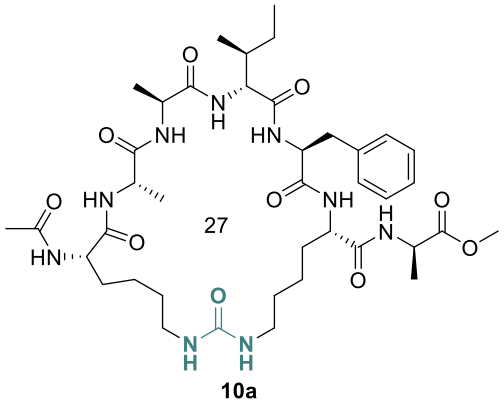

10a

Compound 10a was isolated in 38% yield (3.1 mg, 0.0038 mmol) as a white powder; the HPLC yield was 47% based on absorbance at 220 nm.

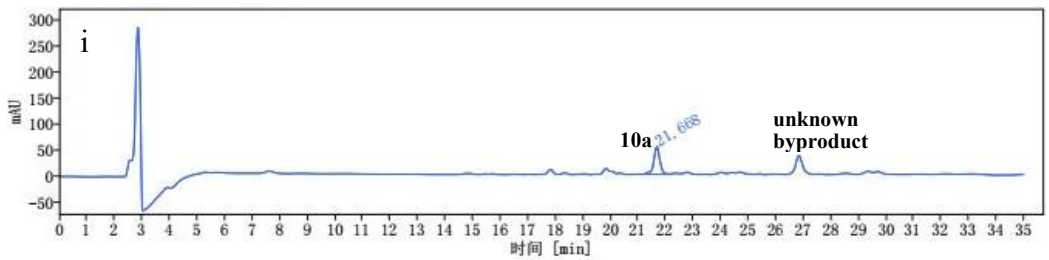

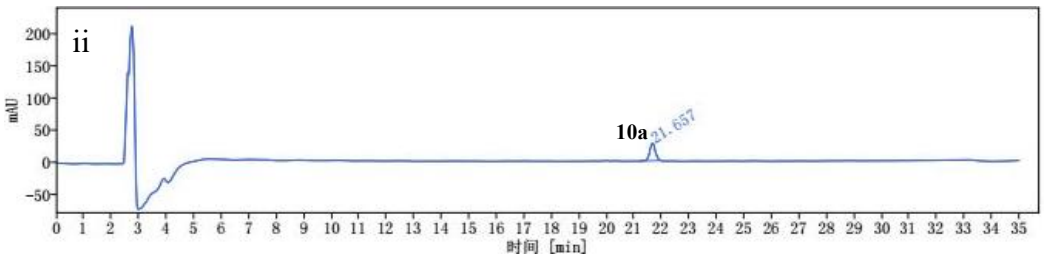

Figure S15. i) HPLC trace of reaction mixture of compound **10a**. ii) HPLC trace of purified compound **10a** [1 mL/min, 10% to 60% MeCN for 30 min, then 60% to 95% MeCN 30-35 min, HPLCONE 10C18A (10 μm, 4.6 x 250 mm), λ = 220 nm].

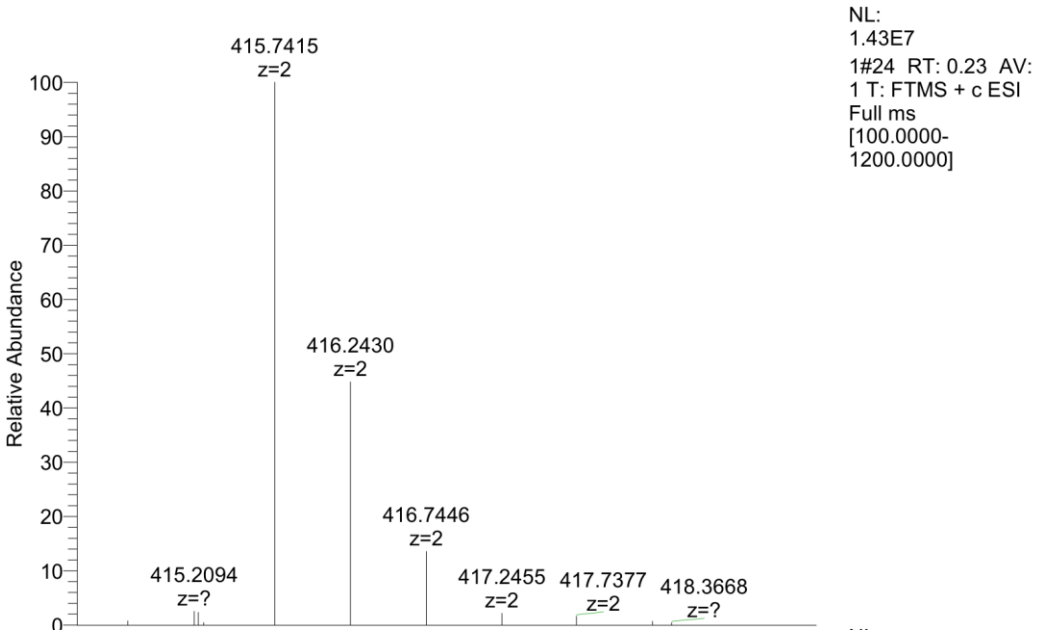

HRMS of compound 10a: Calcd for [(M+2H$^+$)/2] $C_{40}H_{65}N_9O_{10}^{2+}$: 415.7422; found: 415.7415.

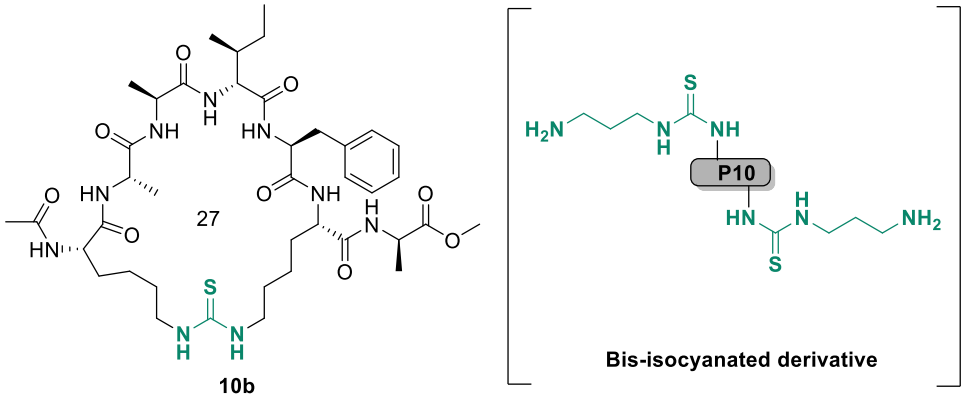

Compound 10b was isolated in 40% yield as (3.4mg, 0.0040 mmol) a white powder; the HPLC yield was 64% based on absorbance at 250 nm.

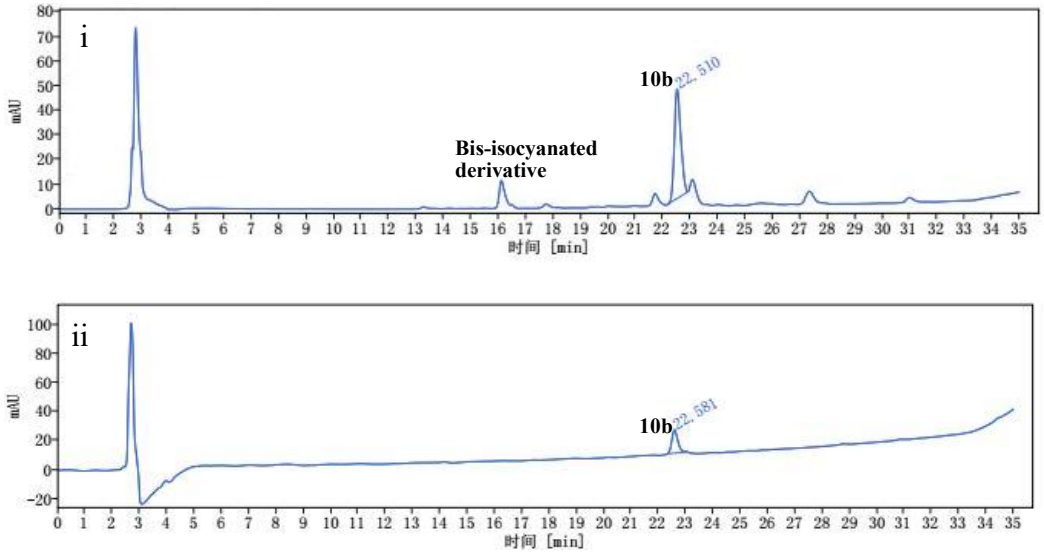

Figure S16. i) HPLC trace of reaction mixture of compound **10b**. ii) HPLC trace of purified compound **10b** [1 mL/min, 10% to 60% MeCN for 30 min, then 60% to 95% MeCN 30-35 min, HPLCONE 10C18A (10 μm, 4.6 x 250 mm), λ = 250 nm].

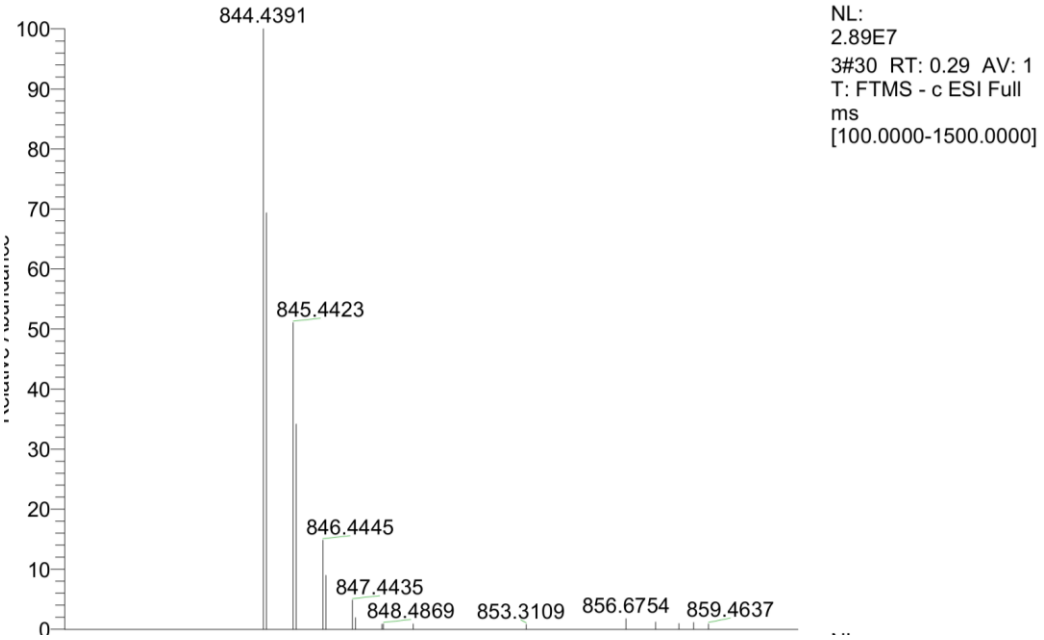

HRMS of compound 10b: Calcd for $[M-H]^-$ $C_{40}H_{62}N_9O_9S^-$: 844.4397; found: 844.4391.

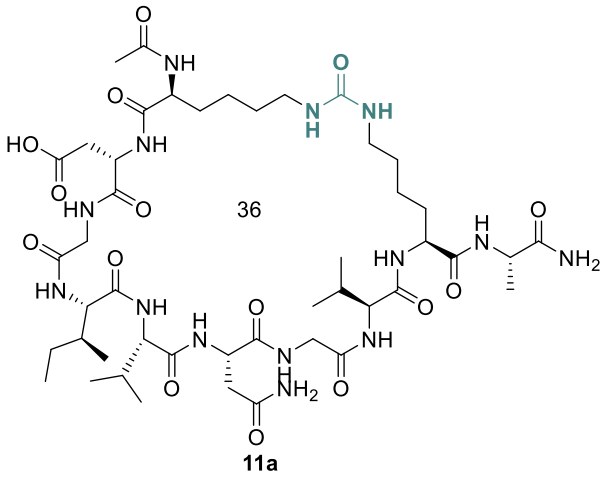

Compound 11a was isolated in 43% yield (4.6 mg, 0.0043 mmol) as a white powder; the HPLC yield was 52% based on absorbance at 220 nm.

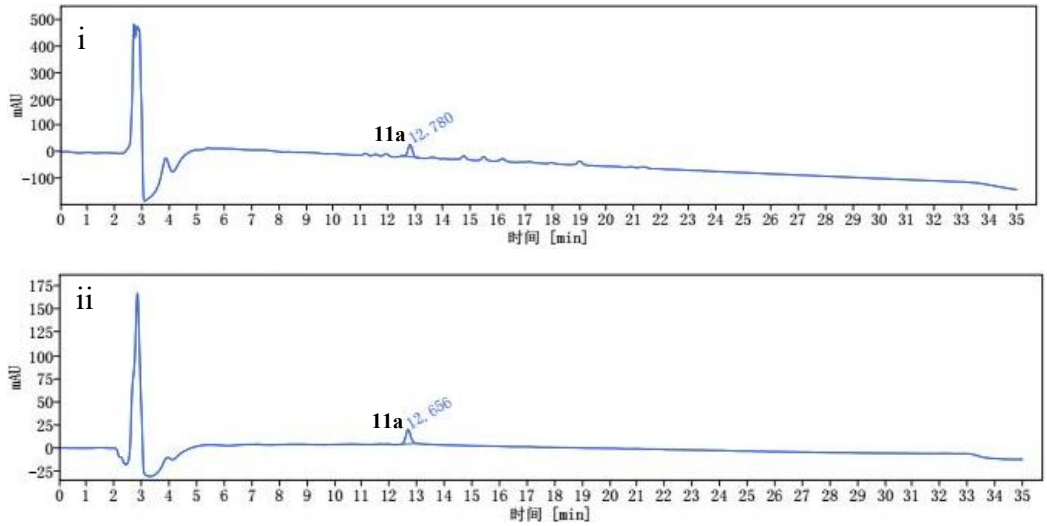

Figure S17. i) HPLC trace of reaction mixture of compound **11a**. ii) HPLC trace of purified compound **11a** [1 mL/min, 10% to 60% MeCN for 30 min, then 60% to 95% MeCN 30-35 min, HPLCONE 10C18A (10 μm, 4.6 x 250 mm), λ = 220 nm].

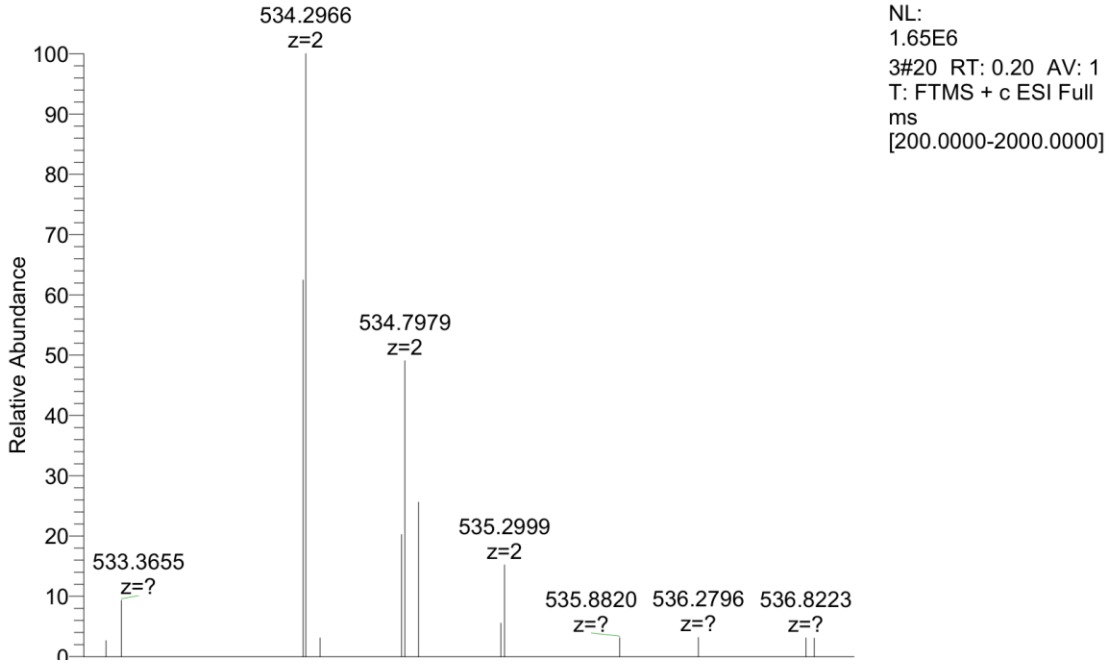

HRMS of compound 11a: Calcd for [(M+2H$^+$)/2] $C_{46}H_{80}N_{14}O_{15}^{2+}$: 534.2958; found: 534.2966.

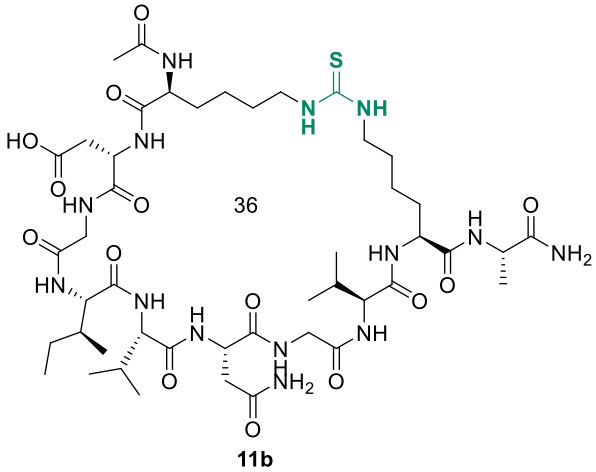

11b

Compound 11b was isolated in 51% yield (5.5 mg, 0.0051 mmol) as a white powder; the HPLC yield was 75% based on absorbance at 240 nm.

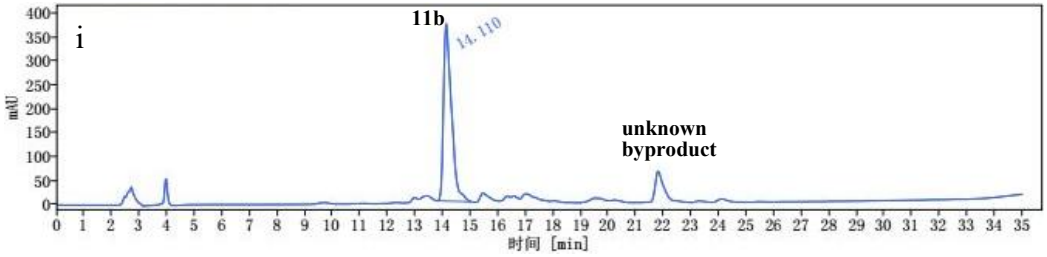

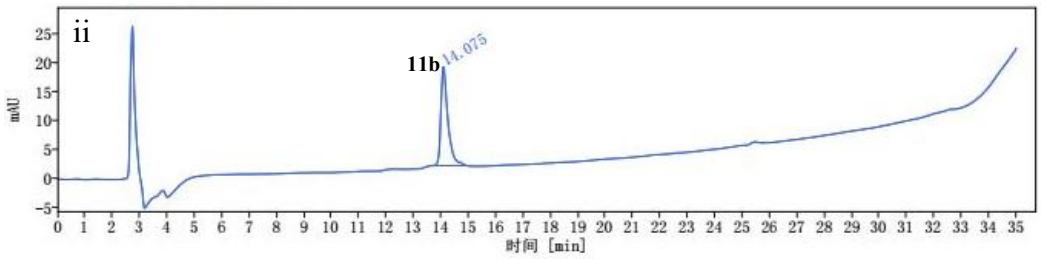

Figure S18. i) HPLC trace of reaction mixture of compound **11b**. ii) HPLC trace of purified compound **11b** [1 mL/min, 10% to 60% MeCN for 30 min, then 60% to 95% MeCN 30-35 min, HPLCONE 10C18A (10 μm, 4.6 x 250 mm), λ = 240 nm].

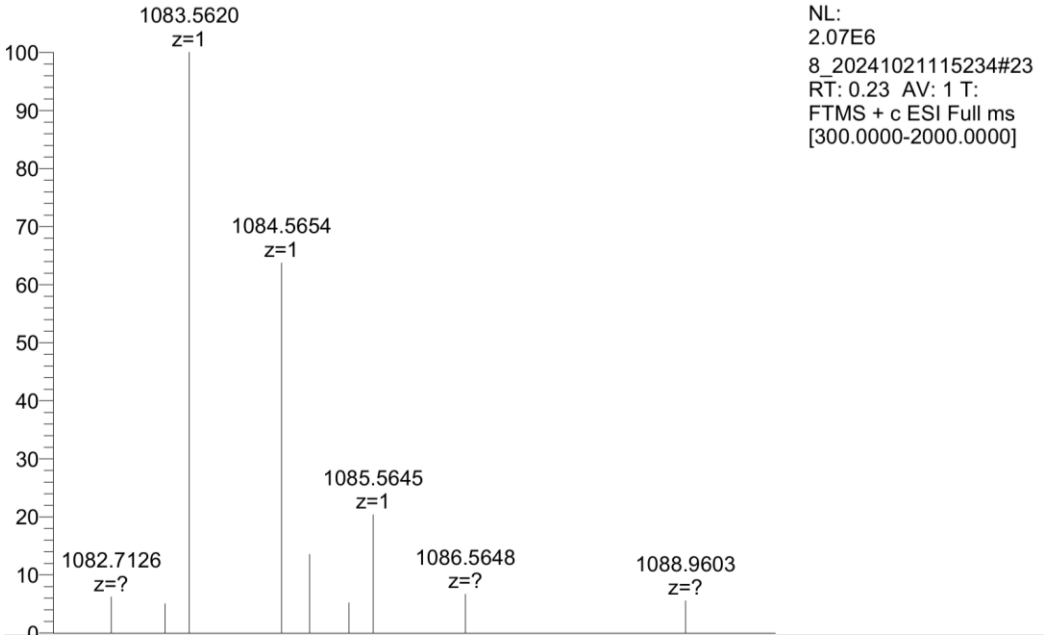

HRMS of compound 11b: Calcd for $[M+H]^+$ $C_{46}H_{79}N_{14}O_{14}S^+$: 1083.5615; found: 1083.5620.

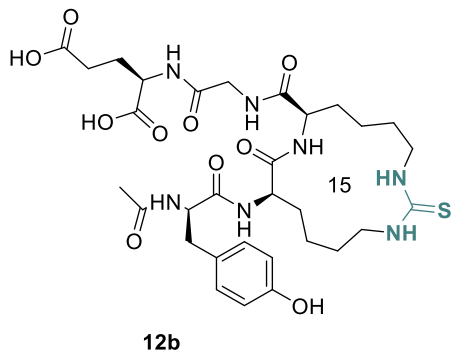

12b

Compound 12b was isolated in 78% yield (5.5 mg, 0.0078 mmol) as a white powder; the HPLC yield was 85% based on absorbance at 220 nm.

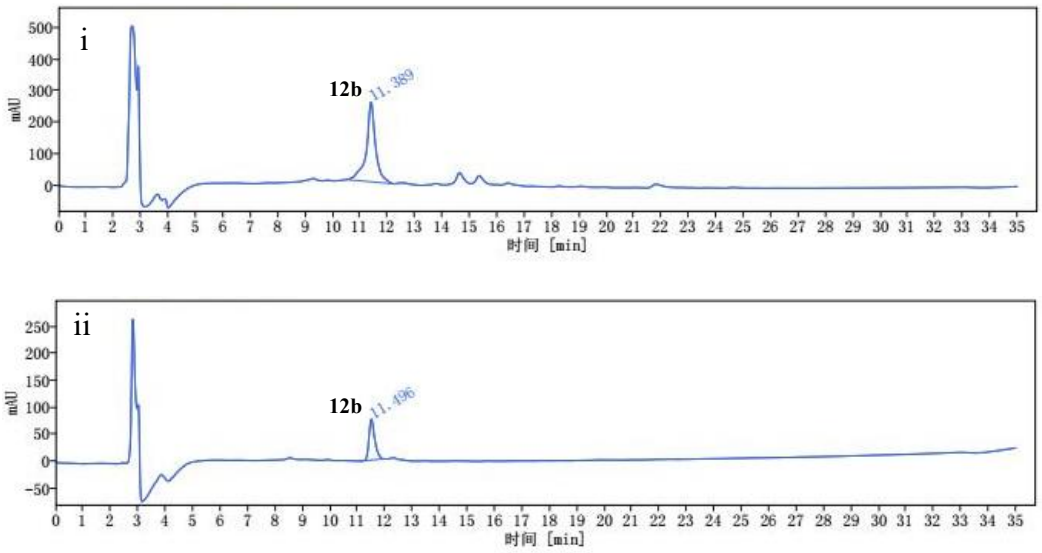

Figure S19. i) HPLC trace of reaction mixture of compound **12b**. ii) HPLC trace of purified compound **12b** [1 mL/min, 10% to 60% MeCN for 30 min, then 60% to 95% MeCN 30-35 min, HPLCONE 10C18A (10 μm, 4.6 x 250 mm), λ = 220 nm].

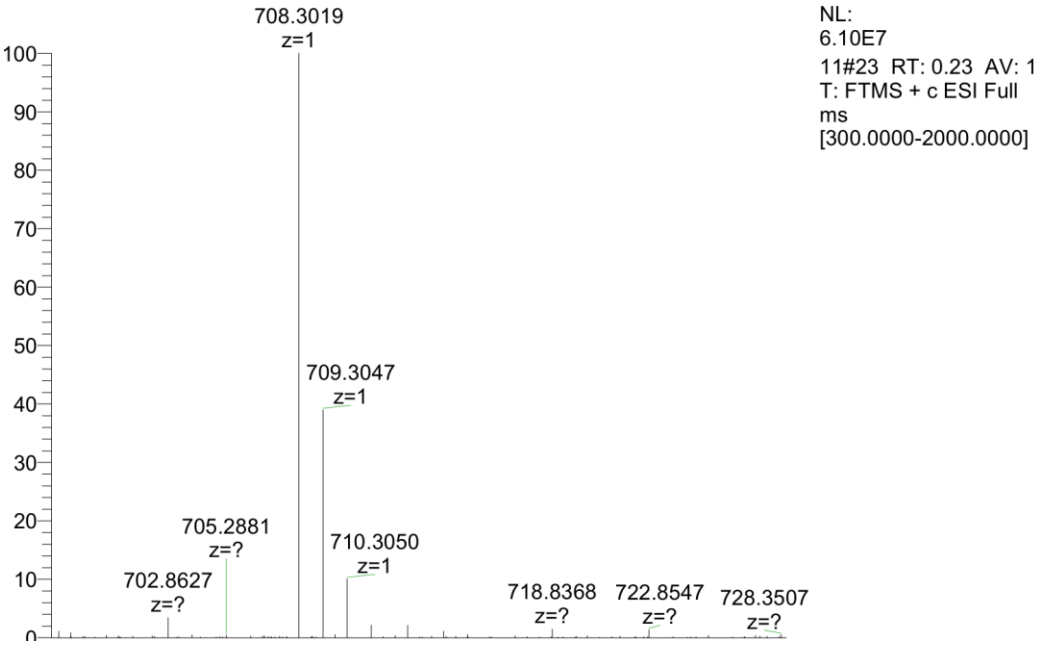

HRMS of compound 12b: Calcd for $[M+H]^+$ $C_{31}H_{46}N_7O_{10}S^+$: 708.3021; found: 708.3019.

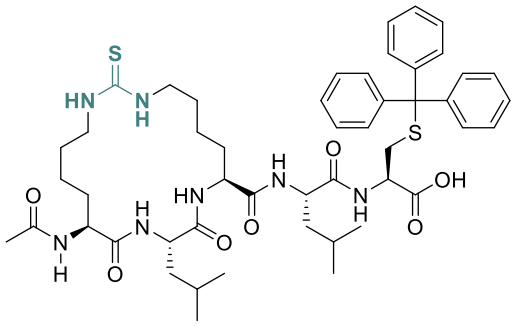

13b

Compound 13b was isolated in 60 % yield (5.6 mg, 0.0060 mmol) as a white powder; the HPLC yield was 63% based on absorbance at 220 nm.

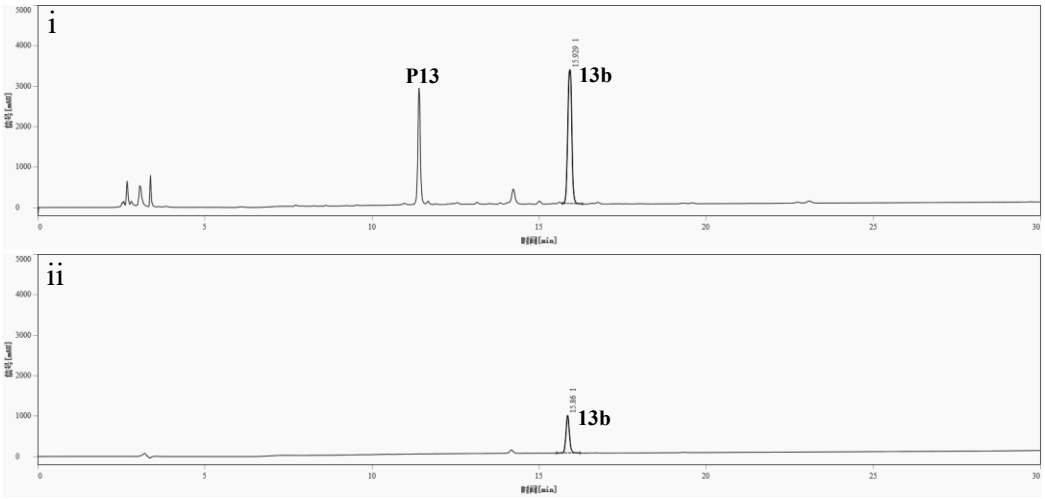

Figure S20. i) HPLC trace of reaction mixture of compound **13b**. ii) HPLC trace of purified compound **13b** [1 mL/min, 10% to 60% MeCN for 8 min, then 60% to 95% MeCN 8-30 min, Supersil ODS2 5µm, E3614696: 4.6mm x 250 mm, λ = 220 nm].

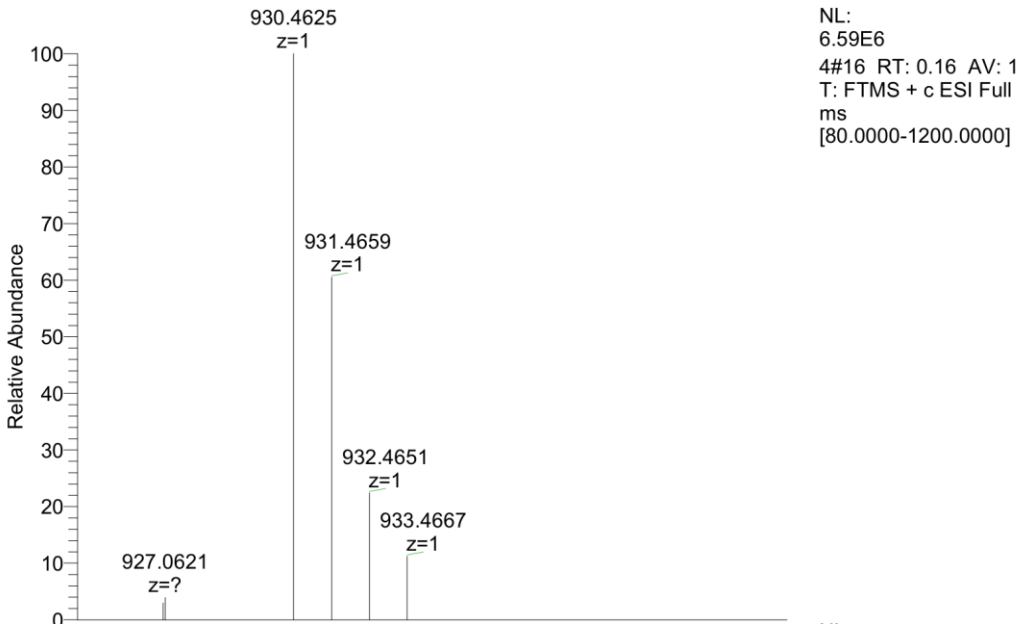

HRMS of compound **13b**: Calcd for $[M+H]^+$ $C_{49}H_{68}N_7O_7S_2^+$: 930.4616; found: 930.4625.

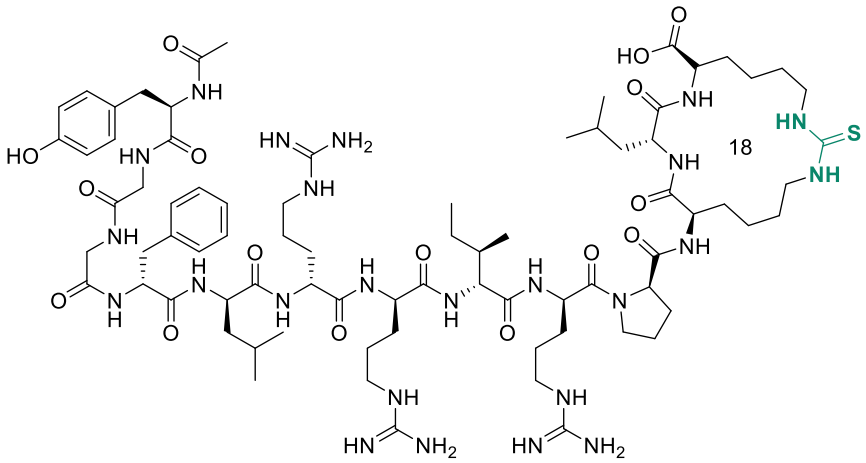

14b

Compound 14b was isolated in 34% yield (5.7 mg, 0.0034 mmol) as a white powder; the HPLC yield was 57% based on absorbance at 220 nm.

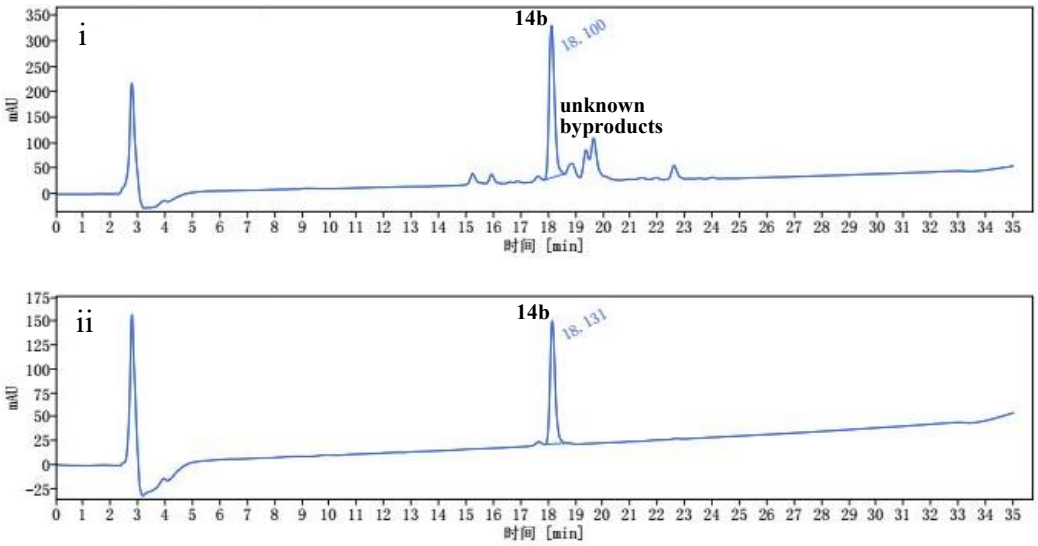

Figure S21. i) HPLC trace of reaction mixture of compound **14b**. ii) HPLC trace of purified compound **14b** [1 mL/min, 10% to 60% MeCN for 30 min, then 60% to 95% MeCN 30-35 min, HPLCONE 10C18A (10 μm, 4.6 x 250 mm), λ = 220 nm].

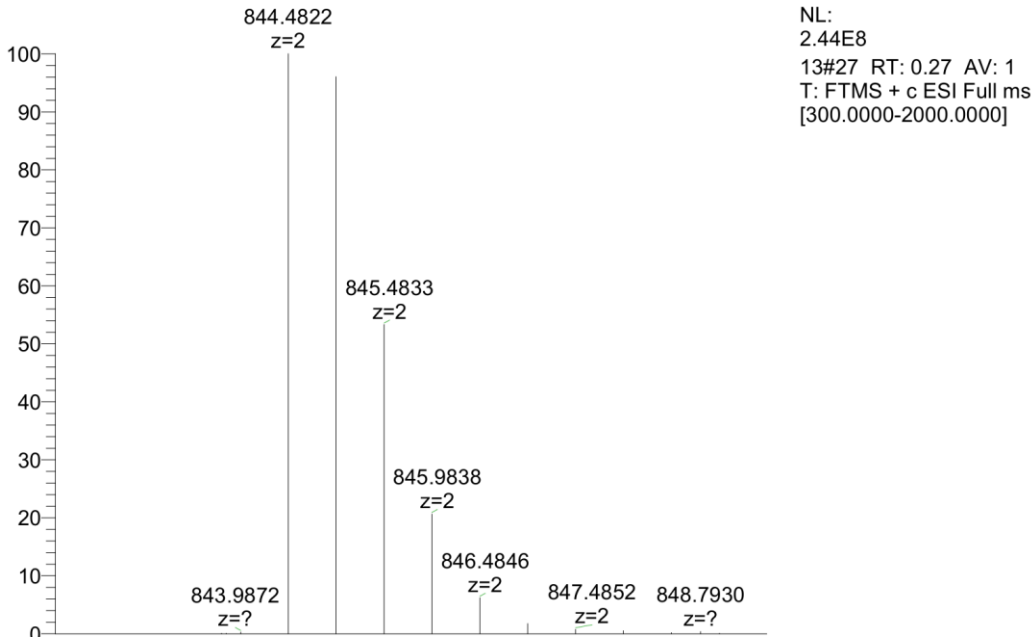

HRMS of compound 14b: Calcd for [(M+2H$^+$)/2] $C_{78}H_{128}N_{24}O_{16}S^{2+}$: 844.4825; found: 844.4822.

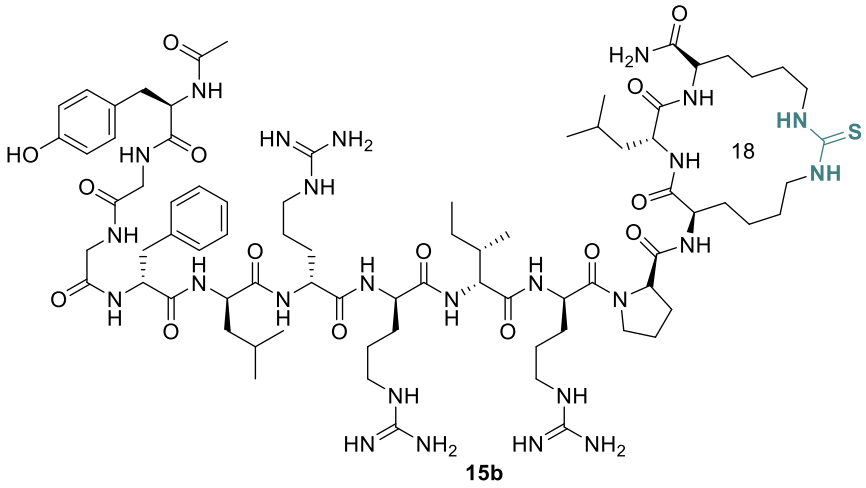

15b

Compound 15b was isolated in 37% yield (6.2 mg, 0.0037 mmol) as a white powder; the HPLC yield was 64% based on absorbance at 220 nm.

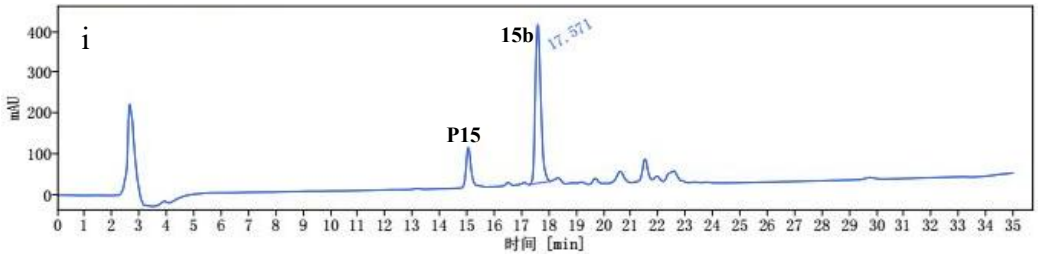

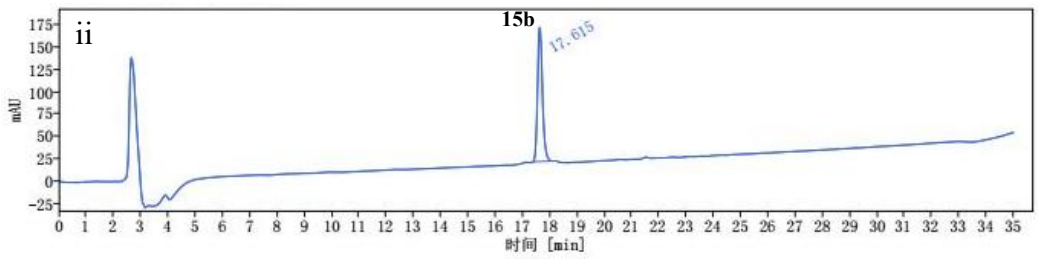

Figure S22. i) HPLC trace of reaction mixture of compound **15b**. ii) HPLC trace of purified compound **15b** [1 mL/min, 10% to 60% MeCN for 30 min, then 60% to 95% MeCN 30-35 min, HPLCONE 10C18A (10 μm, 4.6 x 250 mm), λ = 220 nm].

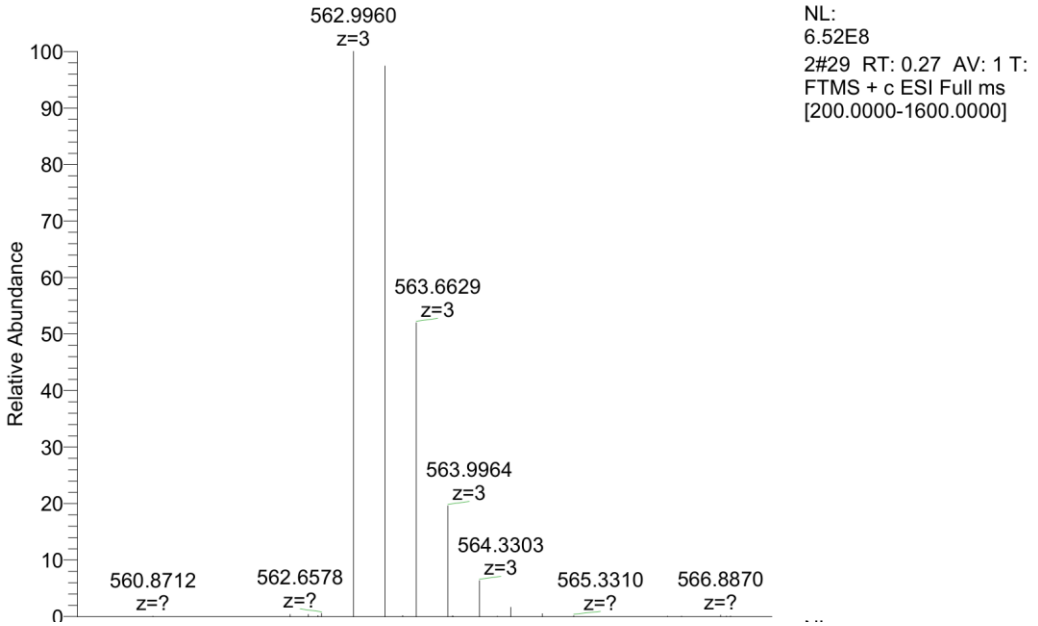

HRMS of compound **15b**: Calcd for $[(M+3H^+)/3]$ $C_{78}H_{130}N_{25}O_{15}S^{3+}$: 562.9961; found:562.9960.

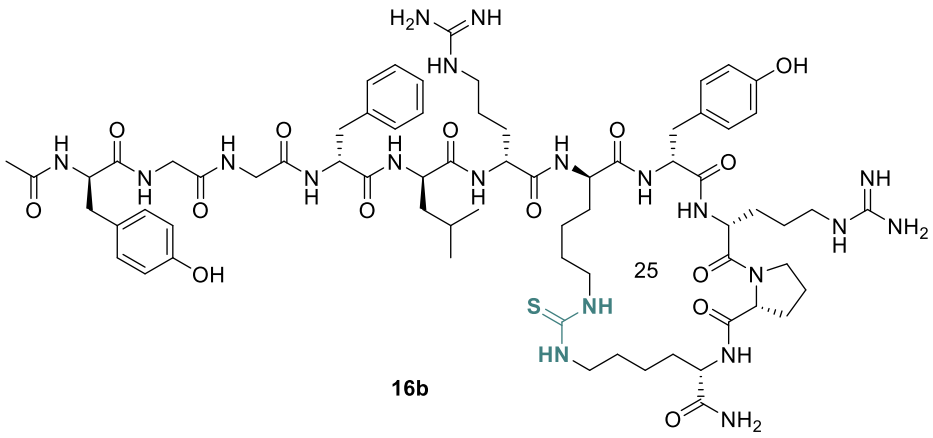

Compound 16b was isolated in 41% yield (6.0 mg, 0.0041 mmol) as a white powder; the HPLC yield was 56% based on absorbance at 220 nm.

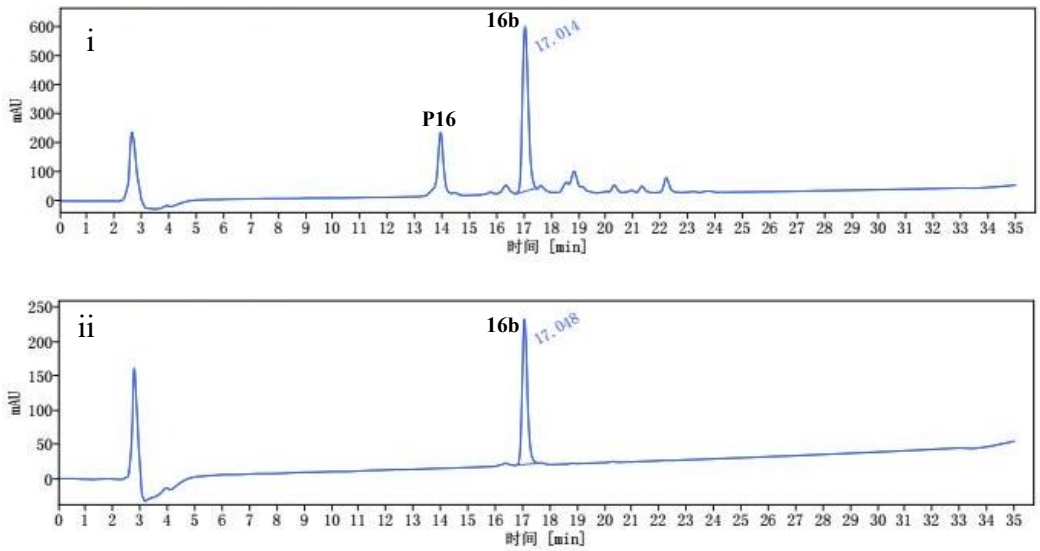

Figure S23. i) HPLC trace of reaction mixture of compound **16b**. ii) HPLC trace of purified compound **16b** [1 mL/min, 10% to 60% MeCN for 30 min, then 60% to 95% MeCN 30-35 min, HPLCONE 10C18A (10 μm, 4.6 x 250 mm), λ = 220 nm].

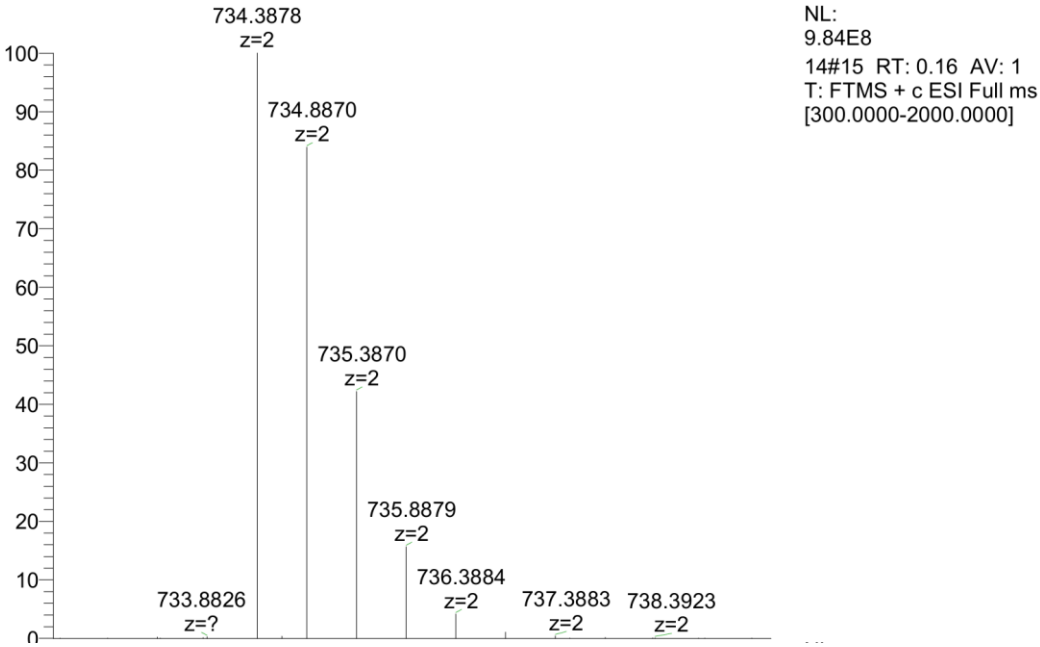

HRMS of compound **16b**: Calcd for $[(M+2H^+)/2]$ $C_{69}H_{104}N_{20}O_{14}S^{2+}$: 734.3875; found: 734.3878.

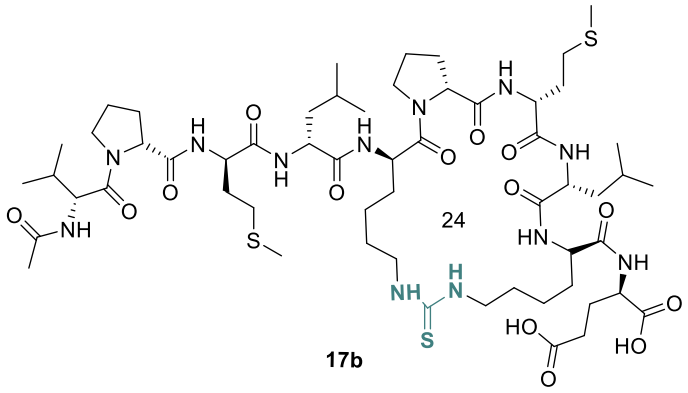

Compound 17b was isolated in 64% yield (8.1 mg, 0.0064 mmol) as a white powder; the HPLC yield was 75% based on absorbance at 240 nm.

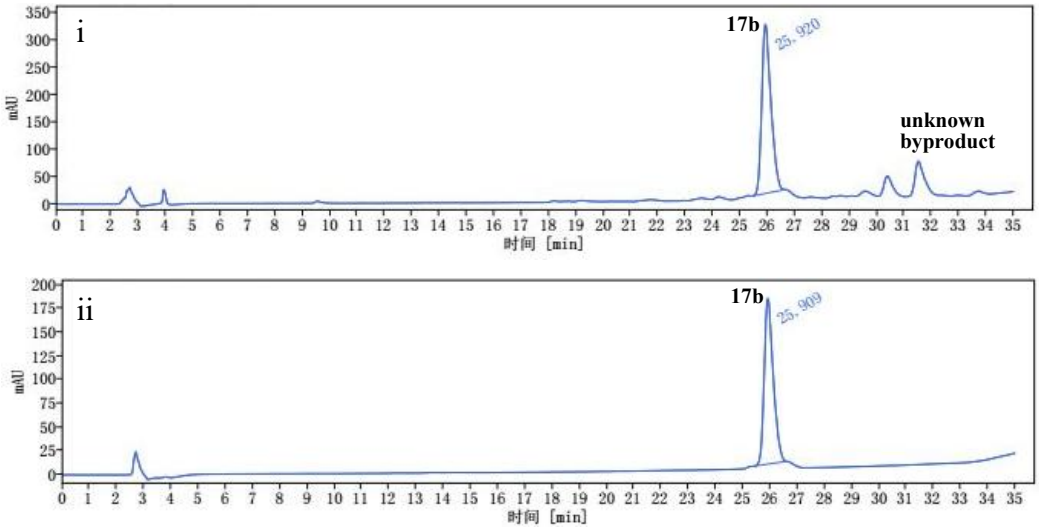

Figure S24. i) HPLC trace of reaction mixture of compound **17b**. ii) HPLC trace of purified compound **17b** [1 mL/min, 10% to 60% MeCN for 30 min, then 60% to 95% MeCN 30-35 min, HPLCONE 10C18A (10 μm, 4.6 x 250 mm), λ = 240 nm].

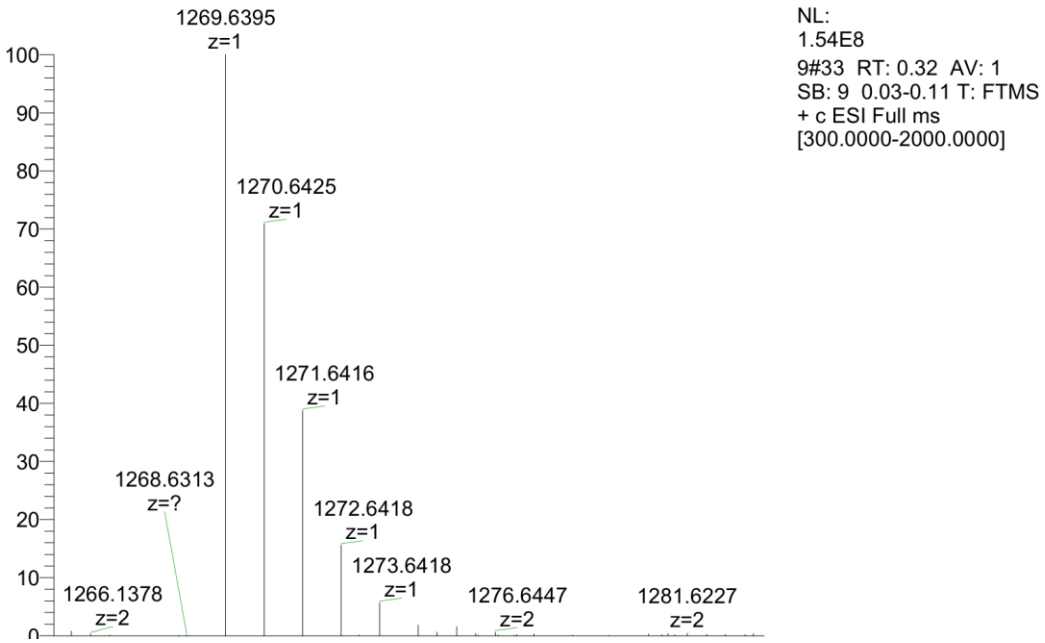

HRMS of compound **17b**: Calcd for $[M+H]^+$ $C_{57}H_{97}N_{12}O_{14}S_3^+$: 1269.6404; found: 1269.6395.

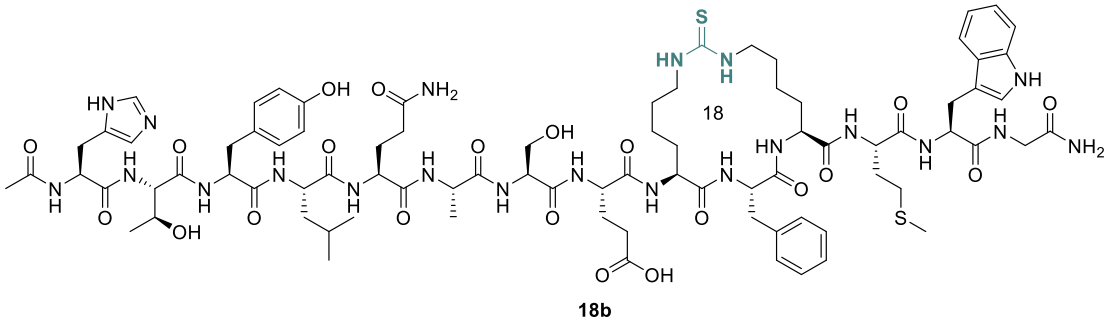

18b

Compound 18b was isolated in 42% yield (7.6 mg, 0.0042 mmol) as a white powder; the HPLC yield was 70% based on absorbance at 250 nm.

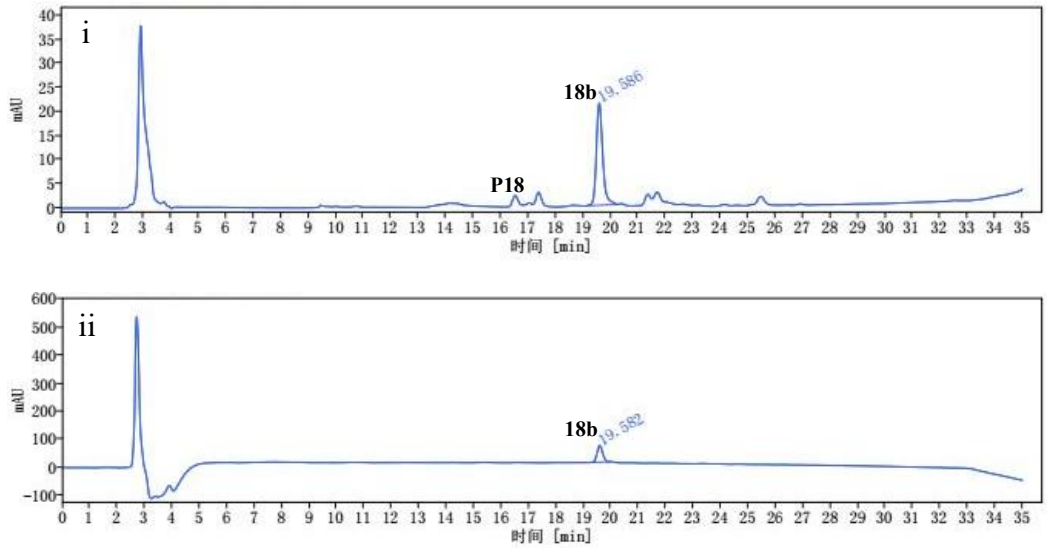

Figure S25. i) HPLC trace of reaction mixture of compound **18b**. ii) HPLC trace of purified compound **18b** [1 mL/min, 10% to 60% MeCN for 30 min, then 60% to 95% MeCN 30-35 min, HPLCONE 10C18A (10 µm, 4.6 x 250 mm), λ = 250 nm].

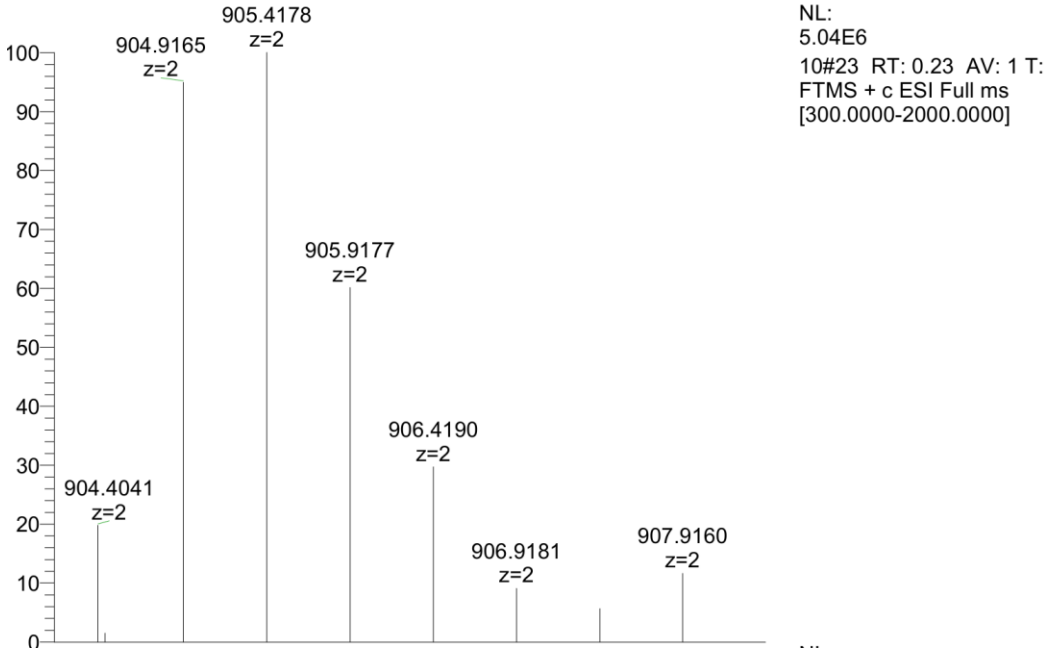

HRMS of compound **18b**: Calcd for [(M+2H$^+$)/2] $C_{83}H_{119}N_{21}O_{21}S_2^{2+}$: 904.9160; found: 904.9165.

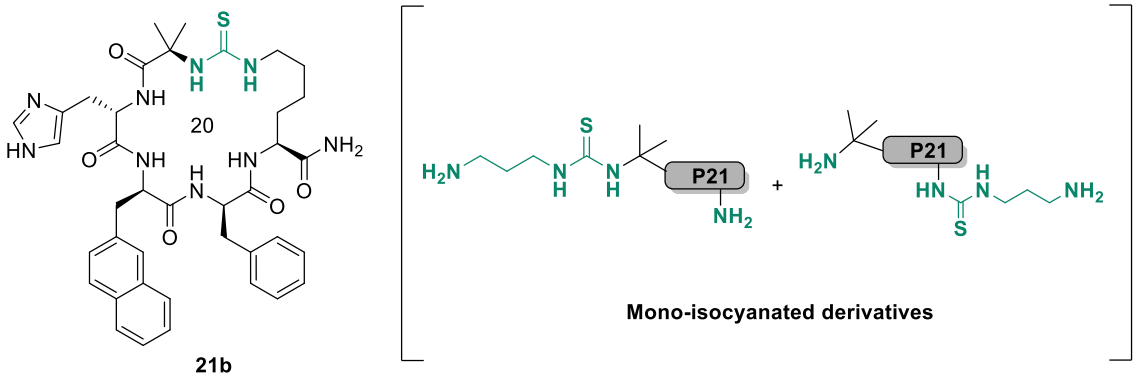

Compound 21b was isolated in 57% yield (4.3 mg, 0.0057 mmol) as a white powder; the HPLC yield was 63% based on absorbance at 270 nm.

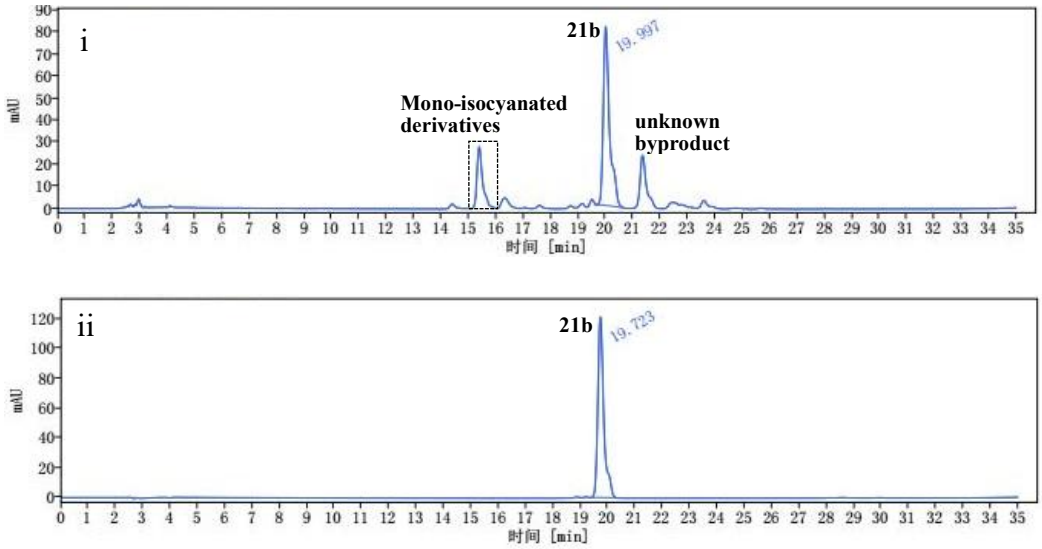

Figure S26. i) HPLC trace of reaction mixture of compound **21b**. ii) HPLC trace of purified compound **21b** [1 mL/min, 10% to 60% MeCN for 30 min, then 60% to 95% MeCN 30-35 min, HPLCONE 10C18A (10 μm, 4.6 x 250 mm), λ = 270 nm].

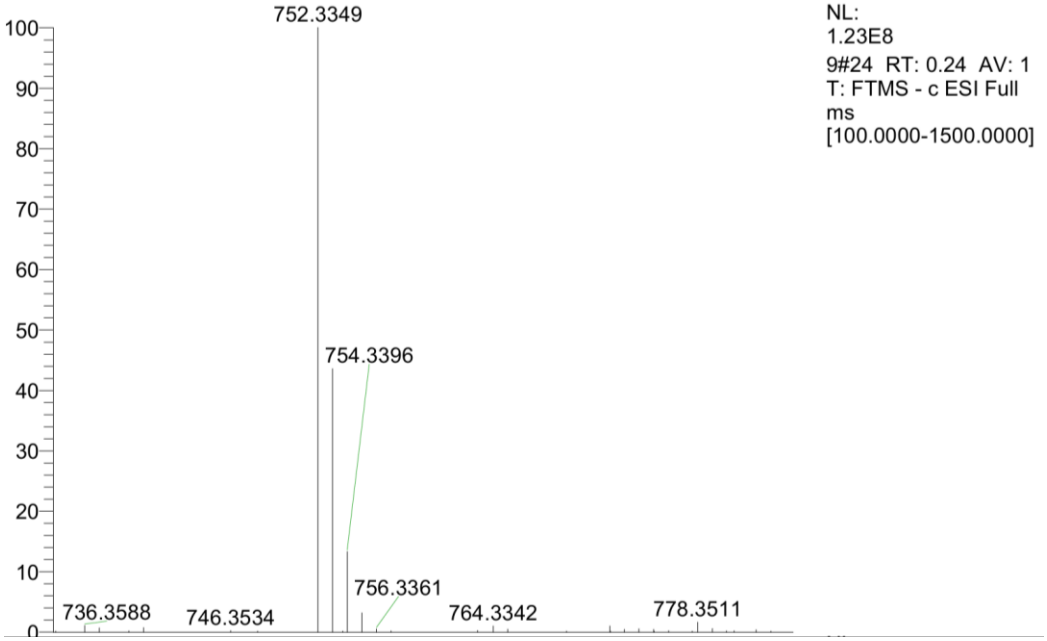

HRMS of compound 21b: Calcd for $[M-H]^-$ $C_{39}H_{46}N_9O_5S^-$:752.3348; found: 752.3349.

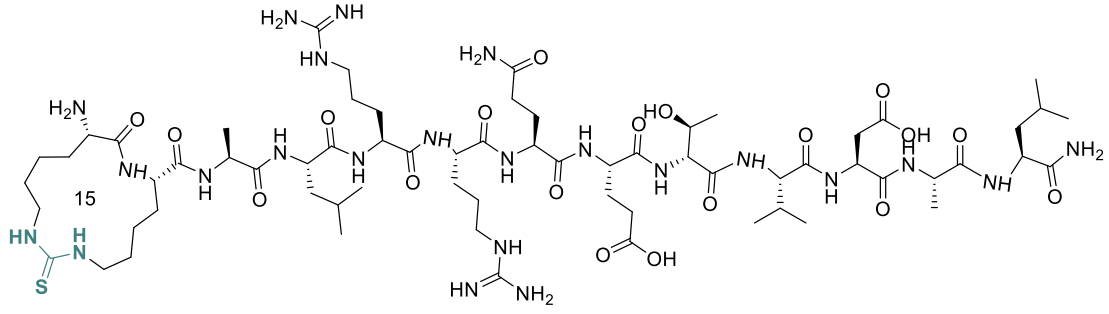

22b

Compound 22b was isolated in 40 % yield (6.3 mg, 0.0040 mmol) as a white powder; the HPLC yield was 63% based on absorbance at 250 nm.

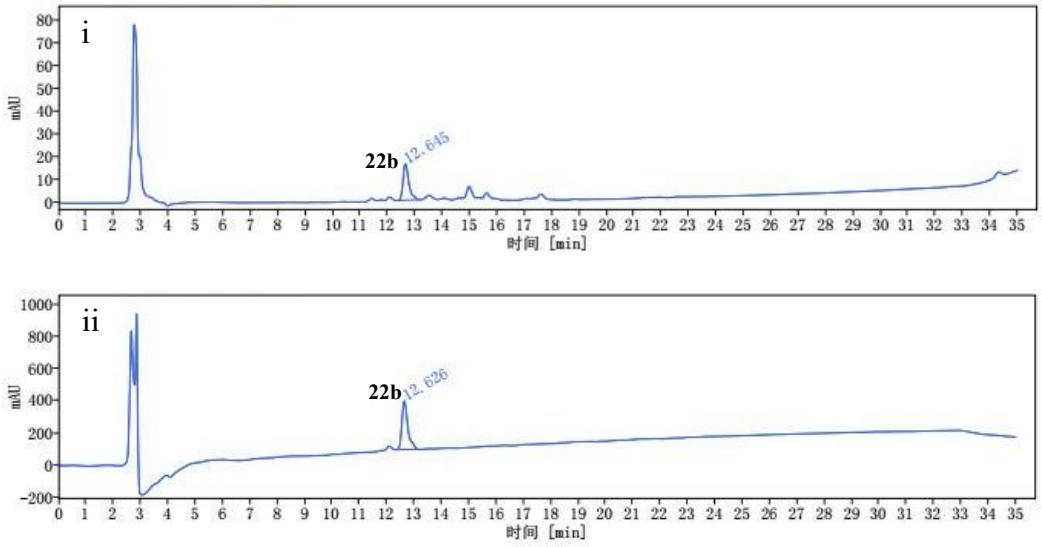

Figure S27. i) HPLC trace of reaction mixture of compound **22b**. ii) HPLC trace of purified compound **22b** [1 mL/min, 10% to 60% MeCN for 30 min, then 60% to 95% MeCN 30-35 min, HPLCONE 10C18A (10 μm, 4.6 x 250 mm), λ = 250 nm].

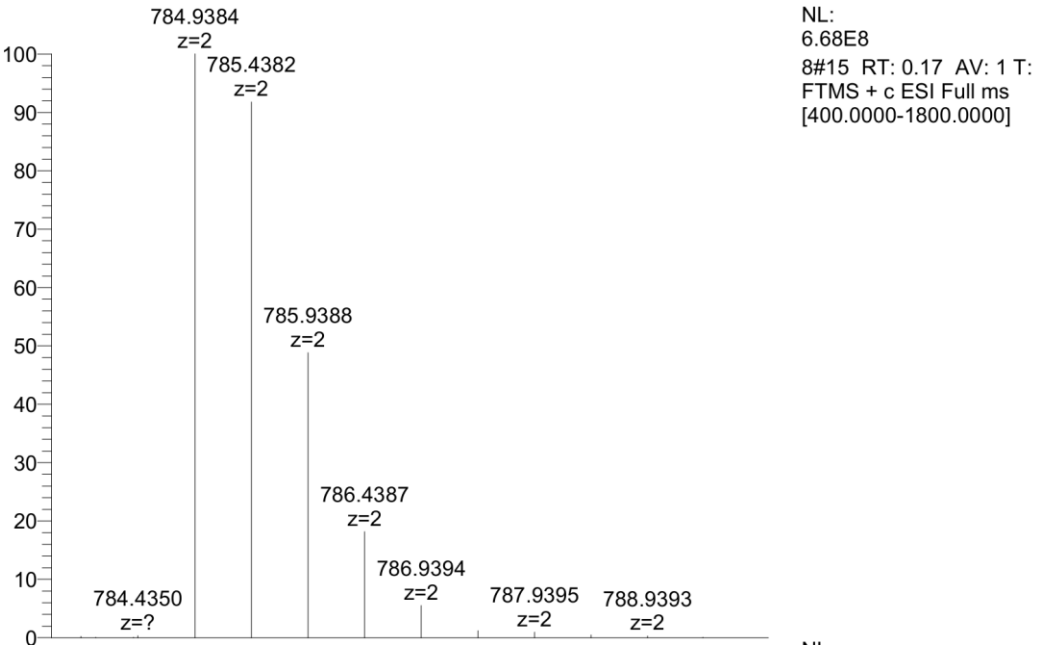

HRMS of compound **22b**: Calcd for $[(M+2H^+)/2]$ $C_{66}H_{119}N_{23}O_{19}S^{2+}$: 784.9381; found: 784.9384.

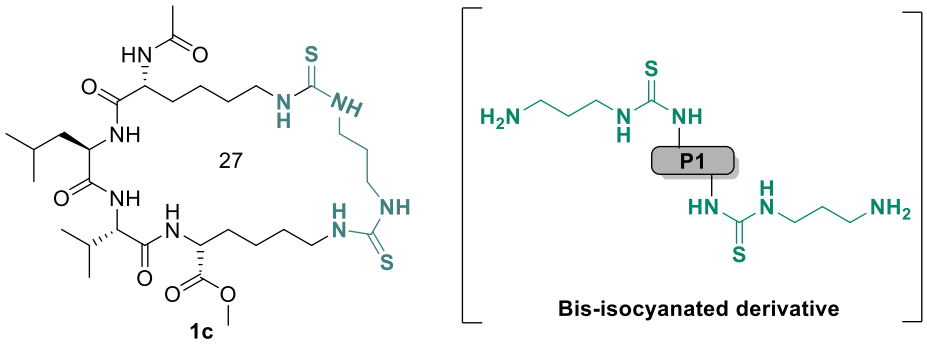

Compound 1c was isolated in 25% yield (1.7 mg, 0.0025 mmol) as a white powder; the HPLC yield was 28% based on absorbance at 220 nm.

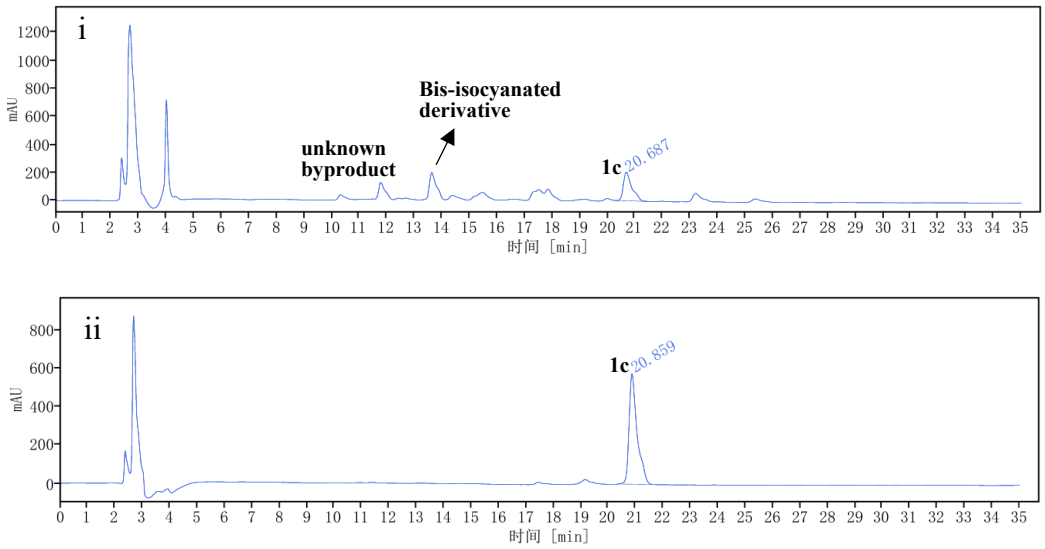

Figure S28. i) HPLC trace of reaction mixture of compound **1c**. ii) HPLC trace of purified compound **1c** [1 mL/min, 10% to 60% MeCN for 30 min, then 60% to 95% MeCN 30-35 min, HPLCONE 10C18A (10 μm, 4.6 x 250 mm), λ = 220 nm].

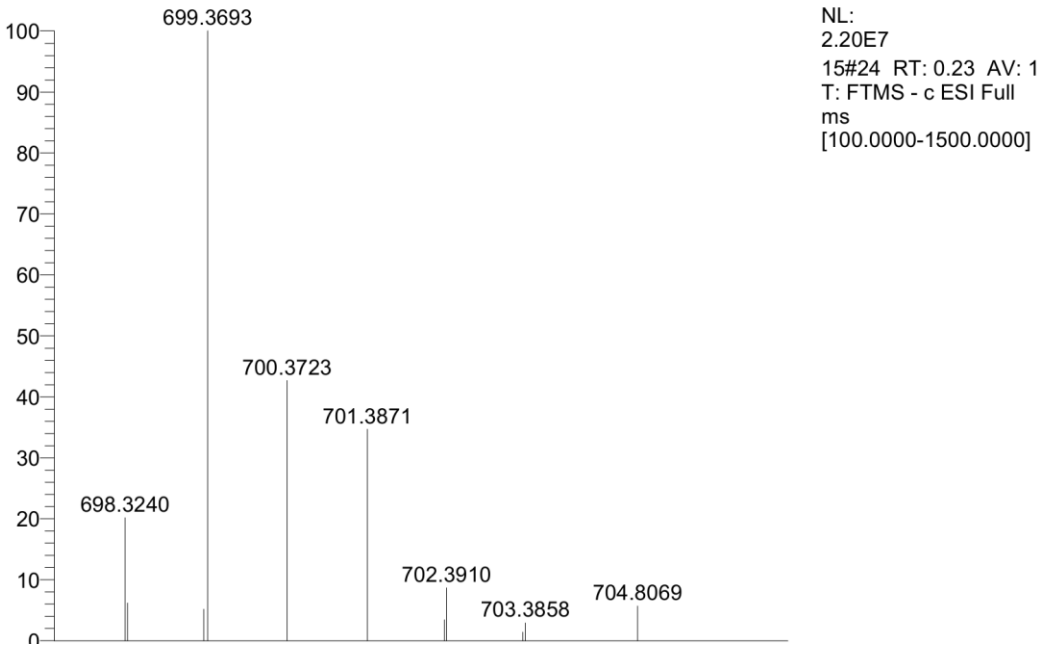

HRMS of compound 1c: Calcd for $[M-H]^-$ $C_{31}H_{55}N_8O_6S_2^-$: 699.3691; found: 699.3693.

D. Characterization of macrocyclic bioactive peptides

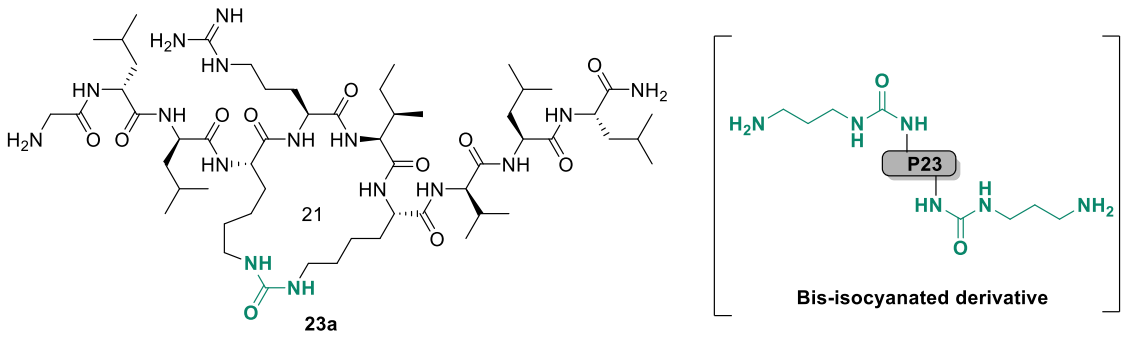

Compound 23a was isolated in 33% yield (3.9 mg, 0.0033 mmol) as a white powder; the HPLC yield was 41% based on absorbance at 210 nm.

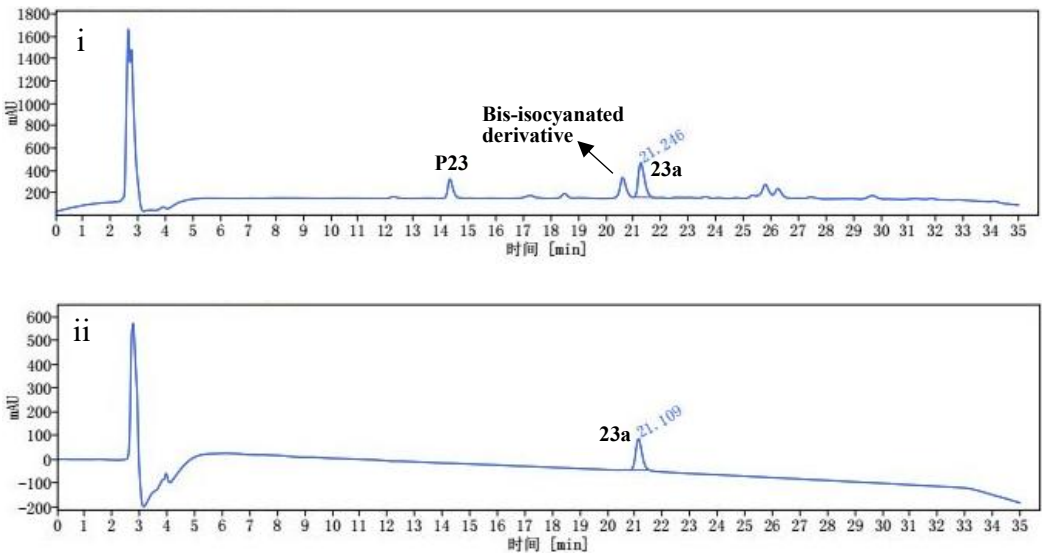

Figure S29. i) HPLC trace of reaction mixture of compound **23a**. ii) HPLC trace of purified compound **23a** [1 mL/min, 10% to 60% MeCN for 30 min, then 60% to 95% MeCN 30-35 min, HPLCONE 10C18A (10 μm, 4.6 x 250 mm), λ = 210 nm].

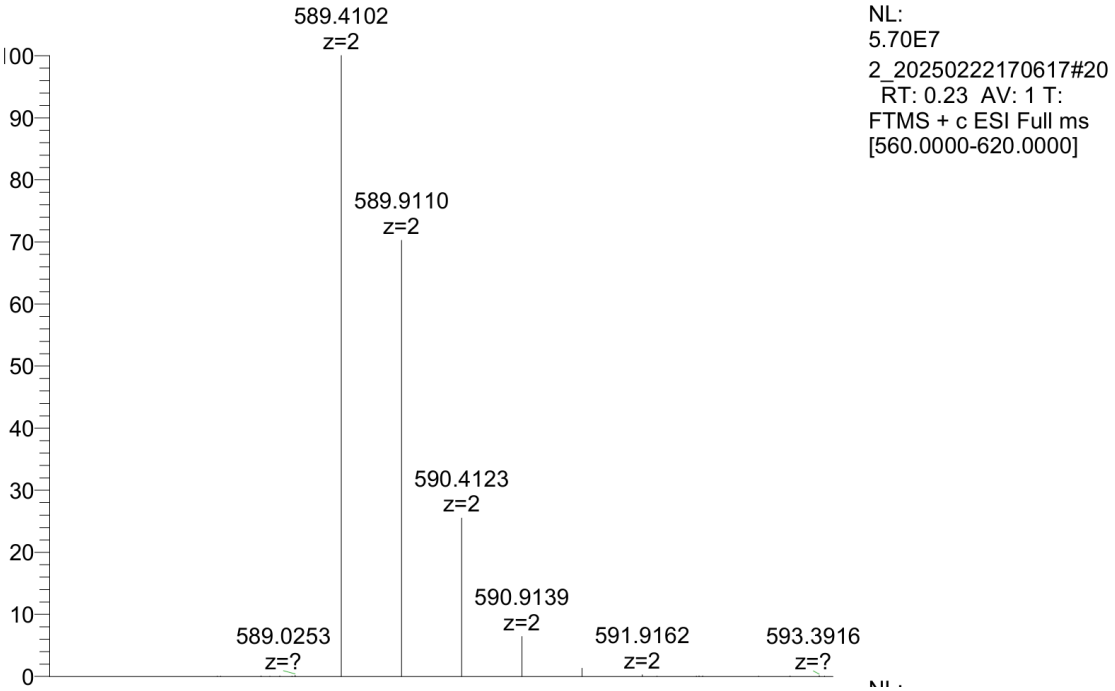

HRMS of compound **23a**: Calcd for [(M+2H$^+$)/2] $C_{56}H_{106}N_{16}O_{11}^{2+}$: 589.4108; found: 589.4102.

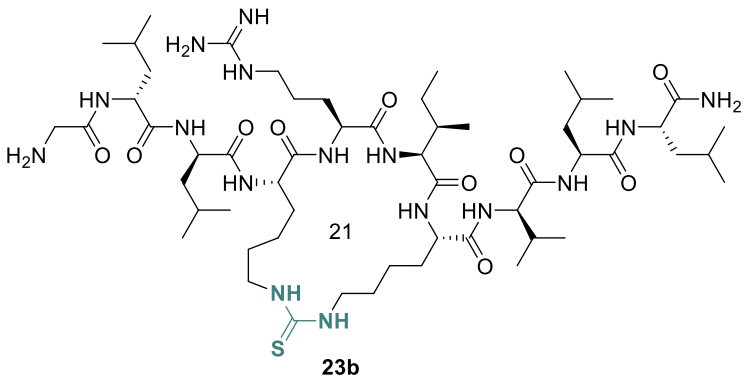

Compound 23b was isolated in 57% yield (6.8 mg, 0.0057 mmol) as a white powder; the HPLC yield was 79% based on absorbance at 240 nm.

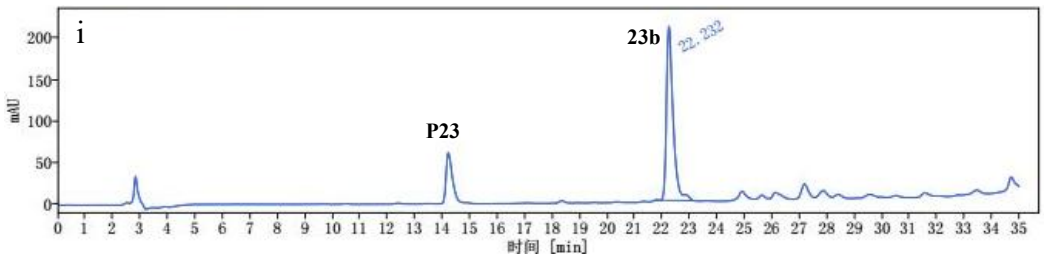

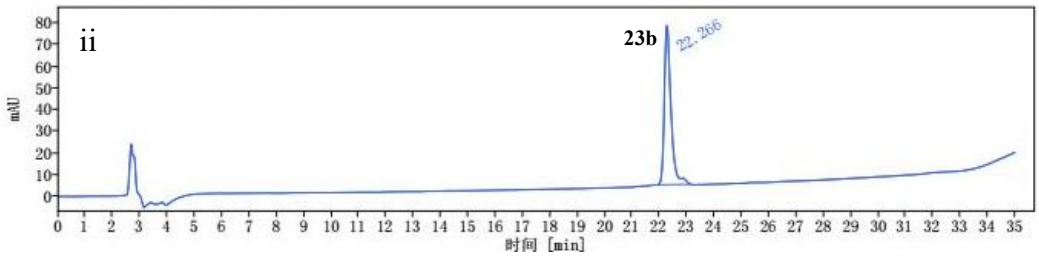

Figure S30. i) HPLC trace of reaction mixture of compound **23b**. ii) HPLC trace of purified compound **23b** [1 mL/min, 10% to 60% MeCN for 30 min, then 60% to 95% MeCN 30-35 min, HPLCONE 10C18A (10 μm, 4.6 x 250 mm), λ = 240 nm].

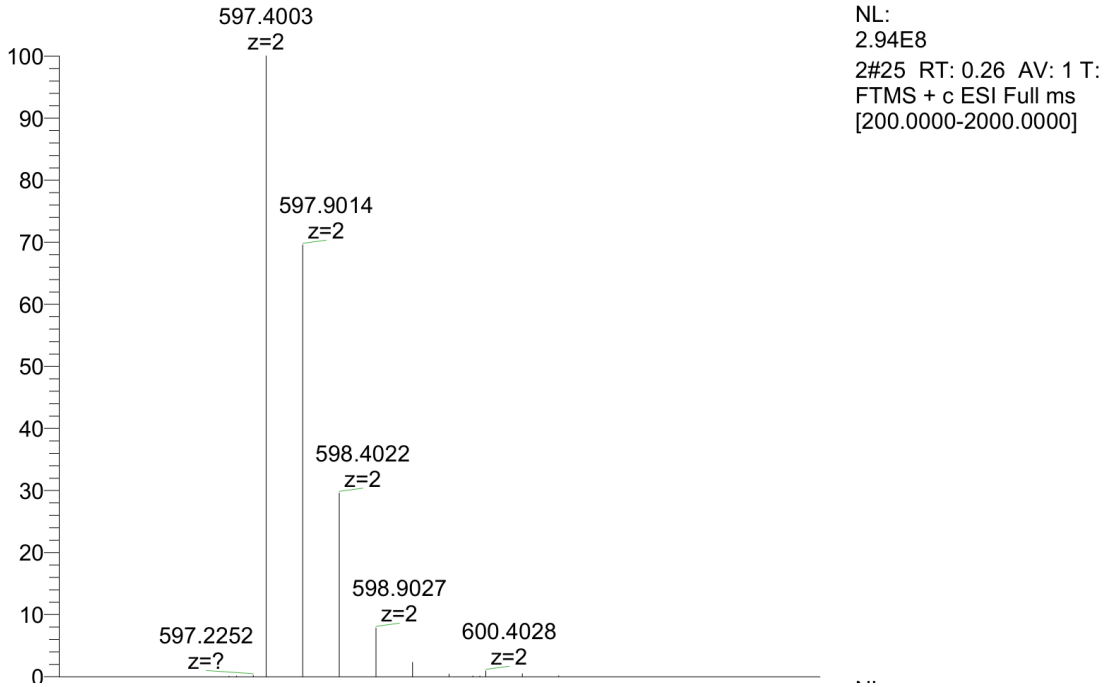

HRMS of compound **23b**: Calcd for $[(M+2H^+)/2]$ $C_{56}H_{106}N_{16}O_{10}S^{2+}$: 597.3994; found: 597.4003.

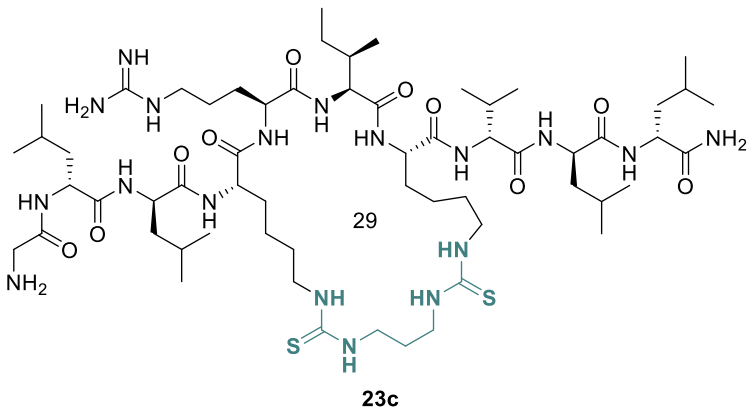

23c

Compound 23c was isolated in 13% yield (1.7 mg, 0.0013 mmol) as a white powder; the HPLC yield was 20% based on absorbance at 220 nm.

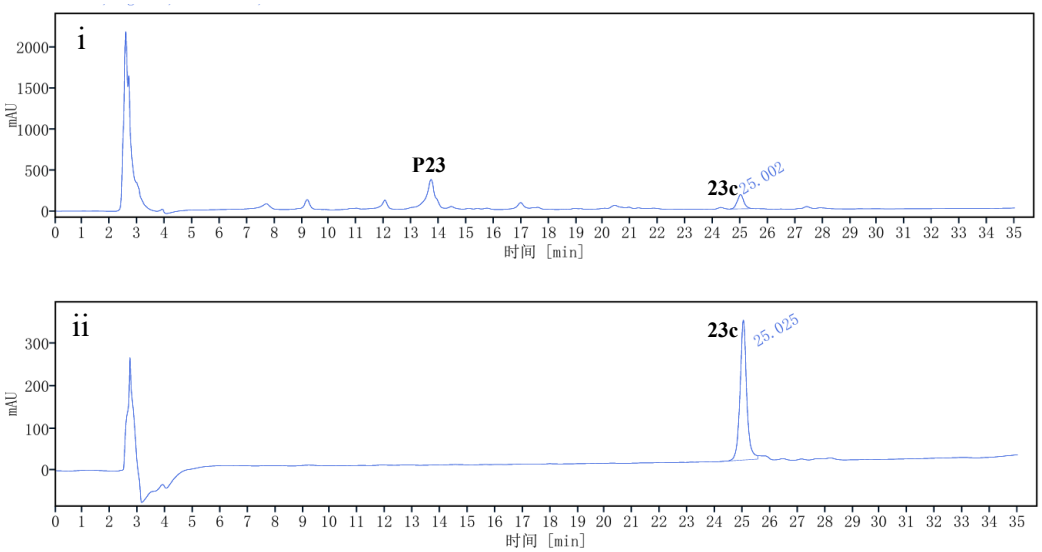

Figure S31. i) HPLC trace of reaction mixture of compound **23c**. ii) HPLC trace of purified compound **23c** [1 mL/min, 10% to 60% MeCN for 30 min, then 60% to 95% MeCN 30-35 min, HPLCONE 10C18A (10 μm, 4.6 x 250 mm), λ = 220 nm].

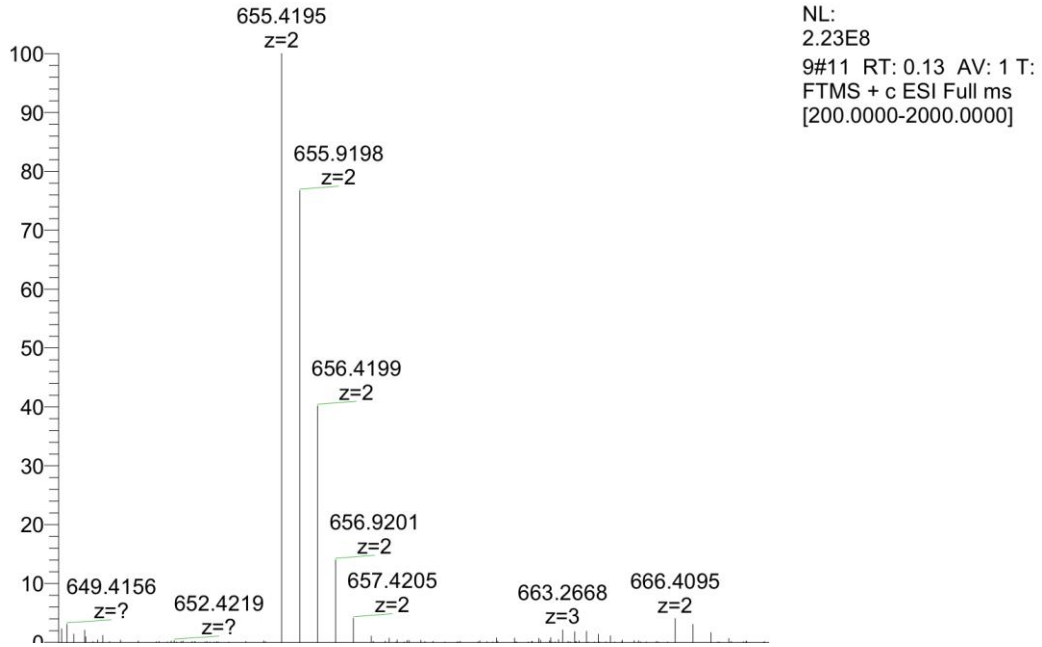

HRMS of compound **23c**: Calcd for [(M+2H$^+$)/2] $C_{60}H_{114}N_{18}O_{10}S_2^{2+}$: 655.4198; found: 655.4195.

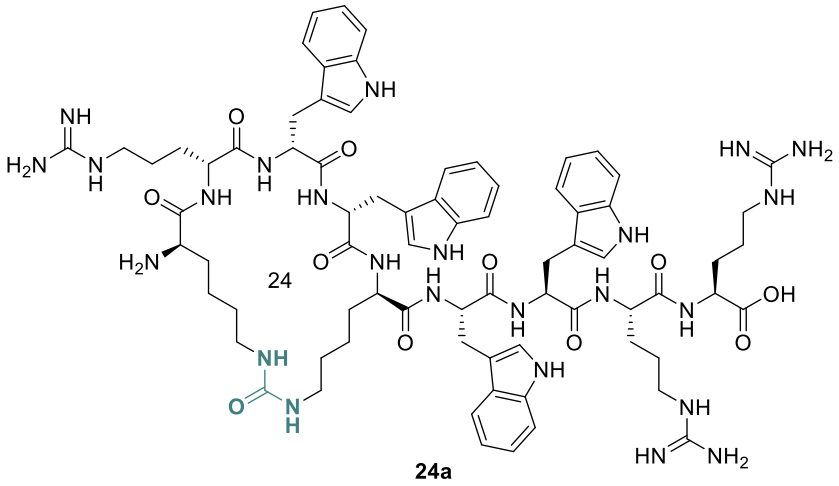

24a

Compound 24a was isolated in 27% yield (4.1 mg, 0.0027 mmol) as a white powder; the HPLC yield was 32% based on absorbance at 250 nm.

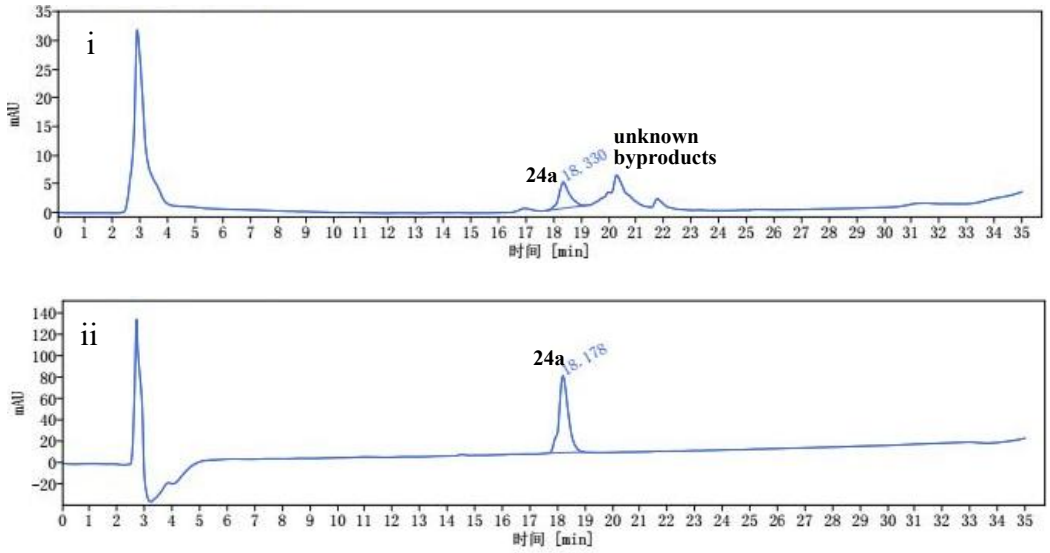

Figure S32. i) HPLC trace of reaction mixture of compound **24a**. ii) HPLC trace of purified compound **24a** [1 mL/min, 10% to 60% MeCN for 30 min, then 60% to 95% MeCN 30-35 min, HPLCONE 10C18A (10 μm, 4.6 x 250 mm), λ = 250 nm].

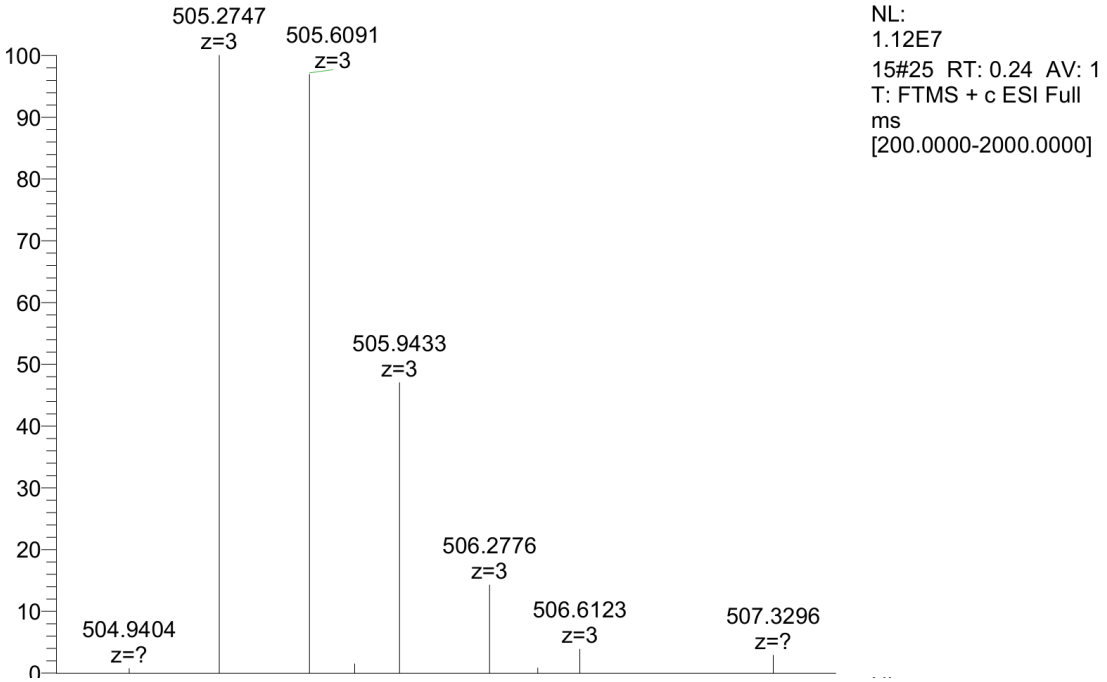

HRMS of compound **24a**: Calcd for [(M+3H$^+$)/3] $C_{75}H_{103}N_{24}O_{11}^{3+}$: 505.2741; found: 505.2747.

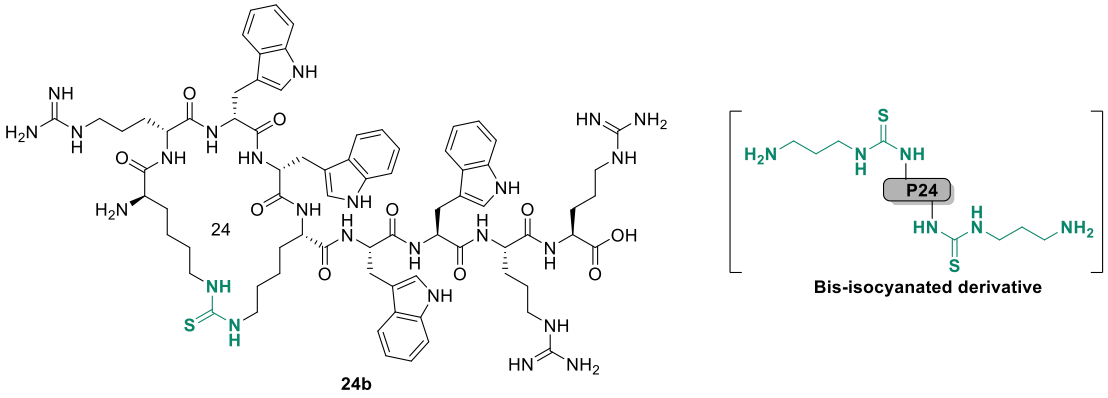

Compound 24b was isolated in 45% yield (6.9 mg, 0.0045 mmol) as a white powder; the HPLC yield was 60% based on absorbance at 240 nm.

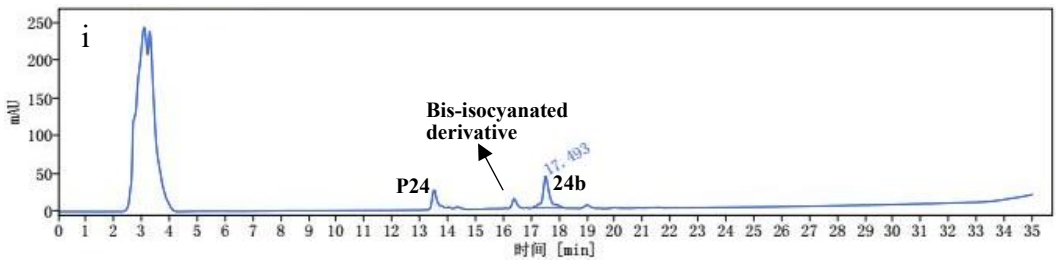

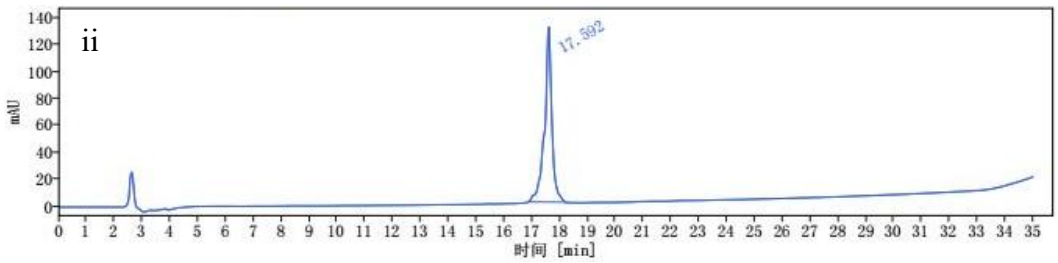

Figure S33. i) HPLC trace of reaction mixture of compound **24b**. ii) HPLC trace of purified compound **24b** [1 mL/min, 10% to 60% MeCN for 30 min, then 60% to 95% MeCN 30-35 min, HPLCONE 10C18A (10 μm, 4.6 x 250 mm), λ = 240 nm].

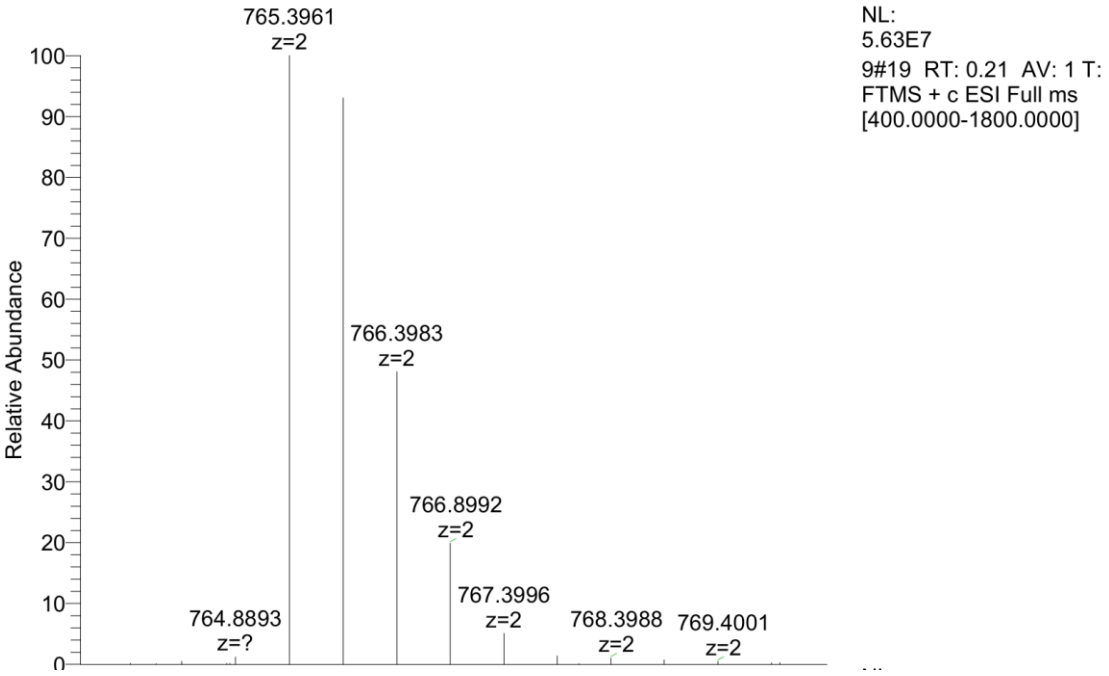

HRMS of compound **24b**: Calcd for [(M+2H$^+$)/2] $C_{75}H_{102}N_{24}O_{10}S^{2+}$: 765.3960; found: 765.3961.

E. Structural verification of peptide 23a

The N-terminal amino acid sequence of peptide product **23a**, modified *via* N, N'-carbonyldiimidazole (CDI)-mediated cyclization, was analyzed using the classical Edman degradation method. As shown in the Figure S3, the sequence data of the first three N-terminal amino acid residues (specifically glycine(A), leucine(B), and leucine(C)) were successfully obtained through multiple cycles of phenyl isothiocyanate (PTC) coupling, acid-catalyzed cleavage, and high-performance liquid chromatography (HPLC) identification. Comparison with the theoretical sequence revealed complete consistency in both the types and order of these amino acids. These results indicate the presence of N-terminal free amino group of **23a** after the cyclization reaction. This finding indirectly confirms that the cyclized product **23a** primarily

underwent side chain-to-side chain lysine cyclization, rather than the cyclization between N-terminal amino and side chain lysine.

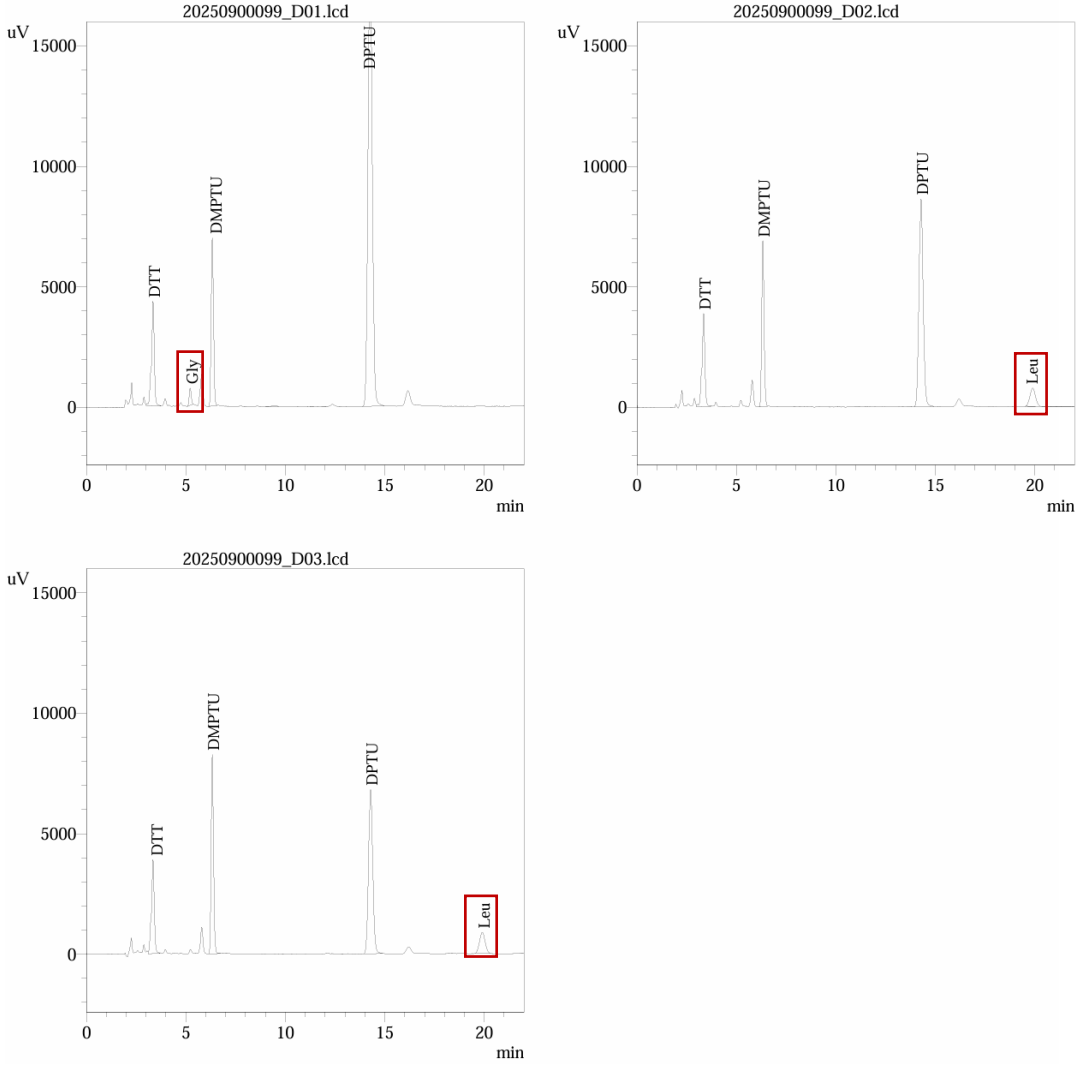

Figure S34. N-terminal sequence determination of peptide **23a** by Edman degradation.

F. Characterization of fluorescently labeled cyclopeptides

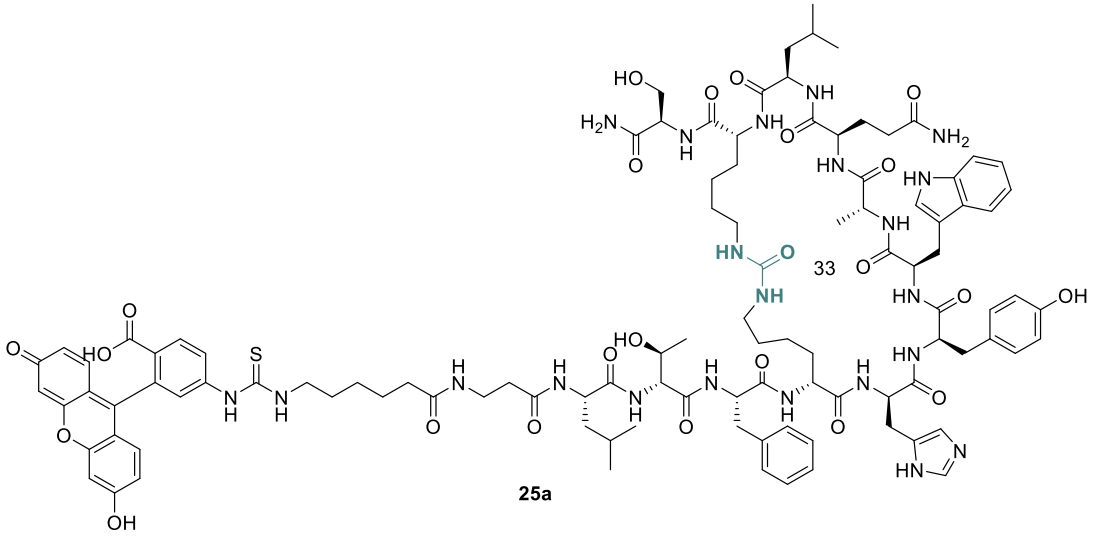

Compound 25a was isolated in 36% yield (7.6 mg, 0.0036 mmol) as a white powder; the HPLC yield was 42% based on absorbance at 210 nm.

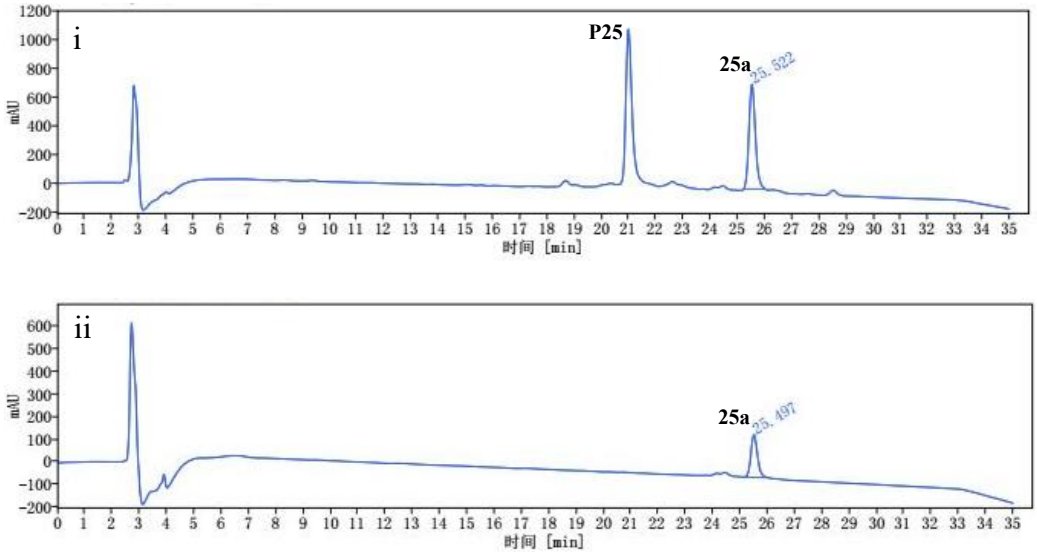

Figure S35. i) HPLC trace of reaction mixture of compound **25a**. ii) HPLC trace of purified compound **25a** [1 mL/min, 10% to 60% MeCN for 30 min, then 60% to 95% MeCN 30-35 min, HPLCONE 10C18A (10 μm, 4.6 x 250 mm), λ = 210 nm].

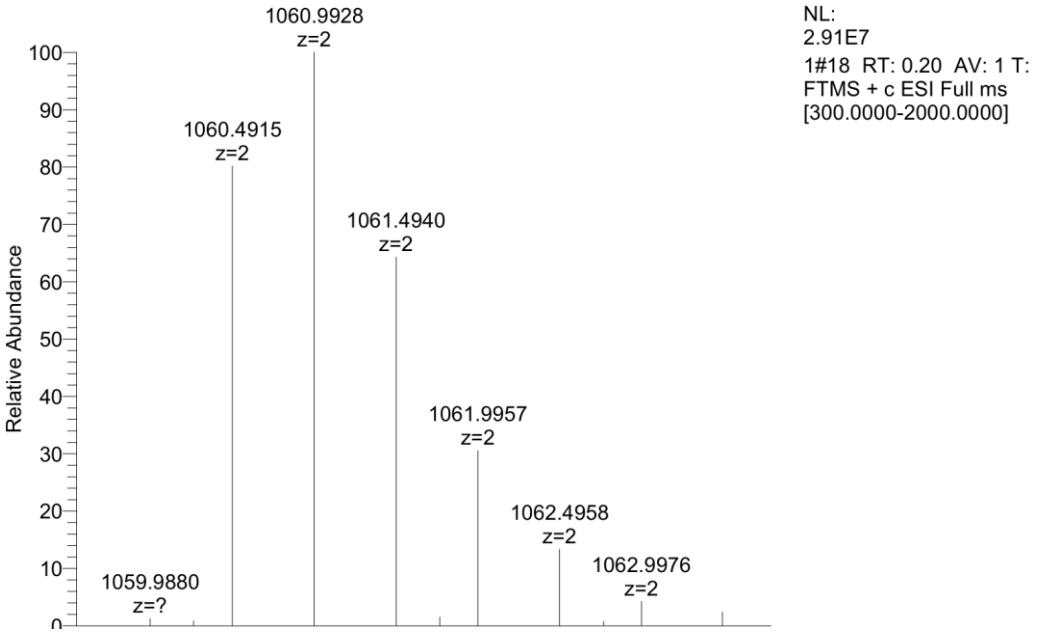

HRMS of compound **25a**: Calcd for [(M+2H$^+$)/2] $C_{105}H_{136}N_{22}O_{24}S^{2+}$: 1060.9921; found: 1060.9928.

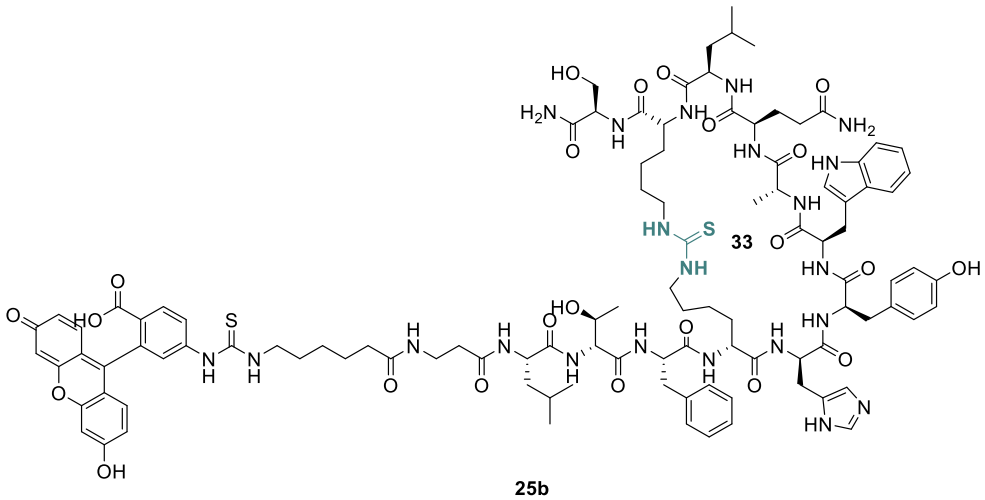

25b

Compound 25b was isolated in 43% yield (9.2 mg, 0.0043 mmol) as a white powder; the HPLC yield was 52% based on absorbance at 220 nm.

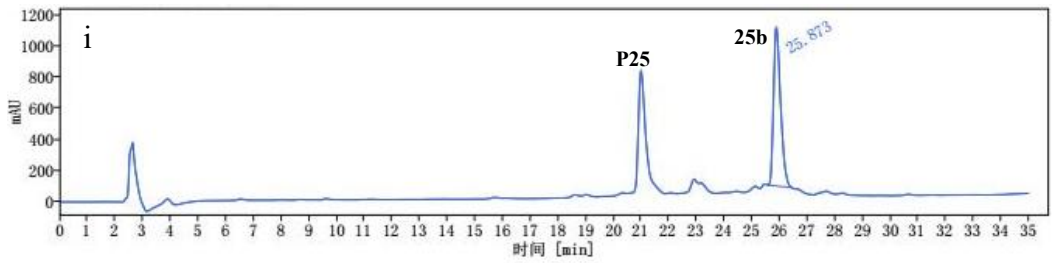

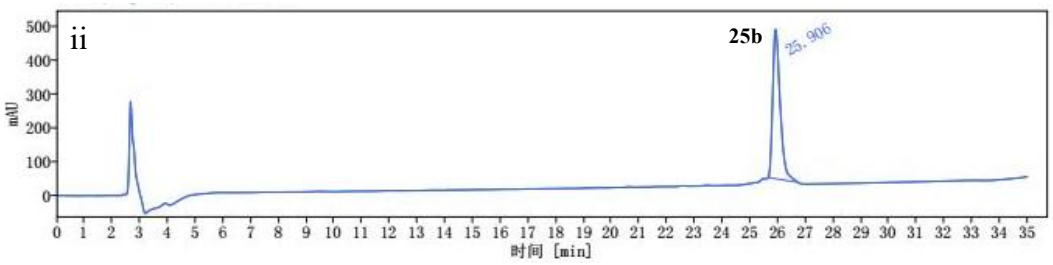

Figure S36. i) HPLC trace of reaction mixture of compound **25b**. ii) HPLC trace of purified compound **25b** [1 mL/min, 10% to 60% MeCN for 30 min, then 60% to 95% MeCN 30-35 min, HPLCONE 10C18A (10 μm, 4.6 x 250 mm), λ = 220 nm].

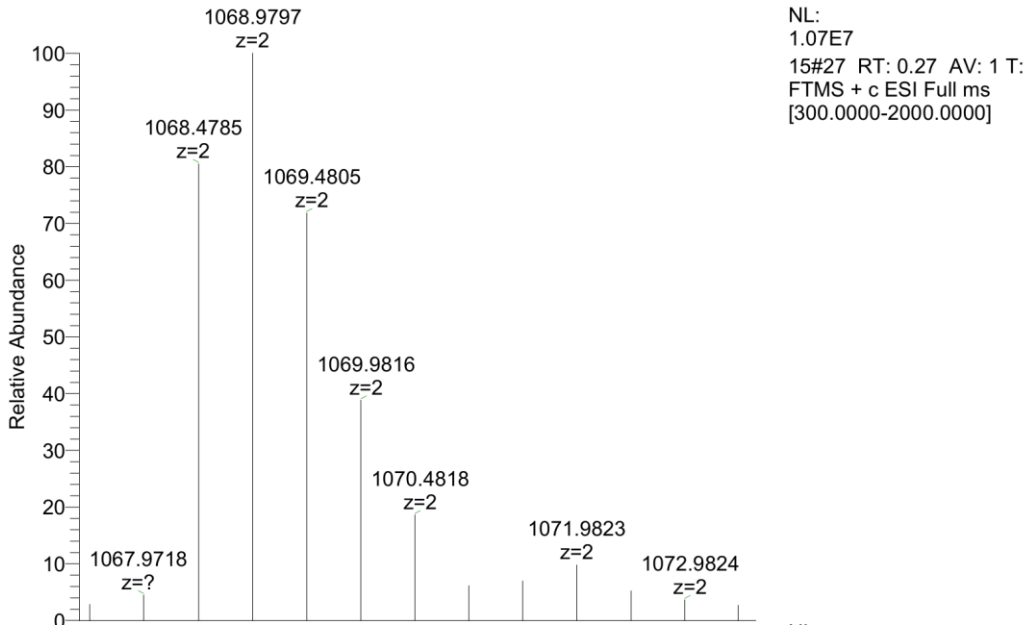

HRMS of compound **25b**: Calcd for $[(M+2H^+)/2]$ $C_{105}H_{136}N_{22}O_{23}S_2^{2+}$: 1068.9806; found: 1068.9797.

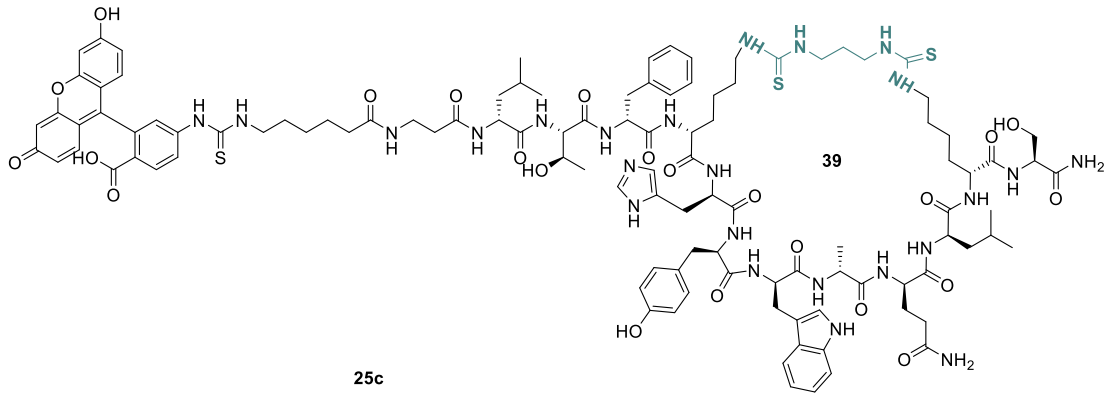

25c

Compound 25c was isolated in 41% yield (9.2 mg, 0.0041 mmol) as a white powder; the HPLC yield was 57% based on absorbance at 220 nm.

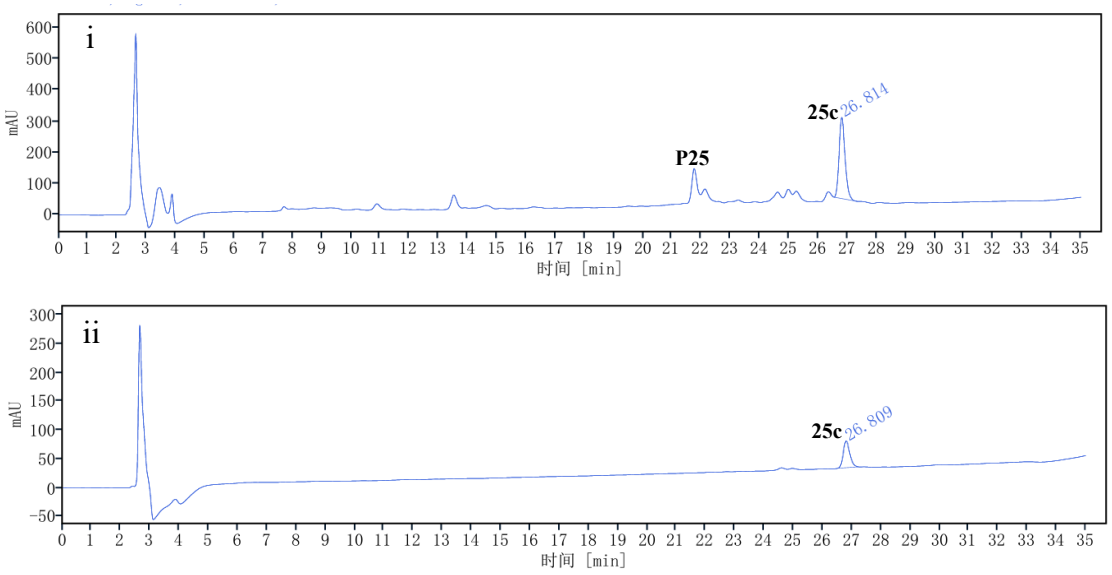

Figure S37. i) HPLC trace of reaction mixture of compound **25c**. ii) HPLC trace of purified compound **25c** [1 mL/min, 10% to 60% MeCN for 30 min, then 60% to 95% MeCN 30-35 min, HPLCONE 10C18A (10 μm, 4.6 x 250 mm), λ = 220 nm].

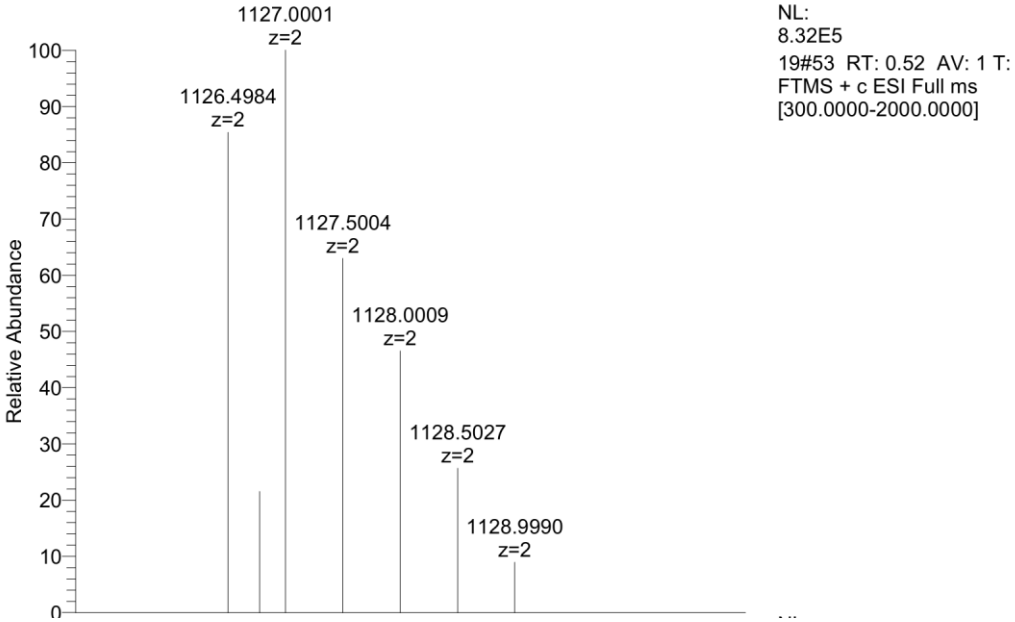

HRMS of compound **25c**: Calcd for $[(M+2H^+)/2]$ $C_{109}H_{144}N_{24}O_{23}S_3^{2+}$: 1127.0010 found: 1127.0001.

G. Characterization of RGD cyclopeptides

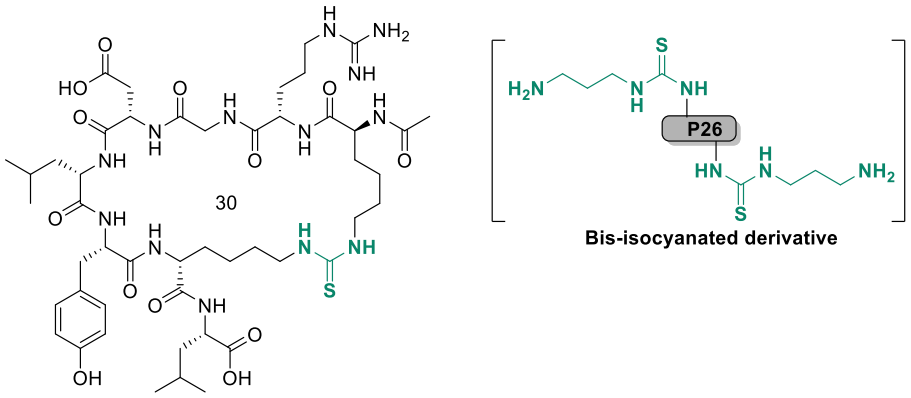

26b

Compound 26b was isolated in 63% yield (6.8 mg, 0.0063 mmol) as a white powder; the HPLC yield was 71% based on absorbance at 220 nm.

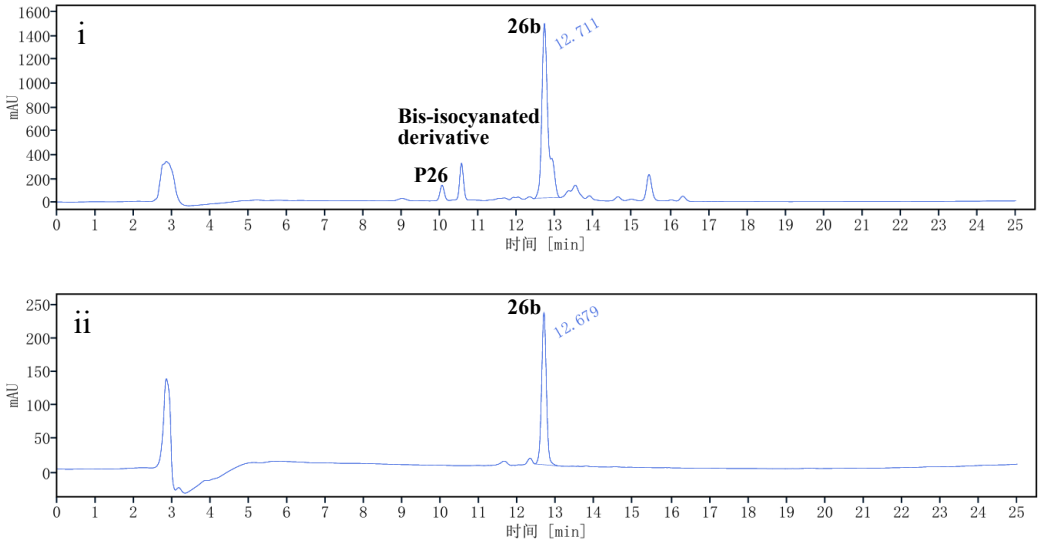

Figure S38. i) HPLC trace of reaction mixture of compound **26b**. ii) HPLC trace of purified compound **26b** [1 mL/min, 10% to 60% MeCN for 30 min, then 60% to 95% MeCN 30-35 min, HPLCONE 10C18A (10 μm, 4.6 x 250 mm), λ = 220 nm].

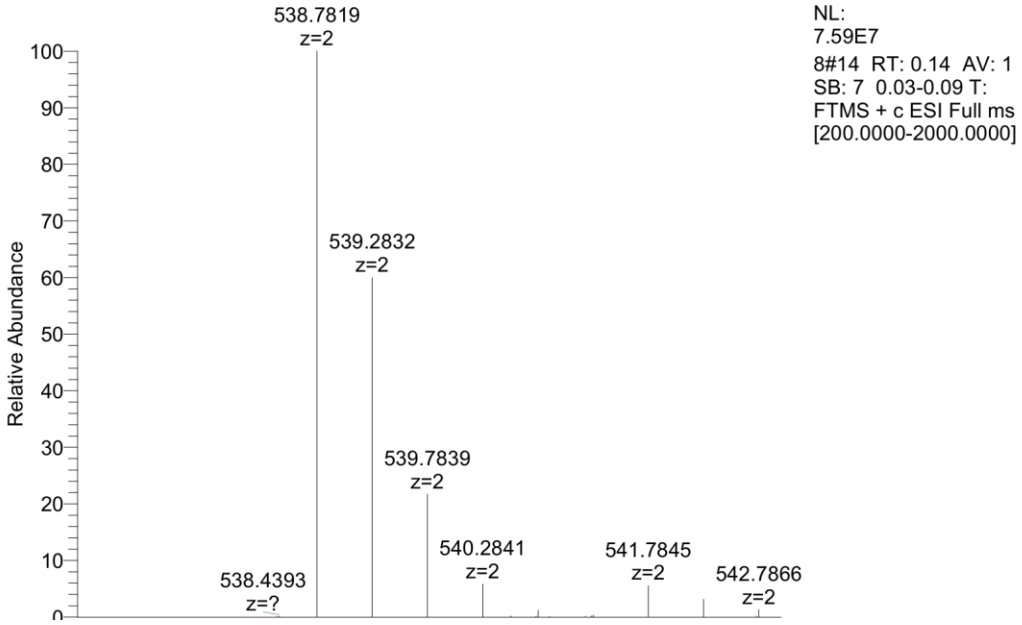

HRMS of compound 26b: Calcd for [(M+2H$^+$)/2] $C_{48}H_{79}N_{13}O_{13}S^{2+}$: 538.7815; found: 538.7819.

H. Evaluation of stability of cyclopeptides

Stability under oxidative conditions

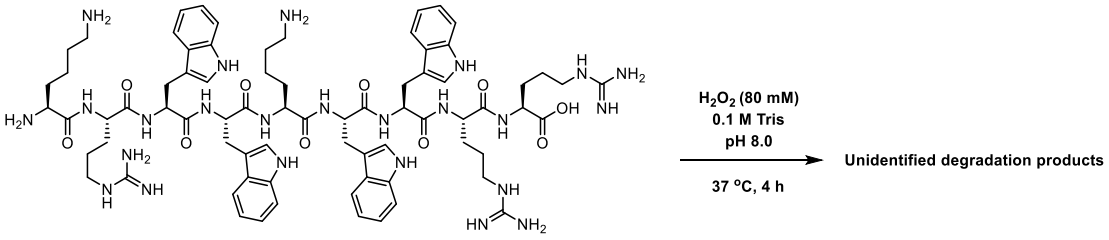

P24
Antimicrobial Peptide HHC-36
H_2N-Lys-Arg-Trp-Trp-Lys-Trp-Trp-Arg-Arg-OH

P24, t = 0 h

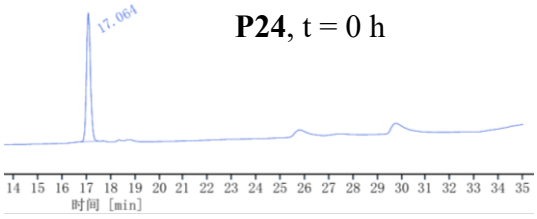

P24, t = 1 h

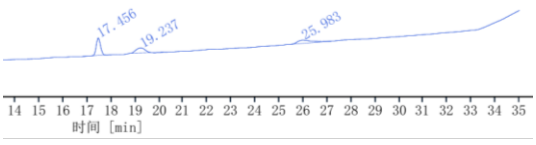

P24, t = 2 h

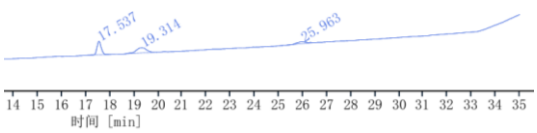

P24, t = 3 h

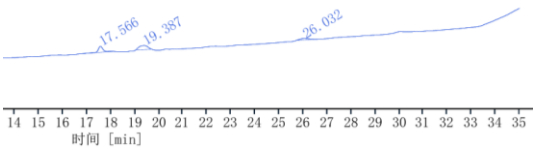

P24, t = 4 h

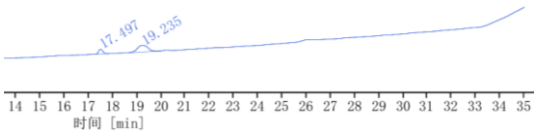

Figure S39. Oxidative stability of **P24** assessed by HPLC over 4 hours.

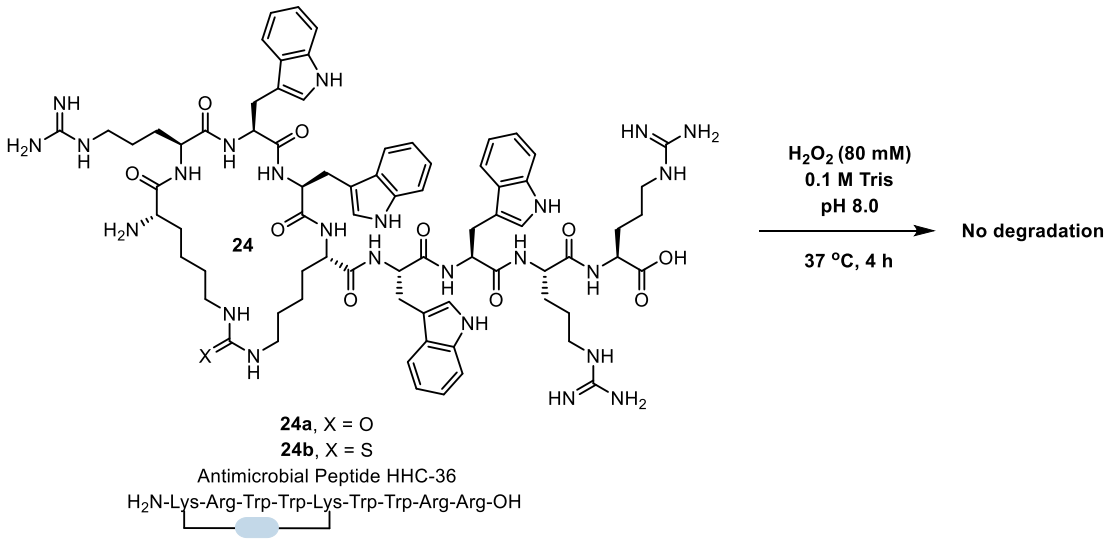

24a, t = 0 h

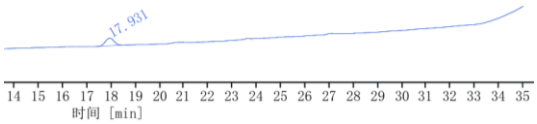

24b, t = 0 h

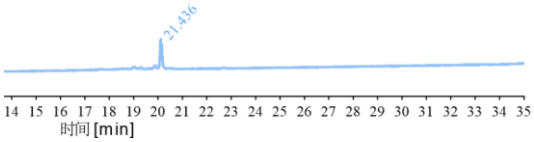

24a, t = 1 h

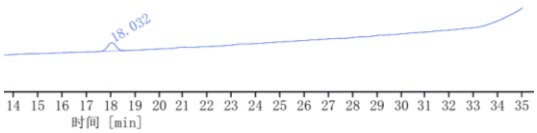

24b, t = 1 h

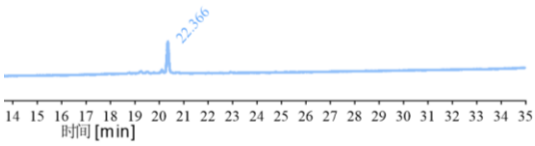

24a, t = 2 h

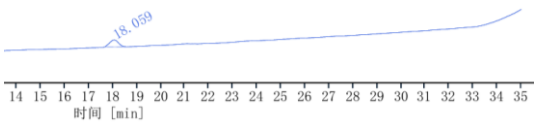

24b, t = 2 h

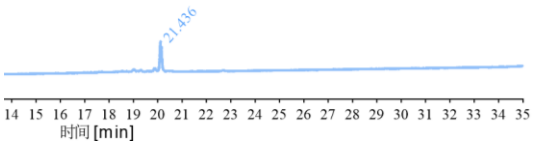

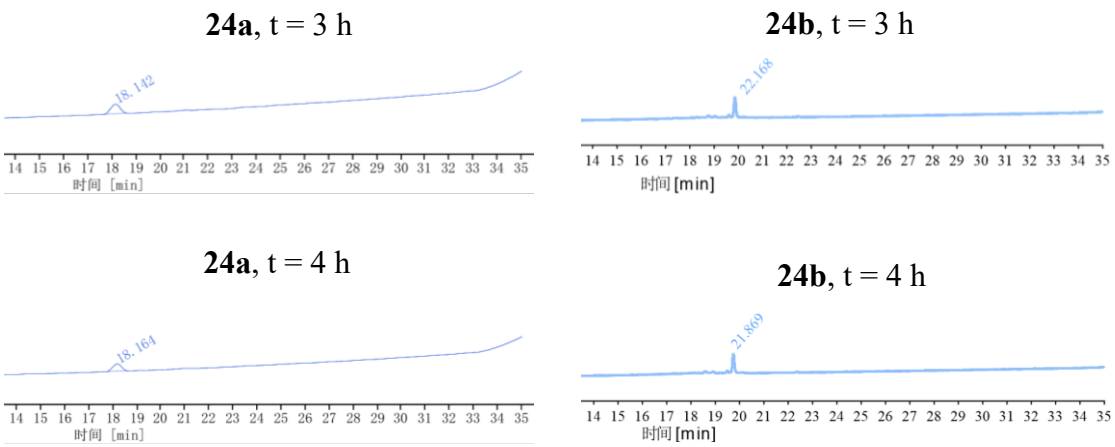

Figure S40. Oxidative stability of **24a** and **24b** assessed by HPLC over 4 hours.

Stability in pH 10.0 buffer conditions

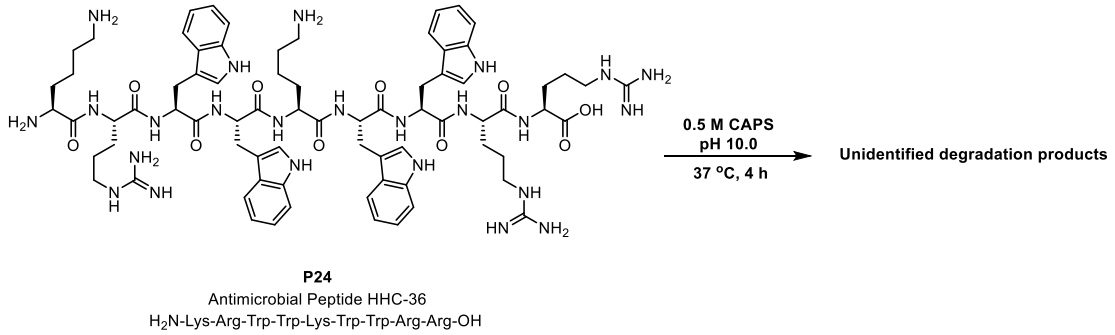

P24
Antimicrobial Peptide HHC-36
H_2N-Lys-Arg-Trp-Trp-Lys-Trp-Trp-Arg-Arg-OH

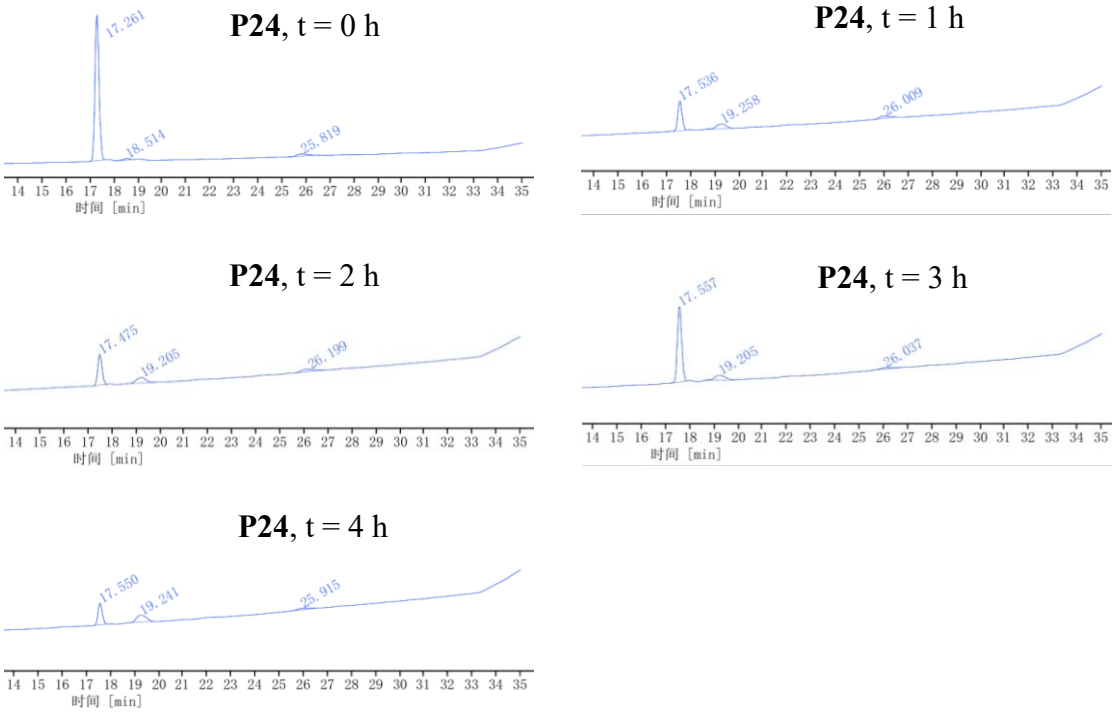

Figure S41. Stability of **P24** in pH 10.0 buffer assessed by HPLC over 4 hours.

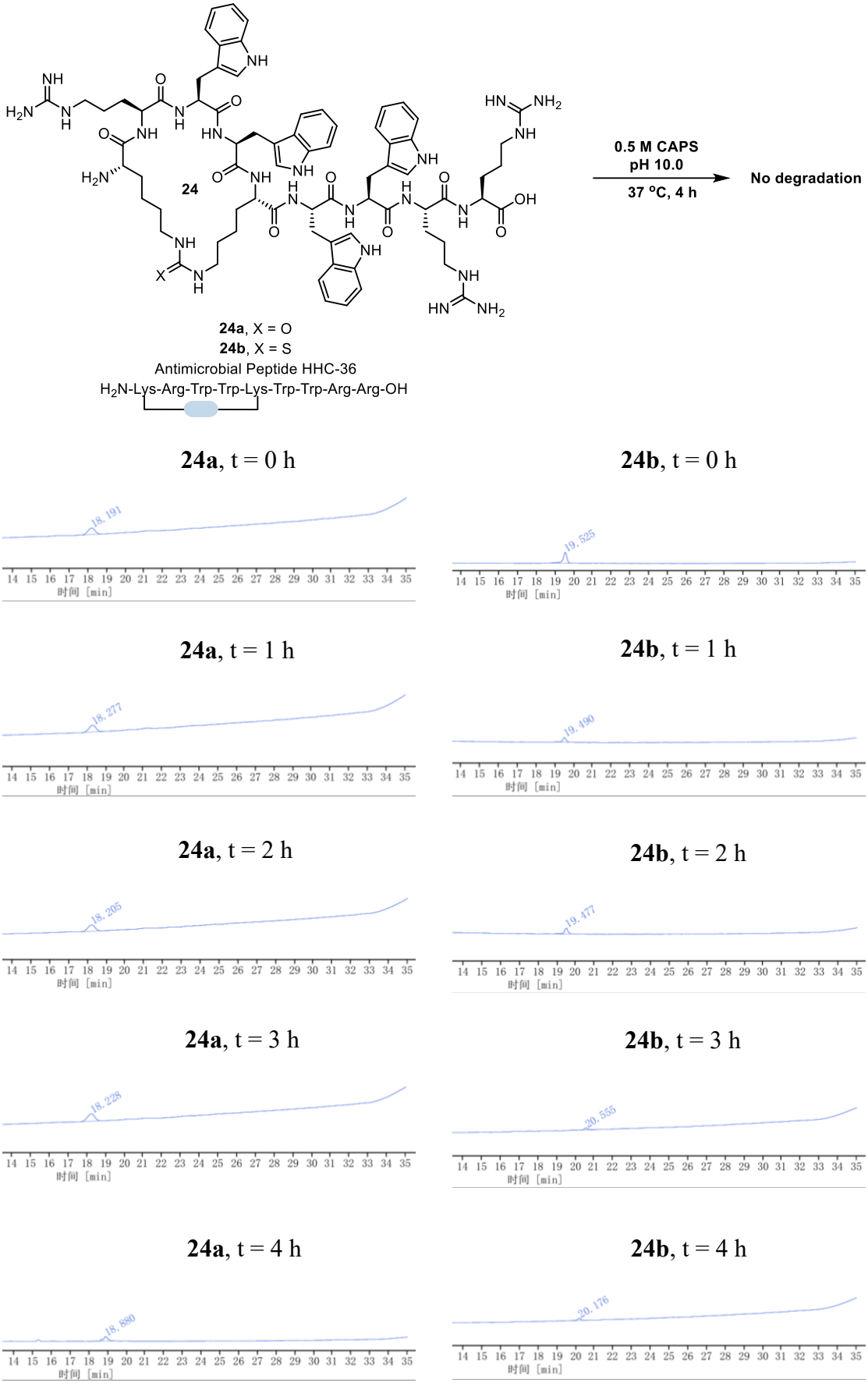

Figure S42. Stability of **24a** and **24b** in pH 10.0 buffer assessed by HPLC over 4 hours.

Stability under trypsin incubation

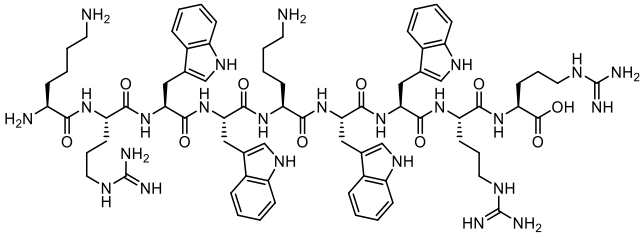

P24
Antimicrobial Peptide HHC-36
H_2N-Lys-Arg-Trp-Trp-Lys-Trp-Trp-Arg-Arg-OH

Unidentified degradation products

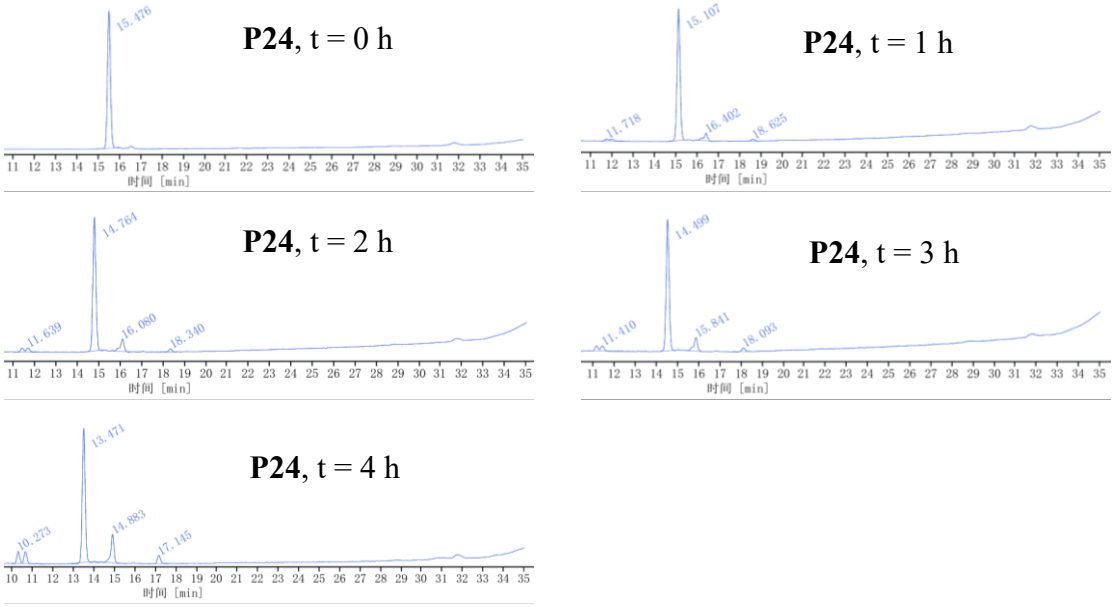

Figure S43. Stability of **P24** during tryptic digestion assessed by HPLC over 4 hours.

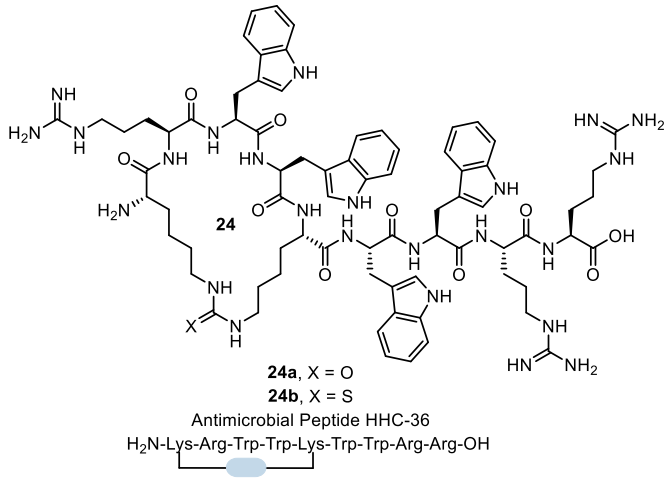

24a, X = O
24b, X = S
Antimicrobial Peptide HHC-36
H_2N-Lys-Arg-Trp-Trp-Lys-Trp-Trp-Arg-Arg-OH

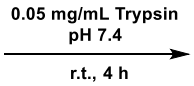

No degradation

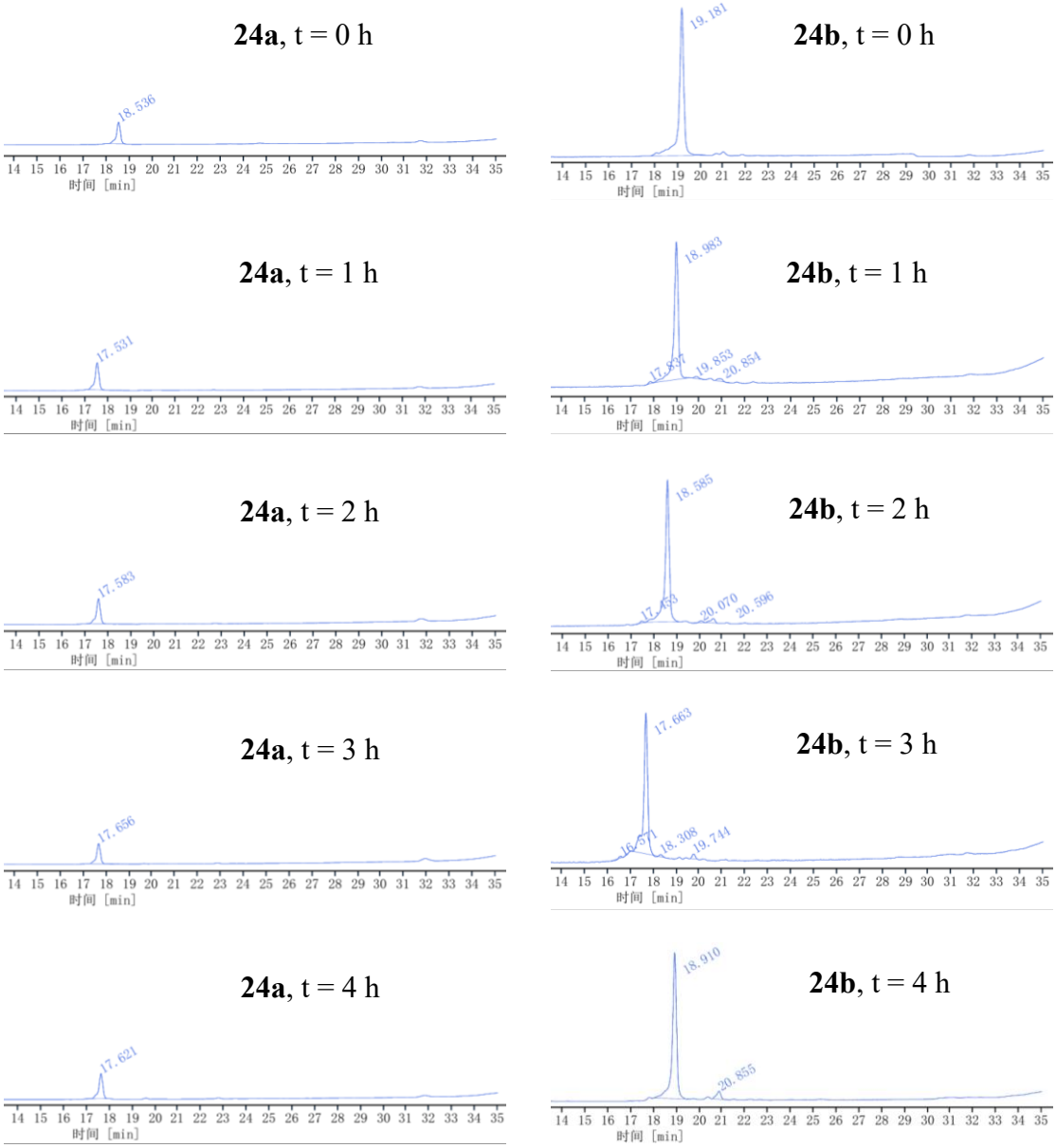

Figure S44. Stability of **24a** and **24b** during tryptic digestion assessed by HPLC over 4 hours.

Results of stability under H_2O_2, pH 10.0 buffer and trypsin incubation

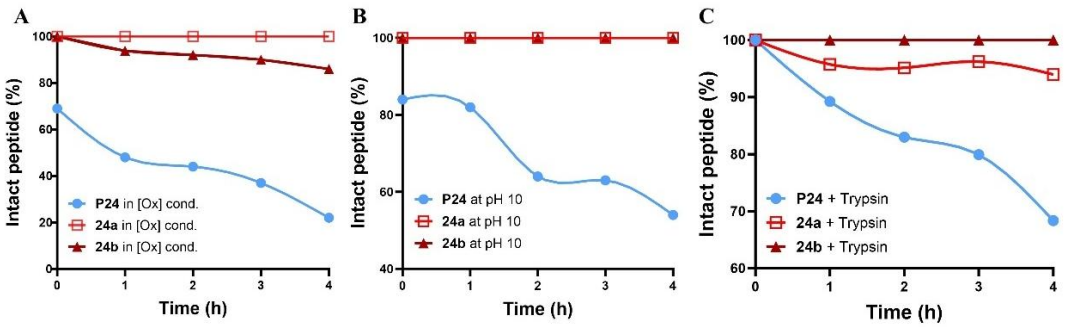

Figure S45. Antimicrobial peptides of chemically stable macrocycles and proteolytic

stability assay. A. Stability of **P24**, **24a**, **24b** at 0-4 h under H_2O_2 (80 mM); B. Stability of **P24**, **24a**, **24b** at 0-4 h in pH 10.0 buffer conditions; C. Stability of **P24**, **24a**, **24b** at 0-4 h under trypsin treatment.

I. Integrin binding assay [1-2]

Flat-bottom 96-well ELISA plates (Corning) were coated overnight at 4 °C with 100 μL/well of 0.4 μg/mL LAP(TGF-β1) (MCE) in carbonate buffer (15 mM Na_2CO_3, 35 mM $NaHCO_3$, pH 9.6). Each well was then washed with PBS-T buffer (PBS, 0.01% Tween 20, pH 7.4, 3 × 200 μL) and blocked for 1 h at room temperature with 150 μL/well of TSB-buffer (20 mM Tris-HCl, 150 mM NaCl, 1 mM $CaCl_2$, 1 mM $MgCl_2$, 1 mM $MnCl_2$, pH 7.5, 1% BSA). After being washed three times with PBS-T, equal volumes of test compounds were mixed with 1.0 μg/mL human integrin αvβ6 (MCE) giving a final dilution in TSB buffer of 0.0001–200 μM for the inhibitors and 0.5 μg/mL for integrin αvβ6. These solutions (100 μL/well) were incubated for 1 h at room temperature. The plate was washed three times with PBS-T buffer and 100 μL/well of 1:400 diluted mouse antihuman αv (Millipore) was added to the plate. After incubation for 1 h at room temperature, the plate was washed three times with PBS-T, and 100 μL/well of 4.0 μg/mL of secondary peroxidase-labeled antibody (anti-mouse IgG-POD, SigmaAldrich) was added to the plate and incubated for 1 h at room temperature. After the plate was washed three times with PBS-T, it got developed by adding 100 μL/well of TMB (Beyotime) and incubated for 1-5 min at room temperature. The reaction was stopped with 100 μL/well of 3 M H_2SO_4, and the absorbance was measured at 450 nm with a plate reader. The resulting inhibition curves were analyzed using Graphpad Prism 10.1.2 software.

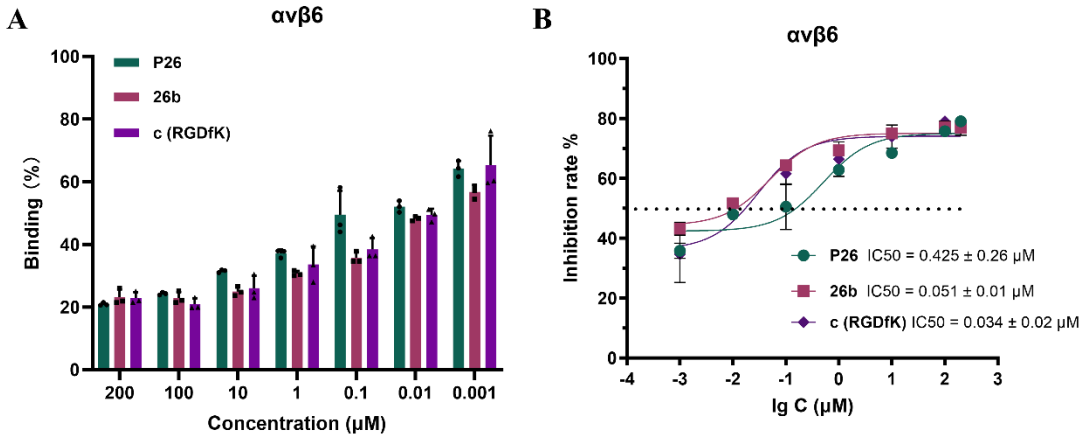

Figure S46. Binding and inhibitory activities of peptides against integrin αvβ6. A. Binding of **P26**, **26b**, **c (RGDfK)** to integrin αvβ6. B. Inhibition of **P26**, **26b**, **c (RGDfK)** to integrin αvβ6. Data are presented as mean ± SD from independent biological replicates (n=3).

J. Cytotoxicity evaluation of cyclopeptides

Cell culture methodology

Cell Line and Culture Conditions: The human non-small cell lung cancer cell line (A549-luc), the human colorectal adenocarcinoma cell line (Caco-2) and the human kidney cancer cell line (A498) were purchased from the Cell Bank of Guangzhou Xinyuan Biotechnology Co., Ltd. (Guangzhou, China). The A549-luc and the Caco-2 were cultured in Roswell Park Memorial Institute (RPMI-1640) medium. The A498 was cultured in Minimum Essential Medium (MEM). The medium was supplemented with 10% fetal bovine serum (FBS), 100 units/ mL of penicillin-streptomycin, and incubated at 37 °C in a humidified atmosphere containing 5% CO_2.

General procedures for cytotoxicity assay

The cell viability was determined by CCK-8 assay. Generally, cells (5000-8000/well) in the above-stated medium containing 10% FBS were cultured in a 96-well plate in a humidified atmosphere of 5% CO_2 at 37 °C for 24 h. Peptide was then added and diluted to final concentrations and incubated for 24 h. Then, 10 μL CCK-8 reagent added per well and incubated for another 1-4 h at 37°C. Next, the absorbance at 450 nm was

measured by a microplate reader. The cell survival rate was calculated with the following formula [3]:

$$Cell\ Viability(\%) = \frac{A_s - A_b}{A_c - A_b} \times 100\% \qquad (2)$$

A_s: Absorbance of peptide-treated cells; A_c: Absorbance of control cells (no peptide); A_b: Absorbance of blank (medium)

Results of data processing

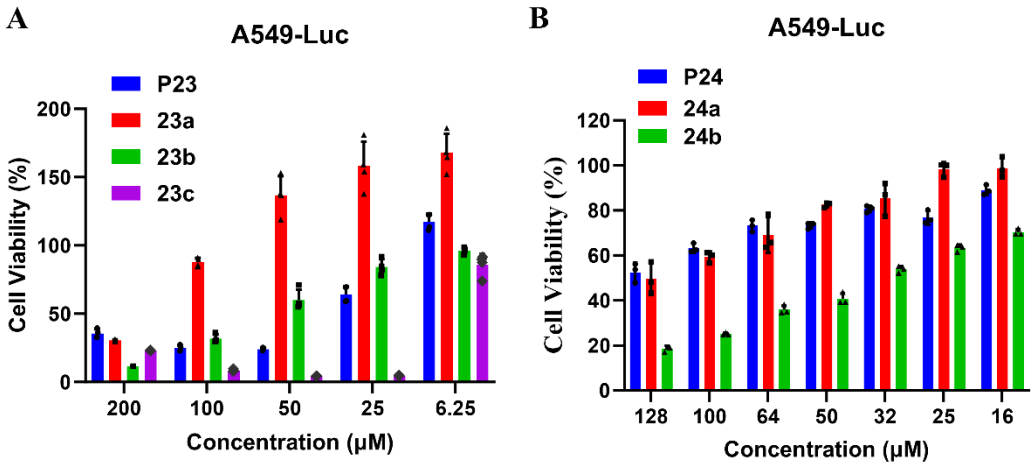

Figure S47. Results of cell viability detection in A549-Luc cells after treatment with polypeptides at serial concentrations. A. The A549-Luc cell viability assay of **P23**, **23a**, **23b**, **23c**; B. The A549-Luc cell viability assay of **P24**, **24a**, **24b.** Data are presented as mean ± SD from independent biological replicates (n≥3).

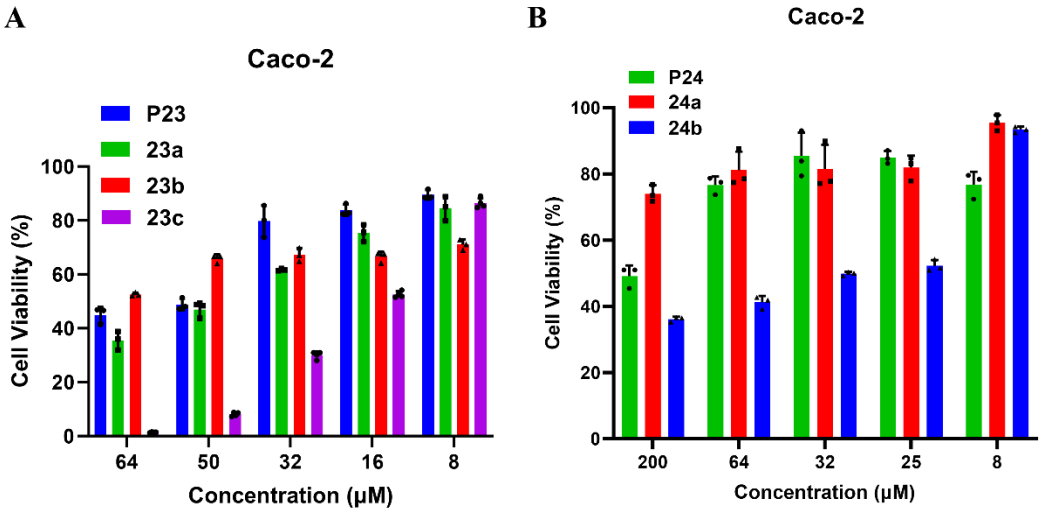

Figure S48. Results of cell viability detection in Caco-2 cells after treatment with polypeptides at serial concentrations. A. The Caco-2 cell viability assay of **P23**, **23a**,

23b, **23c**; B. The Caco-2 cell viability assay of **P24**, **24a**, **24b.** Data are presented as mean ± SD from independent biological replicates (n≥3).

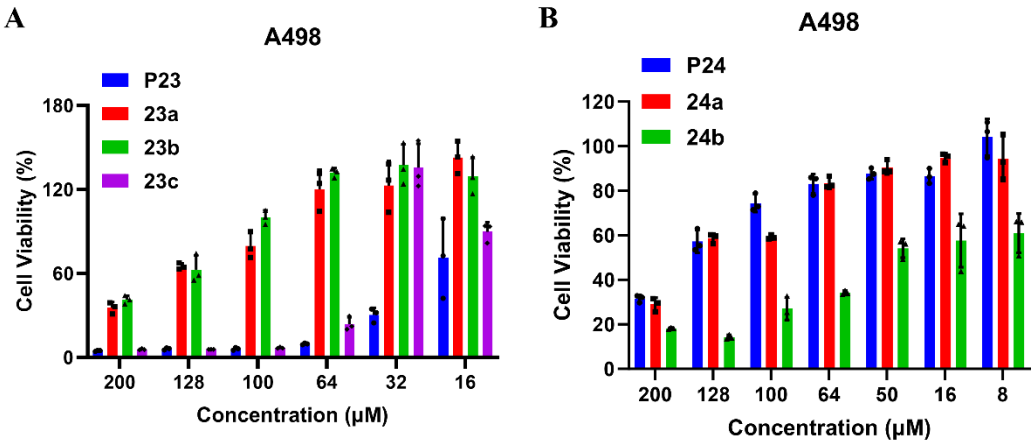

Figure S49. Results of cell viability detection in A498 cells after treatment with polypeptides at serial concentrations. A. The A498 cell viability assay of **P23**, **23a**, **23b**, **23c**; B. The A498 cell viability assay of **P24**, **24a**, **24b.** Data are presented as mean ± SD from independent biological replicates (n=3).

General procedures for cell safety testing

The cell viability was determined using CCK-8 assay. Generally, cells (8000/well) in the above-stated medium containing 10% FBS were cultured in a 96-well plate in a humidified atmosphere of 5% CO_2 at 37 °C for 24 h. Peptide was then added and diluted to final concentrations and incubated for 24 h. Then, 10 μL CCK-8 reagent added per well and incubated for another 1-4 h at 37°C. Next, the absorbance at 450 nm was measured by a microplate reader. The cell survival rate was calculated with the following formula:

$$Cell\ Viability(\%) = \frac{A_s - A_b}{A_c - A_b} \times 100\% \qquad (3)$$

A_s: Absorbance of peptide-treated cells; A_c: Absorbance of control cells (no peptide); A_b: Absorbance of blank (medium)

Results of data processing

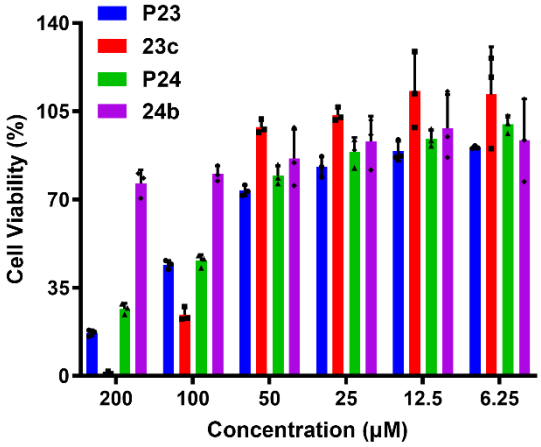

Figure S50. The MCF-10A cell viability assay of **P23**, **23c**, **P24**, and **24b**. Data are presented as mean ± SD from independent biological replicates (n=3).

K. Flow cytometry and cellular uptake of A549-Luc cells

General procedures for cell safety testing

The cell viability was determined using MTT assay. Generally, cells (5000-10000/well) in the above-stated medium containing 10% FBS were cultured in a 96-well plate in a humidified atmosphere of 5% CO_2 at 37 °C for 24 h. Peptide was then added and diluted to final concentrations and incubated for 24 h. Then, 30 μL MTT solution (final concentration: 0.5 mg/mL) added per well and incubated for at 37°C in the dark for 3 hours to form purple formazan crystals. Next, carefully remove the supernatant and add 100 μL of DMSO each well. Shake the plate at low speed for 10–15 minutes to fully dissolve the crystals. Last, the absorbance at 570 nm was measured by a microplate reader. The cell survival rate was calculated with the following formula:

$$Cell\ Viability(\%) = \frac{A_s - A_b}{A_c - A_b} \times 100\% \qquad (4)$$

A_s: Absorbance of peptide-treated cells; A_c: Absorbance of control cells (no peptide); A_b: Absorbance of blank (medium)

Results of data processing

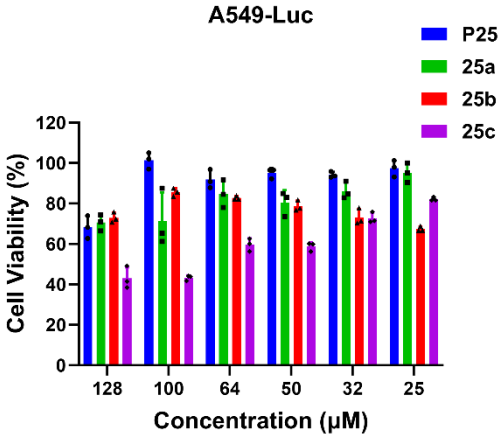

Figure S51. The A549-Luc cell viability assay of **P25**, **25a**, **25b**, **25c**. Data are presented as mean ±SD from independent biological replicates (n=3).

Cellular uptake experiment

A549-Luc cells were seeded into confocal-specific glass-bottom dishes at a density of 100000 cells/well and cultured to 70-90% confluency. FITC-labeled peptides **P25**, **25a**, **25b**, **25c** (dissolved in RPMI-1640 medium containing 0.1% DMSO via 5-minute sonication) were added to the cells and incubated at 37°C, 5% CO_2 for 6 hours. After incubation, the cells were fixed with 4% paraformaldehyde (PFA) for 10-15 minutes and washed twice with PBS. Subsequently, Hoechst 33258 (1-5 μg/mL) was added to stain nuclei, followed by a 20-minute incubation and two additional PBS washes. Finally, imaging was performed using a laser scanning confocal microscope equipped with a 63× oil-immersion objective[4].

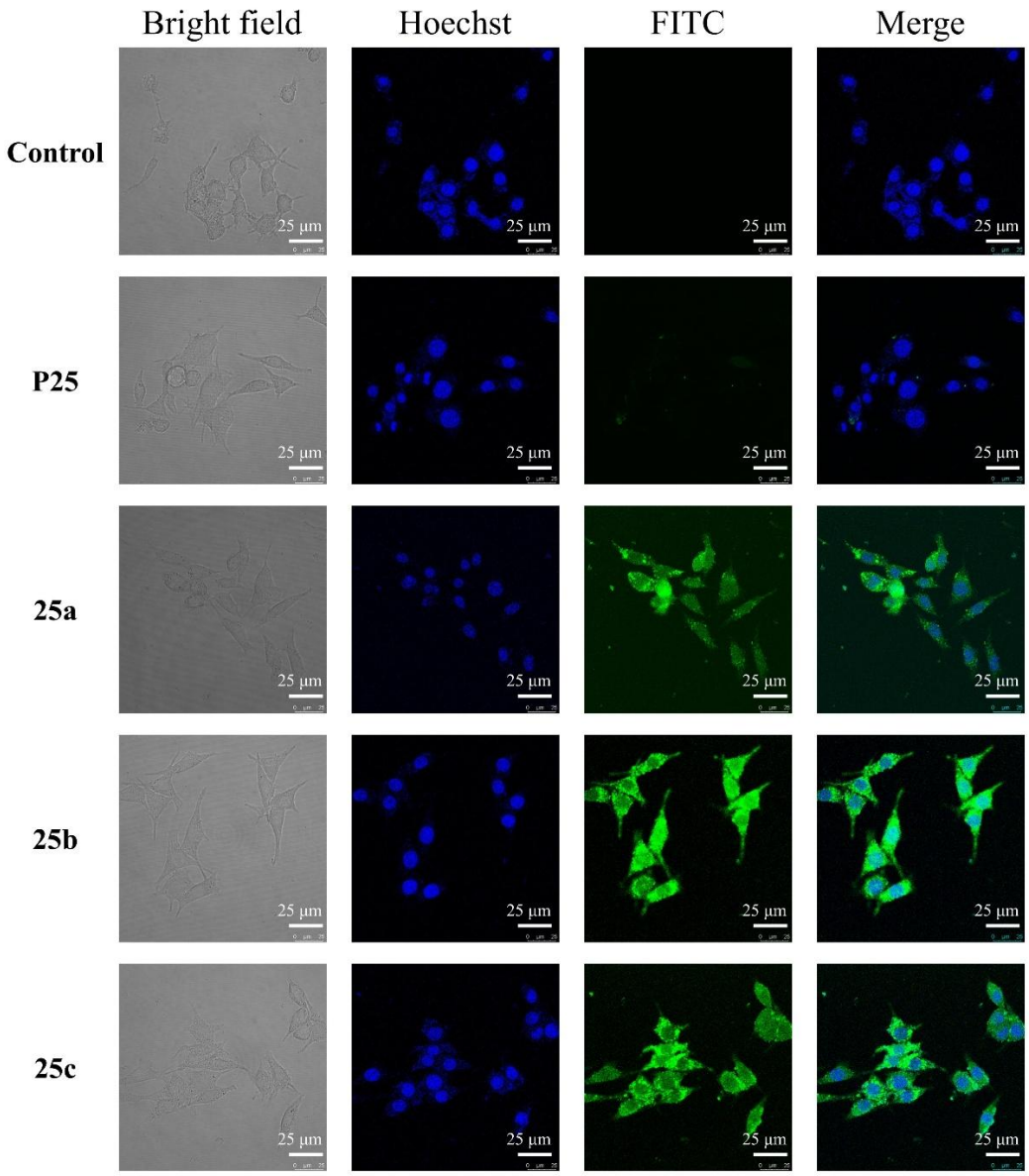

Figure S52. Representative confocal microscopy images of A549-Luc cells treated with peptides from three independent biological replicates. Blue colour: membrane; green colour: FITC labeled peptides. Scale bar: 25 μm.

Flow cytometry

A549-Luc cells were seeded in triplicate in 6-well plates at a density of 1.5×10^5 cells/well and cultured to 90% confluence in RPMI-1640 medium supplemented with 10% fetal bovine serum. Peptides **P25**, **25a**, **25b**, **25c** (dissolved in RPMI-1640 medium containing 0.1% DMSO *via* 5-minute sonication) were administered at a final concentration of 50 μM (1 mL/well). After 6 hours of incubation, the supernatant was

aspirated, and cells were trypsinized with 0.25% trypsin-EDTA for 2 minutes at 37 °C under 5% CO_2. Detached cells were collected, centrifuged at 1000 rpm for 3 minutes at room temperature, washed three times with pre-warmed PBS, resuspended in 1 mL PBS, and filtered through a 40 μm nylon mesh. Flow cytometry analysis was performed on a BD LSRII system (excitation wavelength: 488 nm, detection channel: FITC). Data were analyzed using FlowJo v10.8.1[5].

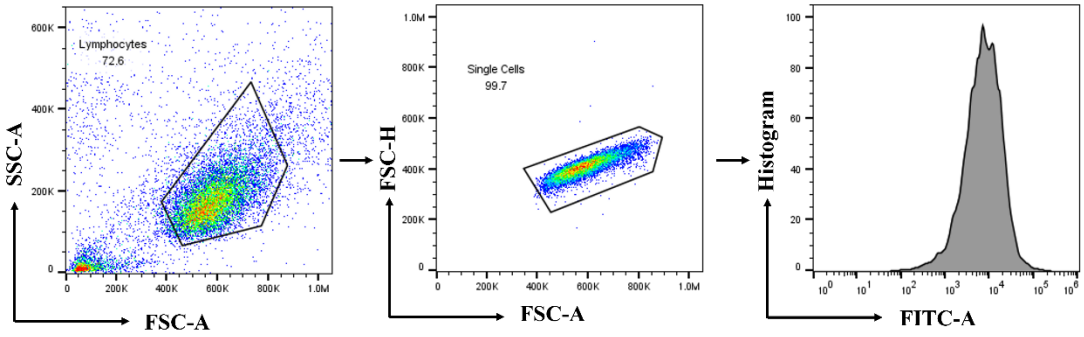

Figure S53. Schematic representation of the flow cytometry gating strategy.

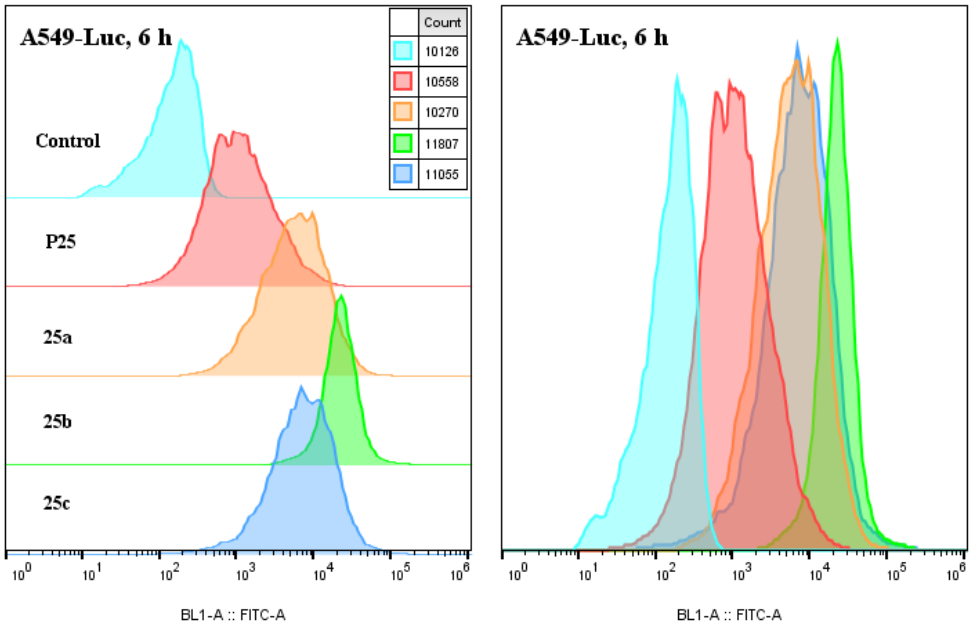

Figure S54. Representative flow cytometry histograms of A549-Luc cells treated with **P25**, **25a**, **25b**, and **25c** for 6 h from three independent biological replicates.

L. Cell apoptosis analysis

A549-Luc and Caco-2 cells, cultured during the logarithmic growth phase, were plated into six-well plates at a seeding density of 1.5×10^5 cells per well and incubated

for 24 h. Thereafter, **23c** was introduced to achieve drug concentrations of 0, 20 μM, 50 μM, and 70 μM for A549-Luc and 0, 20, 35, 60 μM for Caco-2 cells. Following a 48 h treatment period, the cells were centrifuged at 1000 rpm for 3 min and washed three times with cold PBS buffer. The cell apoptosis analysis was carried out using an Annexin V-FITC cell apoptosis kit. According to the manufacturer's procedure, resuspend cells in 500 μL of 1× Binding Buffer and adjust the cell concentration to 1×10^6 cells/mL. Prepare flow cytometry tubes labeled as blank control, single-positive controls (for compensation), and experimental samples. Add 500 μL of the filtered cell suspension (passed through a 200-mesh strainer) to each tube. For single-positive controls, add either 5 μL of Annexin V-Alexa Fluor™488 or 10 μL of propidium iodide (PI) to their respective tubes and mix gently. For sample tubes, first add 5 μL of Annexin V-FITC followed by 10 μL of PI, mixing gently after each addition. Incubate all tubes at room temperature in the dark for 10-20 minutes, then add 500 μL of 1× Binding Buffer and place on ice before flow cytometry analysis. The instrument settings should be configured as follows: Alexa Fluor™488 detection at 488 nm excitation with 530/30 nm emission collection, and PI detection at 561 nm excitation with 610/20 nm emission collection[6].

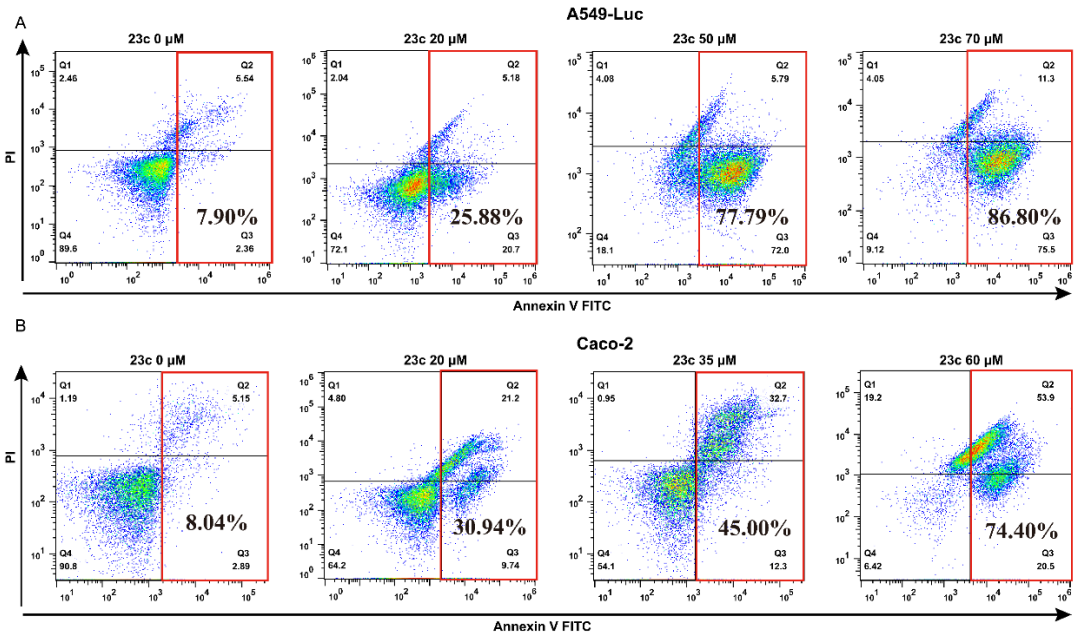

Figure S55. Flow cytometry analysis of cell apoptosis in A549-Luc and Caco-2 cells in the presence of **23c**

M. Circular dichroism spectra of P23, 23a, 23b, and 23c

CD spectra were recorded on a Chirascan CD spectrophotometer at 25 °C to determine the secondary structures of all peptides. Peptide solutions were prepared at a concentration of 100 μM in PBS (pH 7.3), 50% TFE solution. The peptide solution was then transferred into a cuvette with a path length of 0.05 cm. Experimental parameters: scan wavelength: 190 - 260 nm, scan rate: 1 nm/s, bandwidth: 1.0 nm, three repeat scans were performed in reverse direction and averaged. The data from the three scans were averaged, baseline-corrected, and converted to mean residue ellipticity using equation:

$$[\boldsymbol{\theta}]_{\boldsymbol{\lambda}} = \frac{[\boldsymbol{\theta}]_{\boldsymbol{obs}}}{\mathbf{10}\times\boldsymbol{l}\times\boldsymbol{C}\times\boldsymbol{n}} \quad (5)$$

where $[\boldsymbol{\theta}]_{\boldsymbol{\lambda}}$ is the mean residue ellipticity in deg·cm²·dmol⁻¹, $[\boldsymbol{\theta}]_{\text{obs}}$ is the observed ellipticity in millidegrees, $\boldsymbol{C}$ is the peptide concentration in M, $\boldsymbol{l}$ is the path length in cm, and $\boldsymbol{n}$ is the number of amino acid residues.

The percentage of α-helical content was calculated based on the mean residue ellipticity at 222 nm using the following equation:

$$\boldsymbol{\alpha} = \frac{[\boldsymbol{\theta}]_{\mathbf{222}}}{[\boldsymbol{\theta}]_{\boldsymbol{max}}} \times \mathbf{100}\% \quad (6)$$

where $[\boldsymbol{\theta}]_{\mathbf{222}}$ is the mean residue ellipticity at 222 nm, and $[\boldsymbol{\theta}]_{\text{max}} = (-\mathbf{44,000} + \mathbf{250}\boldsymbol{T})(\mathbf{1} - \boldsymbol{k}/\boldsymbol{n})$, with $\boldsymbol{k} = \mathbf{4}$, $\boldsymbol{n}$ being the number of amino acids, $\boldsymbol{T}$=20°C.

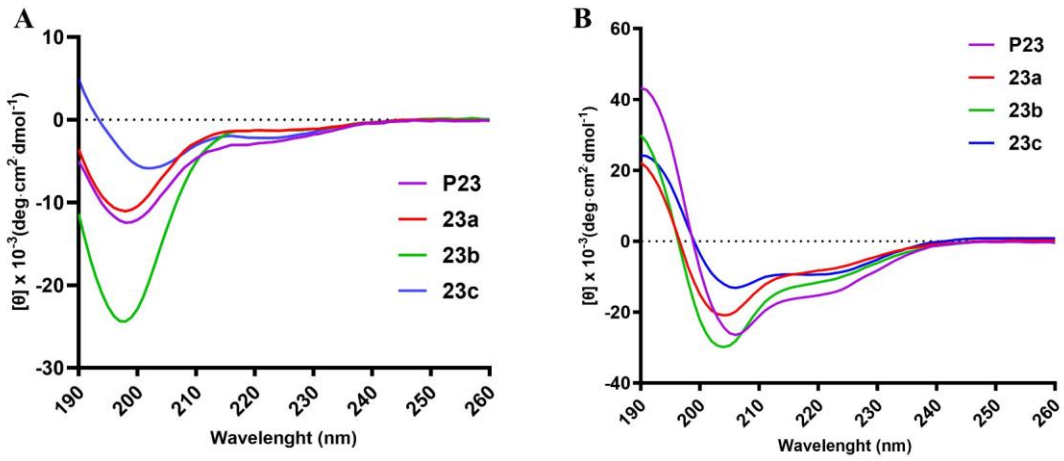

Figure S56. The CD spectrum of **P23**, **23a**, **23b**, and **23c**. A. The CD spectrum of **P23**, **23a**, **23b**, and **23c** in PBS (pH 7.3); B. The CD spectrum of **P23**, **23a**, **23b**, and **23c** in 50% TFE.

N. Detection of endogenous hydrogen sulfide production

Tumor cells were seeded in 12-well plates at a density of 3×10^4 cells/well and cultured in a 37°C, 5% CO_2 incubator until reaching approximately 70-80% confluency. The culture medium was then aspirated and replaced with fresh medium containing the test compounds. The experiment was performed in triplicate, with the following control groups included: a blank control (medium only, without cells), a cell control (cells without drug treatment), and a positive control (cells treated with sodium sulfide, a known H_2S donor). For detection, a strip of lead acetate test paper was attached to the center of each well lid, ensuring that the paper was suspended and did not contact the medium below. The lid was securely replaced, and the plate was further sealed with sealing film to prevent gas leakage. The plate was then incubated at 37°C under 5% CO_2 for 1-2 h. After incubation, the lid was carefully removed. The color change of each test paper was observed and recorded.

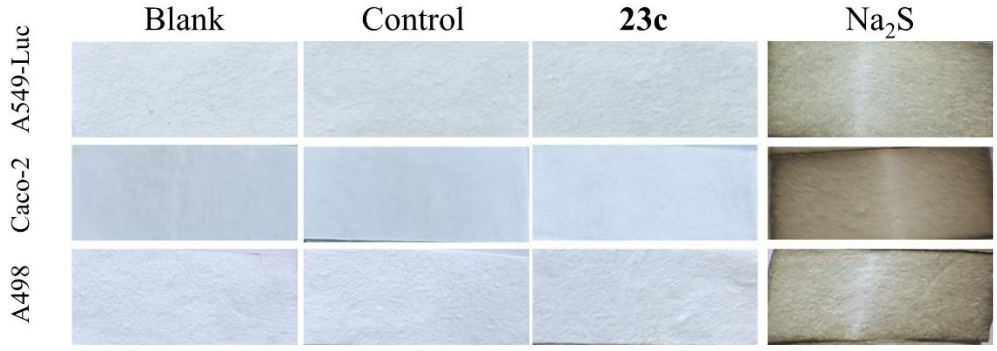

Figure S57. Lead acetate ($Pb(OAc)_2$)- papers strips showing the production of H_2S after different treatments of A549-Luc, Caco-2 and A498.

O. Network pharmacology

Construction of protein interaction networks and screening of targets

The chemical structure of Anoplin was drawn using ChemDraw software to obtain their detailed structural representations. Obtain the targets of Anoplin using Anoplin's SDF file or SMILES in SwissTargetPrediction (https://www.swisstargetprediction.ch/), Targetnet (https://targetnet.scbdd.com/), SEA (https://sea.bkslab.org/) and CHEMBL

(https://www.ebi.ac.uk/chembl/). The obtained targets were translated into gene names through the UniProt database (https://www. uniprot.org/). The analysis was performed by limiting the species to “Homo sapiens”. Finally, the obtained target genes were combined and de-duplicated. The results were the potential targets of Anoplin.

The “non-small cell lung cancer (NSCLC)” keyword was used in the search keywords, and the organism “Homo sapiens” was chosen. This information was entered into four databases, the GeneCards database, the Online Mendelian Inheritance in Man (OMIM) database, the Disgenet database and the National Center for Biotechnology Information (NCBI) database in order to find NSCLC -related targets. The illness targets of this investigation were combined, and duplicate genes were removed. Using the Venny, we next combined the disease targets with the medication targets to identify the possible targets of Anoplin against NSCLC. The protein-protein interaction network data generated from the STRING database was imported into the Cytoscape software (version 3.7.1) for visualization and subsequent analysis. Network topology analysis was then performed using the built-in plugin, cytoNCA. The analysis parameters were set to include seven key centrality metrics: Degree Centrality (DC), Betweenness Centrality (BC), Closeness Centrality (CC), Eigenvector Centrality (EC), Local Average Connectivity based method (LAC) and Network Centrality (NC). The plugin calculated and generated a dataset containing all nodes and their corresponding centrality values. To identify hub nodes within the network, a median-based multi-layer screening strategy was adopted： for each centrality metric, only nodes with values not lower than the median of that metric were retained. Finally, 21 key nodes were identified, which exhibited significant characteristics across the topological metrics examined[7-8].

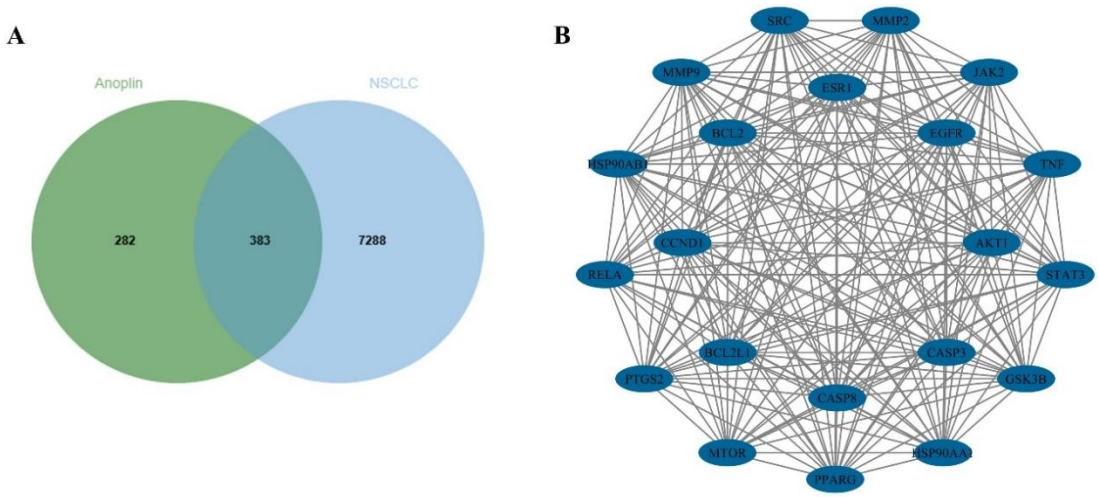

Figure S58. Venny and PPI network. A.Venny diagram showing the common part of Anoplin and NSCLC. B. PPI network of potential targets for Anoplin therapy of NSCLC.

Gene function and pathway enrichment analysis of target proteins

To investigate the biological function of potential targets of Anoplin and NSCLC, data were collected using the Metascape database for GO analysis and KEGG pathway enrichment analysis. We performed GO analysis including assessment of biological processes (BP), cellular components (CC) and molecular functions (MF) to elucidate their main biological functions. In addition, KEGG enrichment analysis was performed to identify important pathways associated with potential targets of NSCLC and to identify the major pathways that gained access to the targets.

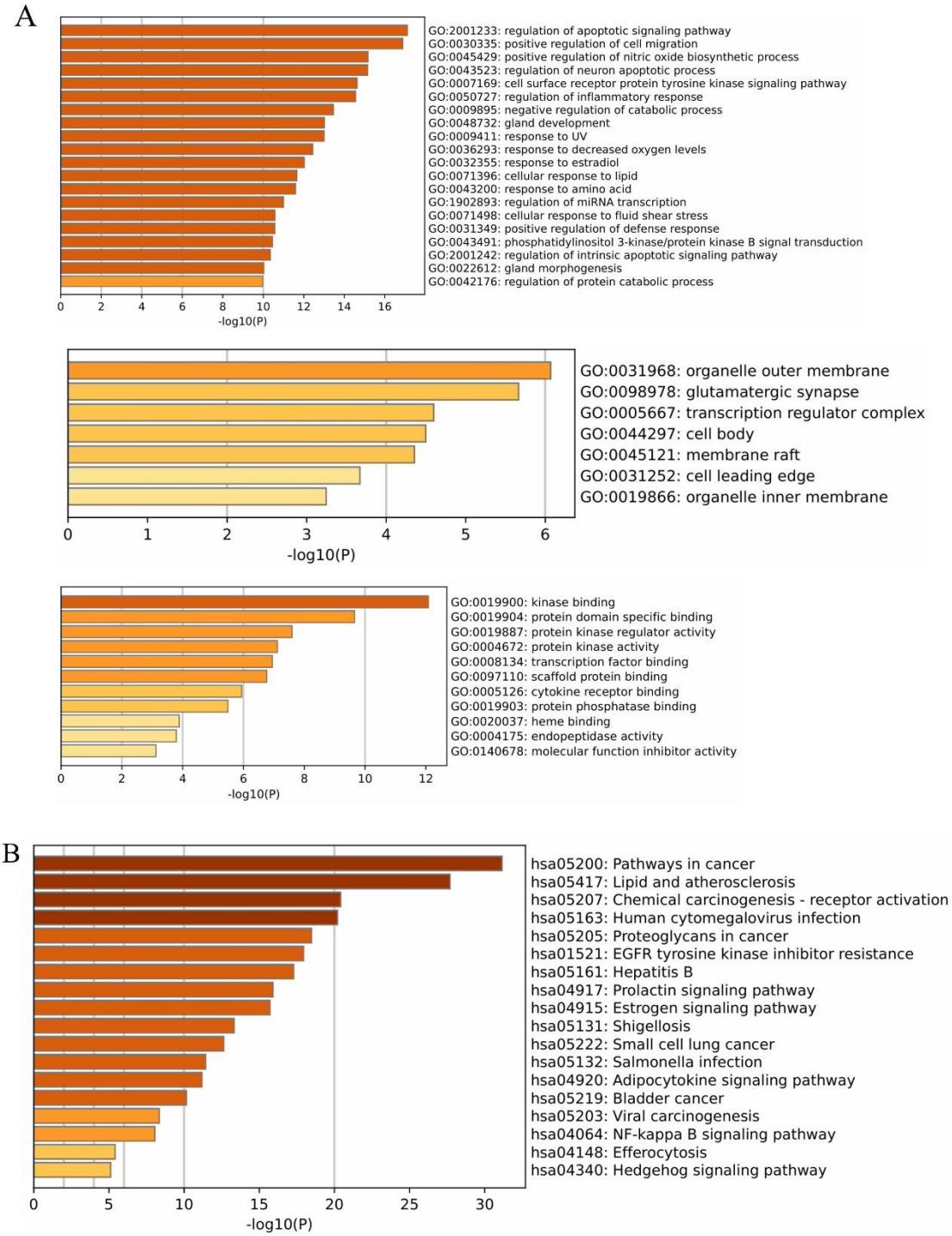

Figure S59. GO functional and KEGG pathway. A. GO functional enrichment analysis of Anoplin in NSCLC. B. KEGG pathway enrichment analysis of Anoplin in NSCLC.

P. Molecular docking

Molecular docking of P26 and 26b

Molecular docking method was used to further analyze the inter molecular interactions between αvβ6 and **P26**, **26b**. The 2D structure of **P26**, **26b** were drawn using

ChemDraw software, and the 2D structure was input into Molecular Operating Environment 2024 (MOE 2024) to produce its 3D structure and saved as a mdb file. Then, the RCSB PDB database (http://www.rcsb.org/) was used to search with the keyword αvβ6 to screen its protein crystal structures, PDB ID: 4UM9. MOE software was used to minimize the energy of the compounds, preprocess the target proteins and find the active pockets. Finally, MOE 2024 was run for molecular docking. The binding activity of both was evaluated according to the magnitude of binding energy and the results were visualized by PyMOL.

Molecular docking of P23 and 23c

Molecular docking method was used to further analyze the inter molecular interactions between NSCLC and **P23**, **23c**. The 2D structure of **P23**, **23c** were drawn using ChemDraw software, and the 2D structure was input into Molecular Operating Environment 2024 (MOE 2024) to produce its 3D structure and saved as a mdb file. Then, based on the PPI interaction network, GO functional enrichment, and KEGG pathway analysis, the interaction between **P23** and NSCLC can involve apoptosis pathways, kinase binding, and pathway in cancer. Therefore, we selected EGFR from the PPI network as the target protein for molecular docking to verify its interaction with **P23** and **23c**. The RCSB PDB database (http://www.rcsb.org/) was used to search with the keyword EGFR to screen its protein crystal structures, PDB ID: 9QXN. MOE software was used to minimize the energy of the compounds, preprocess the target proteins and find the active pockets. Finally, MOE 2024 was run for molecular docking. The binding activity of both was evaluated according to the magnitude of binding energy and the results were visualized by PyMOL.

Table S2. Basic information on the molecular docking of peptides and target proteins

Molecular name	Targets	PDB ID	Residue involved in H bonding	H-bond length(Å)	Docking scores (kcal·mol^{-1})
P26	αvβ6	4UM9	Tyr-178; Thr- 221; Gln-317; Gln-316	2.20; 1.99; 1.98; 2.25; 2.61	-10.71
26b	αvβ6	4UM9	Ile-216; Asp-218; Asp-219; Arg-248; Glu-316; Lys-338	2.27; 2.38; 2.18; 2.33; 1.94; 2.04; 2.87; 2.57	-10.82
P23	EGFR	9QXN	Asp-800; Asp-837; Asp-855; Glu-762; Lys-745	2.12; 1.96; 2.00; 2.01; 2.01; 1.99;	-13.77
23c	EGFR	9QXN	Leu-718; Phe-795; Cys-797; Thr-854	2.28; 2.09; 2.74; 2.05	-14.66

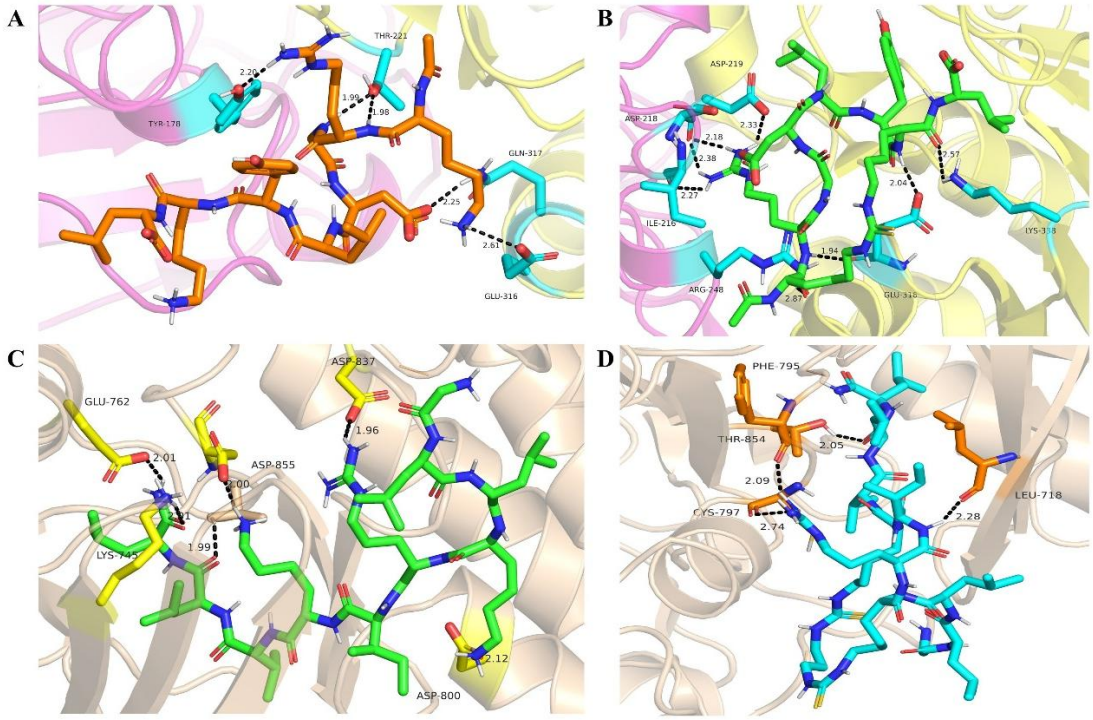

Figure S60. Molecular docking analysis of **P26**, **26b**, **P23**, **23c**, hydrogen bonds are shown in black. A. The docking results indicate that the **P26**compound interacts with the αvβ6 protein, where alphaV (magenta cartoon) and Beta6 (yellow cartoon) form hydrogen bonds. B. The docking results indicate that the **26b** compound interacts with the αvβ6 protein, where alphaV (magenta cartoon) and Beta6 (yellow cartoon) form hydrogen bonds. C. The docking results indicate that the P**23** compound interacts with the EGFR protein. D. The docking results indicate that the **23c** compound interacts with the EGFR protein.

Q. NMR spectra

^{1}H NMR spectra of compound **1a**

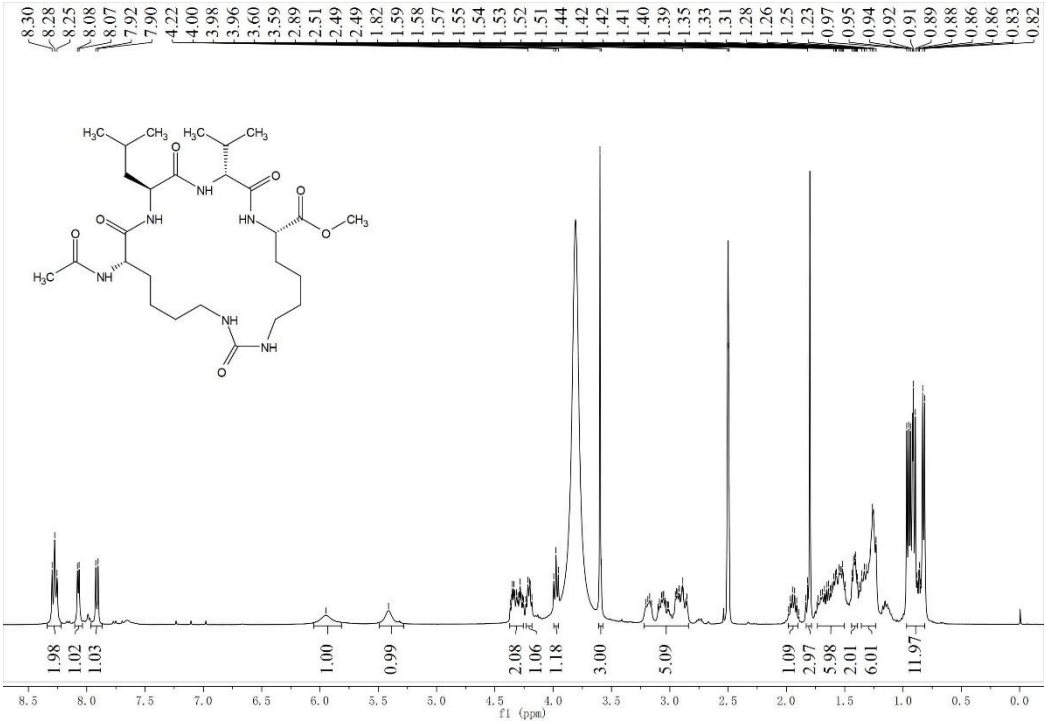

^{13}C NMR spectra of compound **1a**

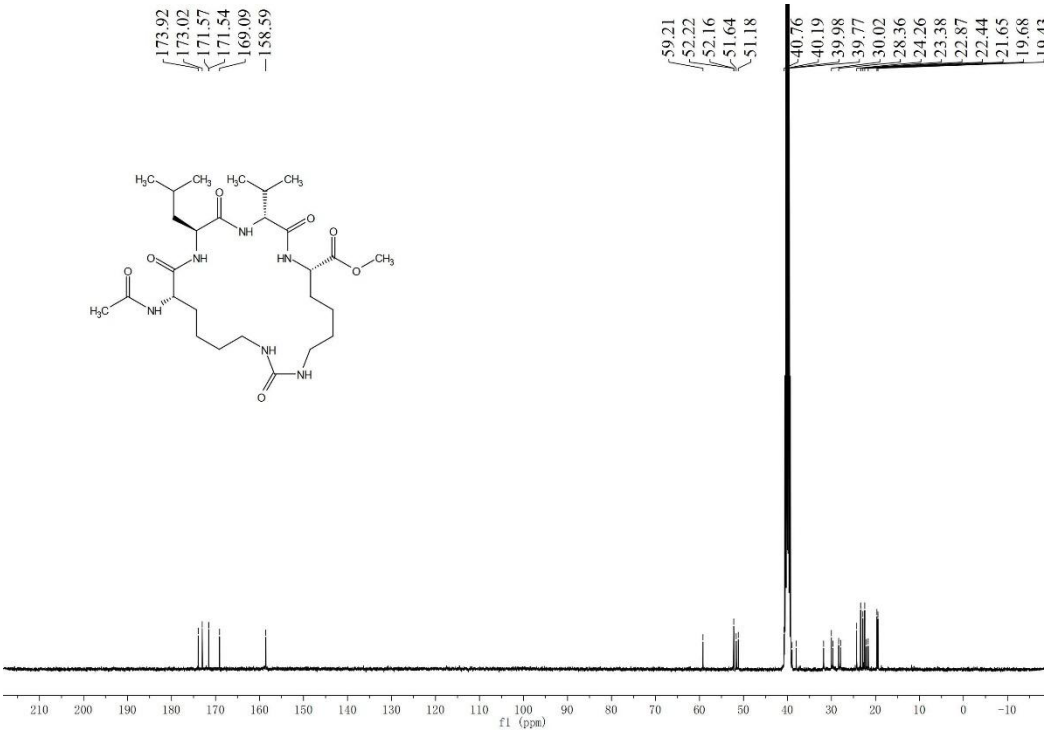

^{1}H NMR spectra of compound **1b**

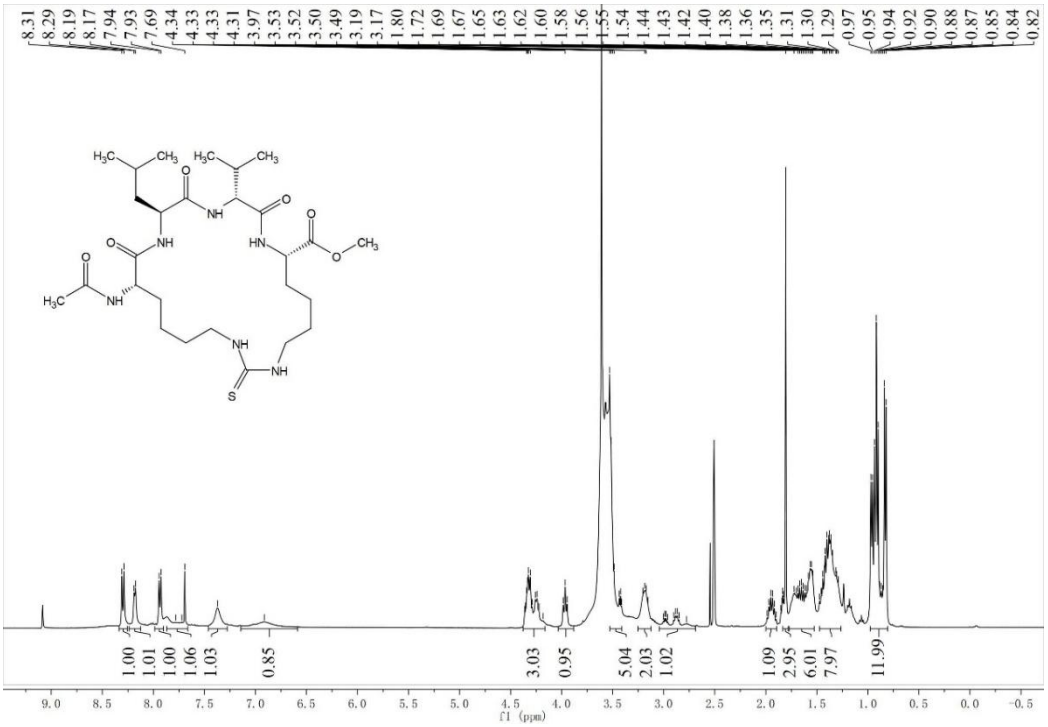

^{1}H NMR spectra of compound **6a**

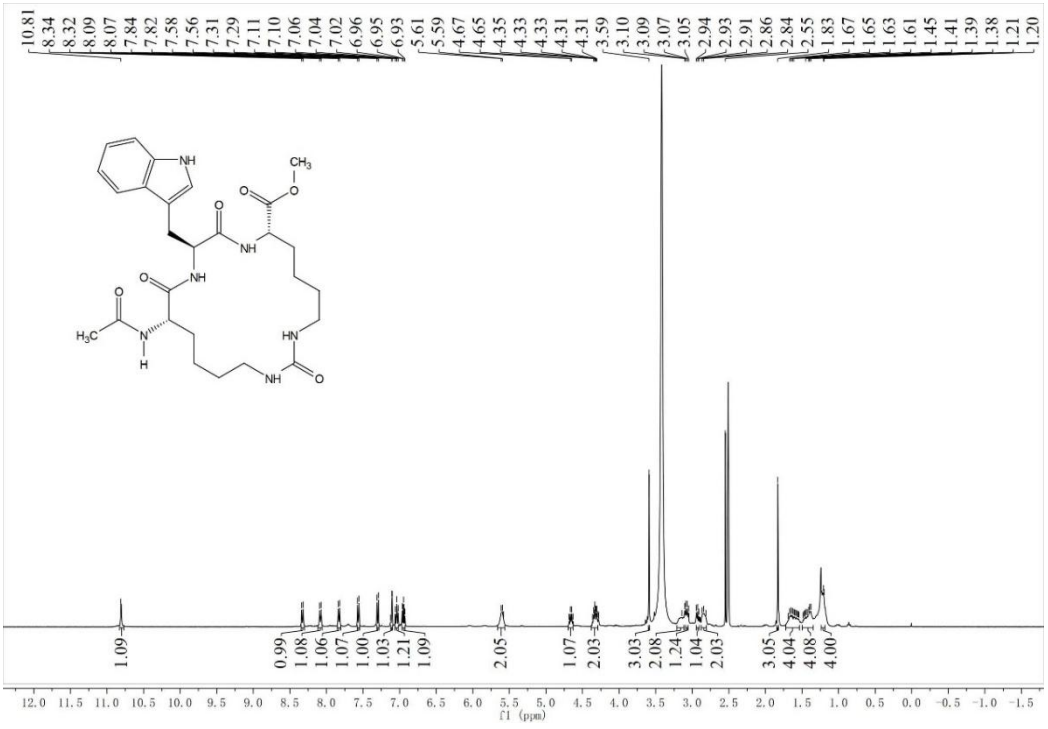

^{13}C NMR spectra of compound **6a**

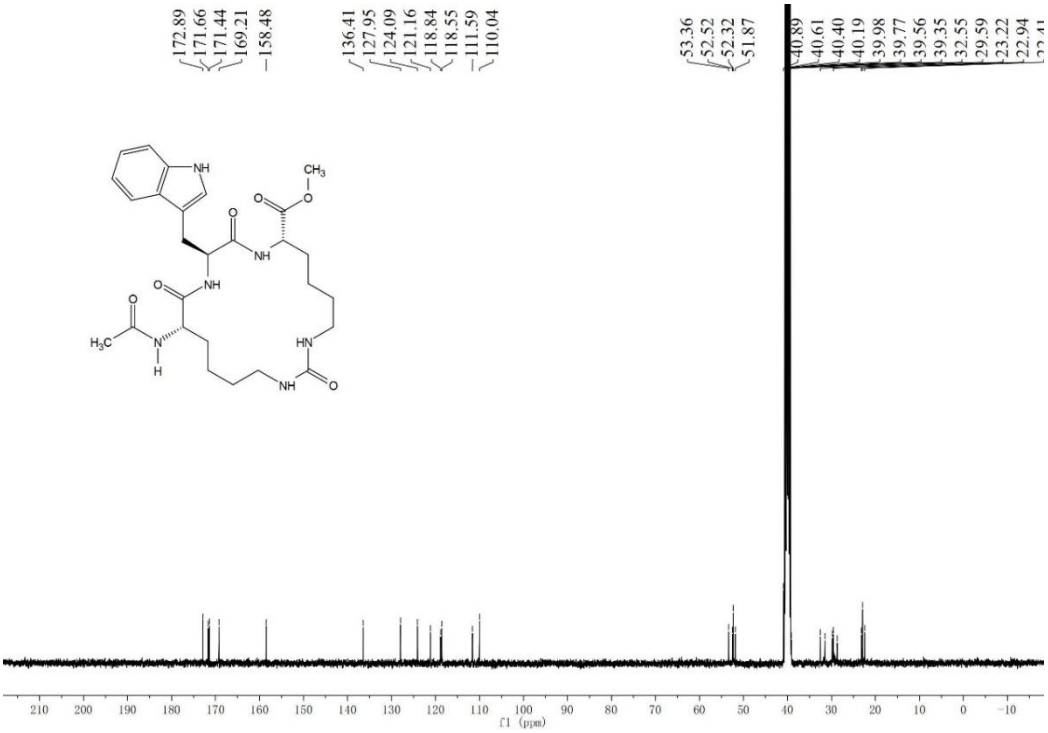

^{1}H NMR spectra of compound **6b**

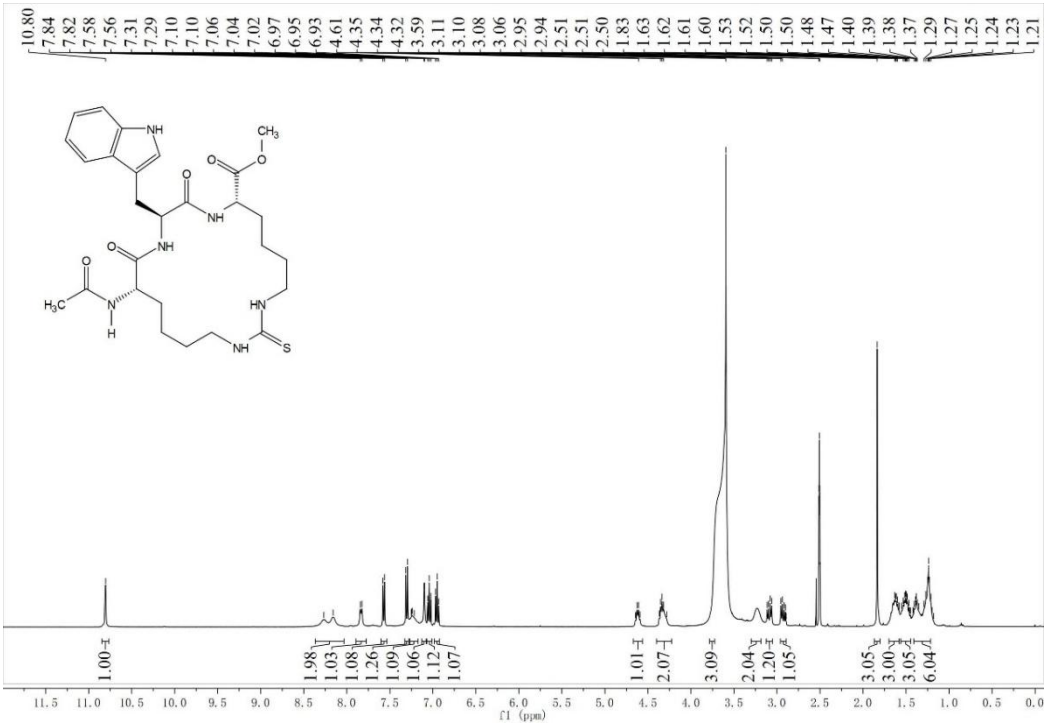

R. Supplementary References

1. Kapp, T. G. et al. A Comprehensive Evaluation of the Activity and Selectivity Profile of Ligands for RGD-binding Integrins. *Sci. Rep.* **7**, 39805 (2017).

2. Di Leva, F. S. et al. From a Helix to a Small Cycle: Metadynamics-Inspired αvβ6 Integrin Selective Ligands. *Angew. Chem. Int. Ed.* **57**, 14645–14649 (2018).

3. Li, Z. *et al.* A Stapled Peptide Inhibitor Targeting the Binding Interface of N6-Adenosine-Methyltransferase Subunits METTL3 and METTL14 for Cancer Therapy. *Angew. Chem. Int. Ed.* **63**, e202402611 (2024).

4. Dougherty, P. G. *et al.* Enhancing the Cell Permeability of Stapled Peptides with a Cyclic Cell-Penetrating Peptide. *J. Med. Chem.* **62**, 10098–10107 (2019).

5. Lautrette, G., Touti, F., Lee, H. G., Dai, P. & Pentelute, B. L. Nitrogen Arylation for Macrocyclization of Unprotected Peptides. J. Am. Chem. Soc. 138, 8340–3 (2016).

6. Xu, L., Fan, X., He, Y., Xia, X. & Zhang, J. Design, Synthesis, and Biological Evaluation of Lysine-Stapled Peptide Inhibitors of p53-MDM2/MDMX Interactions with Potent Antitumor Activity *In Vivo*. *J. Med. Chem.* **67**, 17893–17904 (2024).

7. Lan, Y., Peng, Q., Fu, B. & Liu, H. Effective analysis of thyroid toxicity and mechanisms of acetyltributyl citrate using network toxicology, molecular docking, and machine learning strategies. *Toxicol.* **511**, 154029 (2025).

8. He, Q. et al. Exploring the mechanism of curcumin in the treatment of colon cancer based on network pharmacology and molecular docking. *Front. Pharmacol*. **14**, 1102581 (2023).